(4)

FINAL PROJECT REPORT

ONR Contract Number: N00014-86-K-0549

Office of Naval Research
Electronics Division
Arlington, Virginia 22217-5000

ELECTROMAGNETIC INTERACTIONS IN HIGH-SPEED INTEGRATED ELECTRONIC CIRCUITS

Reporting Period: [illegible]

Principal Investigator: [illegible]
[illegible]

[illegible]

4

FINAL PROJECT REPORT

ONR Contract Number: N00014-86-K-0609

Office of Naval Research
Electronics Division
Arlington, Virginia 22217-5000

ELECTROMAGNETIC INTERACTIONS IN HIGH-SPEED INTEGRATED ELECTRONIC CIRCUITS

Reporting Period: June 1, 1986 to December 31, 1988

Prepared by: Dennis P. Nyquist
Principal Investigator

Division of Engineering Research
College of Engineering
Michigan State University
East Lansing, Michigan 48824

March 31, 1989

UNCLASSIFIED

SECURITY CLASSIFICATION OF THIS PAGE

REPORT DOCUMENTATION PAGE

1a. REPORT SECURITY CLASSIFICATION Unclassified	1b. RESTRICTIVE MARKINGS N/A
2a. SECURITY CLASSIFICATION AUTHORITY N/A	3. DISTRIBUTION / AVAILABILITY OF REPORT Approved for public release Distribution unlimited
2b. DECLASSIFICATION / DOWNGRADING SCHEDULE N/A	
4. PERFORMING ORGANIZATION REPORT NUMBER(S) N/A	5. MONITORING ORGANIZATION REPORT NUMBER(S)
6a. NAME OF PERFORMING ORGANIZATION Div. of Engineering Research Michigan State University 6b. OFFICE SYMBOL (If applicable)	7a. NAME OF MONITORING ORGANIZATION Office of Naval Research
6c. ADDRESS (City, State, and ZIP Code) East Lansing, MI 48824-1326	7b. ADDRESS (City, State, and ZIP Code) Electronics Division (Code 1114) Office of Naval Research Arlington, VA 22217-5000
8a. NAME OF FUNDING / SPONSORING ORGANIZATION Office of Naval Research 8b. OFFICE SYMBOL (If applicable) ONR	9. PROCUREMENT INSTRUMENT IDENTIFICATION NUMBER N00014-86-K-0609
8c. ADDRESS (City, State, and ZIP Code) Electronics Division (Code 1114) Office of Naval Research Arlington, VA 22217-5000	10. SOURCE OF FUNDING NUMBERS PROGRAM ELEMENT NO. / PROJECT NO. / TASK NO. / WORK UNIT ACCESSION NO

11. TITLE (Include Security Classification)

Electromagnetic Interactions in High-Speed Integrated Electronic Circuits

12. PERSONAL AUTHOR(S)
Dennis P. Nyquist

13a. TYPE OF REPORT	13b. TIME COVERED	14. DATE OF REPORT (Year, Month, Day)	15. PAGE COUNT
Final	FROM 6/1/86 TO 12/31/88	3/31/89	

16. SUPPLEMENTARY NOTATION

17. COSATI CODES			18. SUBJECT TERMS (Continue on reverse if necessary and identify by block number)
FIELD	GROUP	SUB-GROUP	Integrated microstrip circuits; electromagnetic interactions; excitation, scattering and resonances

19. ABSTRACT (Continue on reverse if necessary and identify by block number)

The objective of this research was to investigate electromagnetic interactions among components within microstrip-based circuits fabricated adjacent to the layered surround characteristic of a high-speed MMIC environment. EM fields maintained by currents immersed in layered dielectric/ferrimagnetic media are exploited to study the complete propagation-mode spectrum of microstrip lines and their interactions with the coupled microstrip devices which they interconnect. Topics studied include: 1) electromagnetics of layered dielectric/ferrimagnetic media; 2) mathematical methods -- analytical and numerical; 3) EM interactions among integrated microstrip guiding structures; 5) coupling between adjacent microstrip lines; 6) EM response of microstrip patch devices and antennas; and 7) experimental measurement of EM interactions in MMIC's.

20. DISTRIBUTION / AVAILABILITY OF ABSTRACT	21. ABSTRACT SECURITY CLASSIFICATION
☒ UNCLASSIFIED/UNLIMITED ☐ SAME AS RPT. ☐ DTIC USERS	Unclassified

22a. NAME OF RESPONSIBLE INDIVIDUAL	22b. TELEPHONE (Include Area Code)	22c. OFFICE SYMBOL
Dr. Arthur K. Jordan	(202) 696-4217	ONR (Code 1114)

DD FORM 1473, 84 MAR 83 APR edition may be used until exhausted. All other editions are obsolete.

SECURITY CLASSIFICATION OF THIS PAGE

Table of Contents

1. Introduction

This is the final project report on the research program entitled "Electromagnetic Interactions in High-Speed Integrated Electronic Circuits" supported by the Office of Naval Research under ONR Contract Number N00014-86-K-0609. It reports research conducted during the contract period of June 1, 1986 to December 31, 1988.

The objective of this research was to investigate electromagnetic interactions among components within microstrip-based circuits fabricated adjacent to the layered surround characteristic of a high-speed MMIC environment. EM fields maintained by currents immersed in layered dielectric/ferrimagnetic media are exploited to study the complete propagation-mode spectrum of microstrip lines and their interactions with the coupled microstrip devices which they interconnect. Seven related research topics were investigated in connection with this program, and they are described in Section 4 of this report.

The seven scientific collaborators who contributed to the research program are identified in Section 2 of this report. Section 3 details bibliographical information on the eighteen research papers which were precipitated by the investigations supported by this contract. Finally, Section 4 includes a technical description of the project and results; the seven sub-sections there provide details of research on the major topics investigated in connection with the program. Extensive reference is made to sciectific papers from Section 3, copies of which are included in Section 4.

2. Scientific Collaborators on Project

The following individuals have participated in, and contributed to, the research program during the contract period.

Faculty:

1. Dennis P. Nyquist, Professor of Electrical Engineering, Principal Investigator.
2. Byron C. Drachman, Professor of Mathematics, Co-Principal Investigator.

Doctoral-Level Students:

1. Michael J. Cloud, Graduate Assistant, Electrical Engineering Ph.D. Degree awarded in December 1987.
2. Yi Yuan, Graduate Assistant, Electrical Engineering Ph.D. Degree expected in June 1990.

Master's-Level Students:

1. Eric W. Blumbergs, Graduate Assistant, Electrical Engineering M.S. Degree expected in June 1989.

Undergraduate Students:

1. Paul F. Havala, Undergraduate Assistant, Electrical Engineering B.S. Degree awarded in June 1987; presently completing his M.S. Degree.
2. Darius Adamczyk, Undergraduate Assistant, Electrical Engineering B.S. Degree awarded in June 1988.

3. Contributed Papers Arising from Research Program

The following eighteen scientific papers, reporting results of this research, were produced during the Contract period.

[1] B. C. Drachman, D. P. Nyquist, and M. J. Cloud, "Accurate evaluation of Sommerfeld integrals using the fast Fourier transform," Nat. Radio Science (USNC/URSI) Meeting, University of Colorado, Boulder, CO, digest p. 73, Jan. 1987.

[2] J. S. Bagby and D. P. Nyquist, "Radiative and surface-wave losses in microstrip transmission lines," Nat. Radio Science (USNC/URSI) Meeting, University of Colorado, Boulder, CO, digest p. 226, Jan. 1987.

[3] J. S. Bagby and D. P. Nyquist, "Dyadic Green's functions for integrated electronic and optical circuits," IEEE MTT-S Trans. 35, 2, 206-210 (Feb. 1987).

[4] M. S. Viola, D. P. Nyquist, and B. C. Drachman, "On the Sommerfeld integral representation of the electric dyadic Green's function for layered media," URSI Radio Science Meeting, Virginia Tech, Blacksburg, VA, digest p. 278, June 1987.

[5] M. J. Cloud and D. P. Nyquist, "Complete propagation-mode spectrum of microstrip guiding structures," URSI Radio Science Meeting, Virginia Tech, Blacksburg, VA, digest p. 120, June 1987.

[6] E. W. Blumbergs, D. P. Nyquist, and P. F. Havala, "Integral equation formulation for a circular patch antenna in a layered environment," URSI Radio Science Meeting, Virginia Tech, Blacksburg, VA, digest p. 149, June 1987.

[7] M. J. Cloud, "Electromagnetic Interactions in Integrated Electronic Circuits," Ph.D. Dissertation, Department of Electrical Engineering, Michigan State University, East Lansing, MI, December 1987.

[8] D. P. Nyquist, M. S. Viola, M. J. Cloud, and M. Havrilla, "On Sommerfeld-integral electric field kernels for microstrip-based circuits," Nat. Radio Science (USNC/URSI) Meeting, University of Colorado, Boulder, CO, digest p. 112, Jan. 1988.

[9] M. S. Viola and D. P. Nyquist, "An observation on the Sommerfeld integral representation of the electric dyadic Green's function for layered media," IEEE MTT-S Trans. 36, 8, 1289-1292 (August 1988).

[10] C. H. Lee, J. S. Bagby, Y. Yuan and D. P. Nyquist, "Entire basis MoM analysis of coupled microstrip transmission lines," Nat. Radio Science (USNC/URSI) Meeting, University of Colorado, Boulder, CO, digest p. 179, Jan. 1989.

[11] Y. Yuan and D. P. Nyquist, "EFIE-based perturbation approximation for coupled microstrip lines," Nat. Radio Science (USNC/URSI) Meeting, University of Colorado, Boulder, CO, digest p. 180, Jan. 1989.

[12] B. Drachman, M. Cloud, and D. Nyquist, "Accurate evaluation of Sommerfeld integrals using the fast Fourier transform," to appear in IEEE AP-S Trans., April 1988.

[13] Y. Yuan and D. P. Nyquist, "Electric dyadic Green's function for layered media with dielectric/magnetic contrast," to be presented at 1989 URSI Nat. Radio Science (USNC/URSI) Meeting, SanJose, CA, June 26-30, 1989.

[14] Y. Yuan, J. Vezmar, G. King and D. P. Nyquist, "Coupled microstrip transmission lines: full-wave perturbation theory and experimental validation," to be presented at 1989 URSI Radio Science (USNC/URSI) Meeting, SanJose, CA, June 26-30, 1989.

[15] D. P. Nyquist "Dyadic Green's functions for EM fields in the layered PC/IC environment--representation, properties, and applications," to be presented at PIERS (Progress in Electromagnetics Research Symposium), MIT, Cambridge, Massachusetts, July 1989.

[16] D. P. Nyquist, "Deduction of EM phenomena in microstrip circuits from an integral-operator description of the system," Proceedings of the URSI Triennial EM Theory Symposium, Stockholm, Sweden, August 14-17, 1989.

[17] M. J. Cloud and D. P. Nyquist, "A note on the mixed potential representation of electric fields in layererd media," to appear in IEEE MTT-S Trans., August 1989.

[18] C. H. Lee, J. S. Bagby, Y. Yuan, and D. P. Nyquist, "Entire-domain basis MoM analysis of coupled microstrip transmission lines," submitted to IEEE MTT-S Trans., February 1989.

4. Technical Description of Project and Results

A technical description of the seven major research topics investigated in connection with the project is included in the corresponding sub-sections to follow. All bibliographic references are to scientific papers precipitated by that research, as listed in Section 3. Reproductions of research papers relevant to each subsection are included following those sections.

4.1 Electromagnetics of layered dielectric/ferrimagnetic media

A major accomplishment during the contract period was the development of a full-wave theory for the electromagnetics of layered dielectric/ferrimagnetic media. A dyadic Green's function for the electric field maintained by electric currents, immersed in a tri-layered substrate/film/cover surround having general linear, isotropic dielectric and magnetic properties, was obtained. In the special case where the substrate layer becomes perfectly conducting (negative infinite imaginary permittivity), the tri-layered background becomes that appropriate for the MMIC environment. This formulation and its results are reported in papers [3,4,9,13,15,17].

The Hertz potential boundary conditions of [3] are generalized in [13,17] to allow magnetic permeability contrast between the various isotropic, homogeneous media layers. A two-dimensional spectral analysis subsequently leads to the transform-domain Hertz potential maintained by currents immersed in the tri-layered environment. The space-domain electric field is recovered by inverse Fourier transformation, which leads to a Sommerfeld-type integral representation for that field. Subsequent complex analysis in the 2-d transform plane provides for a decomposition of the field into discrete surface-wave and continuous radiation-mode spectral components. The complete propagation mode spectrum of the tri-layered environment, into which the field of any immersed currents can be expanded, is consequently identified. The surface-wave contribution arises from poles of implicated spectral-domain reflection and coupling coefficients; those TE/TM poles of the tri-layered media are located by the solutions to generalized eigenvalue equations which involve the dielectric and magnetic properties of each layer and the film thickness. A specialization of the TM eigenvalue equation leads to precisely the recently reported TM surface waves supported by a grounded, lossy planar ferrite slab.

The source-point singularity in the Sommerfeld-integral representation of the electric Green's dyad for a layered IC environment was studied for the

first time in [4,9]. An innate principal volume and associated depolarizing dyad to properly accomodate that singularity were identified. A new mixed-potential formulation for the electric field maintained by currents immersed in the cover layer of the tri-layered IC environment was exposed in [17]. That formulation avoids the source-point singularity which arises from certain derivitives of the corresponding Hertz potential, resulting in Sommerfeld integral representations which are relatively rapidly convergent.

The electromagnetic analysis of tri-layered substrate/film/cover media provides the basis for study of electromagnetic interactions in MMIC's. It provides, through Hertz potential and electric Green's dyads, a concise and elegant description for EM excitation of such an integrated-circuit environment, in which no phenomena have been neglected. If the film layer is ferrimagnetic with moderately high permittivity, new physical phenomena are expected since the surface-wave regime may couple with important microstrip propagation modes unless the film is very thin. Each of the subsequent research topics exploits this EM analysis of the tri-layered environment; its consequences and physical implications are consequently investigated in connection with each topic.

T-MTT/35/2/11631

Research Paper No. [3]

Dyadic Green's Functions for Integrated Electronic and Optical Circuits

J. S. Bagby
D. P. Nyquist

Reprinted from: IEEE TRANSACTIONS ON MICROWAVE THEORY AND TECHNIQUES, Vol. MTT-35, No. 2, FEB. 1987.

Dyadic Green's Functions for Integrated Electronic and Optical Circuits

JONATHAN S. BAGBY, MEMBER, IEEE, AND
DENNIS P. NYQUIST, MEMBER, IEEE

Abstract—Layered structures play an important role in both integrated microwave circuits and optical integrated circuits. Accurate prediction of device behavior requires evaluation of fields in the system. An increasingly used mathematical formulation relies on integral equations: the electric field in the device is expressed in terms of the device current integrated into an electric Green's function. Details of the development of the specialized Green's functions used by various researchers have not appeared in the literature. We present the development of general dyadic electric Green's functions for layered structures; this dyadic formulation allows extension of previous analyses to cases where currents are arbitrarily directed. The electric-field Green's dyads are found in terms of associated Hertzian potential Green's dyads, developed via Sommerfeld's classic method. Incidently, boundary conditions for electric Hertzian potential are utilized; these boundary conditions, which have been a source of confusion in the research community, are developed in full generality. The dyadic forms derived herein are reducible in special cases to the Green's functions used by other workers.

I. INTRODUCTION

Layered dielectric structures, such as those depicted in Fig. 1, play an important role in both integrated electronic circuits and integrated optical circuits. In integrated electronics, conducting "devic .s" are affixed to a dielectric film layer which is deposited over a conducting ground plane. For integrated optical circuits, a dielectric waveguiding region is typically placed on top of a dielectric film layer; the film layer is, in turn, deposited on a

Manuscript received July 14, 1986; revised September 6, 1986.

J. S. Bagby is with the Department of Electrical Engineering, University of Texas at Arlington, Arlington, TX 76019.

D. P. Nyquist is with the Department of Electrical Engineering and Systems Science, Michigan State University, East Lansing, MI 48824.

IEEE Log Number 8611631.

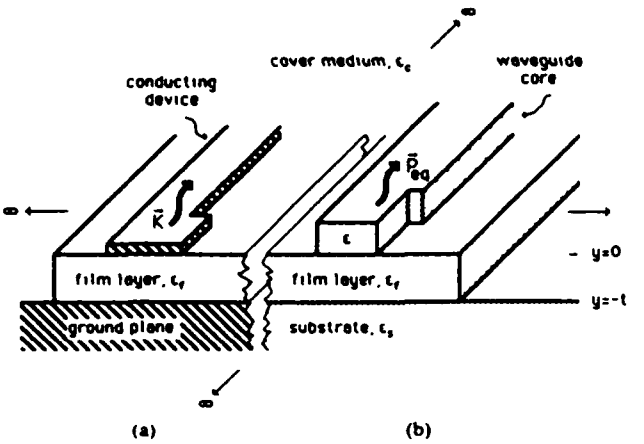

Fig. 1. Typical structures for (a) integrated electronic circuits and (b) integrated optical circuits.

substrate. In both cases, accurate prediction of device behavior requires evaluation of the fields in the system.

Exact formulations for the electric field in terms of differential equations [1], [2] are rendered ineffective for these more complicated geometries by the inseparability of boundary conditions at the device boundaries, and approximations based on such formulations have been found to neglect important radiative phenomena [3], [4]. Alternative formulations have been gaining favor; these formulations rely on integral equations to describe the behavior of the system [4]–[8]. The electric field in the system is expressed in terms of a current integrated into an electric Green's function; boundary conditions are incorporated in their full generality in the Green's function. However, details of the development of the Green's functions used by different researchers have not appeared in the literature.

We present a general dyadic formulation for the electric Green's functions for such layered structures. The dyadic forms derived here allow extension of previous analyses to cases where normally directed currents exist, such as in thick devices. The electric-field Green's dyads are found in terms of associated Hertzian potential Green's dyads; these, in turn, are developed by an extension of Sommerfeld's classic method [9], with components expressed as 2-D spatial frequency integrals of the Sommerfeld type. Incidently, boundary conditions for electric Hertzian potential are utilized; an adaptation of Sommerfeld's [9] development of these boundary conditions, which have been a source of confusion (compare, e.g., [10] and [11]), is given in the Appendix for the reader's convenience. Application of the Green's dyads to the analysis of integrated microstrip circuits and integrated optical waveguides is discussed.

II. Prototype Potential Solutions

In this section, we develop prototype solutions for the Hertzian potential excited in layered background structures by impressed currents. These solutions will later be specialized to the cases in Fig. 1 by application of boundary conditions. The resultant expressions for the potential in terms of the impressed current allow identification of Hertzian potential dyadic Green's functions, from which associated electric-field Green's dyads can be found.

Consider the situation depicted in Fig. 2. An impressed current $\vec{J}$ (or an impressed polarization $\vec{P} = \vec{J}/j\omega$) radiates in the ith layer of an infinite, multilayered dielectric structure, generating electric Hertzian potential in each layer. The total potential in each layer is the sum of a primary part $\vec{\Pi}^p$ and a scattered part,

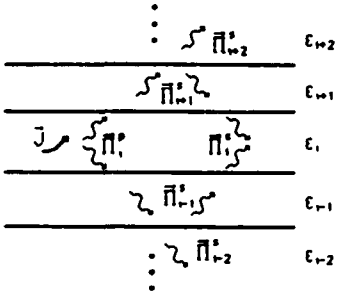

Fig. 2. Multilayered dielectric background structure with source in ith layer

$\vec{\Pi}^s$; the primary potential propagates directly from the source to a field point in the ith layer, whereas the scattered potential arrives at a field point after being scattered (reflected or transmitted) from interfaces between adjacent layers. These potentials satisfy the following Helmholtz equations:

$$\left(\nabla^2 + k_l^2\right)\begin{Bmatrix}\vec{\Pi}_l^p\\ \vec{\Pi}_l^s\end{Bmatrix} = \begin{cases} -\vec{J}/j\omega\epsilon_i, & l = i \\ 0, & \text{all } l. \end{cases} \tag{1}$$

The solution for the primary potential in terms of the impressed current is

$$\vec{\Pi}_i^p(\vec{r}) = \int G^p(\vec{r}|\vec{r}')\frac{\vec{J}(\vec{r}')}{j\omega\epsilon_i}\,dV' \tag{2}$$

where $G^p(\vec{r}|\vec{r}') = \exp(-jk_iR)/4\pi R$ is the free-space Green's function.

We solve (1) for the scattered potential by Fourier transformation on spatial variables tangential to the layer interfaces. Define the transform pair $F(\vec{r}) \leftrightarrow f(\vec{\lambda}, y)$, where $\vec{\lambda}$ is the 2-D transform variable $\vec{\lambda} = \xi\hat{x} + \zeta\hat{z}$. Then we have

$$\left(\frac{\partial^2}{\partial y^2} - p_l^2\right)\vec{\pi}_l^s = 0 \tag{3}$$

where $p_l^2 = \lambda^2 - k_l^2 = \xi^2 + \zeta^2 - k_l^2$. Equation (3) has solutions

$$\vec{\pi}_l^s(\vec{\lambda}, y) = \vec{W}(\vec{\lambda})\exp(\mp p_l y) \tag{4}$$

where the coefficient $\vec{W}(\vec{\lambda})$ is determined by application of boundary conditions; (2) can also be transformed to facilitate application of boundary conditions:

$$\vec{\pi}_i^p(\vec{\lambda}, y) = \int g^p(\vec{\lambda}; y, y')\frac{\vec{j}(\vec{\lambda}, y')}{j\omega\epsilon_i}\,dy'. \tag{5}$$

Here, $\vec{J}(\vec{r}) \leftrightarrow \vec{j}(\vec{\lambda}; y)$ and $g^p(\vec{\lambda}; y, y') = \exp(-p_i|y - y'|)/2p_i$.

We will use (4) and (5) as prototype solutions for the transformed Hertzian potential in the structures of Fig. 1. Since the coefficients $\vec{W}(\vec{\lambda})$ will depend on the transformed impressed current through (5), inverse transformation of these expressions will allow identification of the Hertzian potential Green's dyads $\vec{G}(\vec{r}|\vec{r}')$ for these structures, with the total potential given by

$$\vec{\Pi}_i(\vec{r}) = \int \vec{G}(\vec{r}|\vec{r}')\cdot\frac{\vec{J}(\vec{r}')}{j\omega\epsilon_i}\,dV'. \tag{6}$$

Once the Hertzian potential has been determined, the corresponding electric field can be found as $\vec{E}_i = (\nabla\nabla\cdot + k_i^2)\vec{\Pi}_i$, or

$$\vec{E}_i(\vec{r}) = \left(\nabla\nabla\cdot + k_i^2\right)\int \vec{G}(\vec{r}|\vec{r}')\cdot\frac{\vec{J}(\vec{r}')}{j\omega\epsilon_i}\,dV'$$

$$= \int \vec{G}^e(\vec{r}|\vec{r}')\cdot\frac{\vec{J}(\vec{r}')}{j\omega\epsilon_i}\,dV' \tag{7}$$

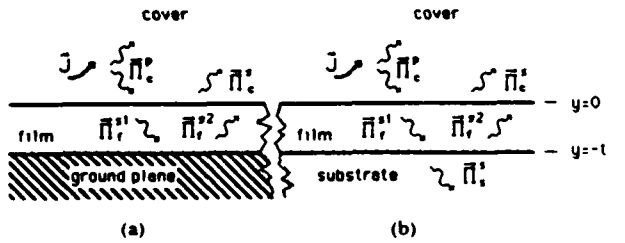

Fig. 3. Detail of potential components in (a) integrated electronic circuit and (b) integrated optical circuit.

where the electric-field Green's dyad $\bar{\bar{G}}(\bar{r}|\bar{r}')$ is defined by

$$\bar{\bar{G}}^e(\bar{r}|\bar{r}') = \text{P.V.}\left(\nabla\nabla\cdot + k_i^2\right)\bar{\bar{G}}(\bar{r}|\bar{r}') + \bar{\bar{L}}\delta(\bar{r}-\bar{r}'). \quad (8)$$

P.V. indicates that spatial integration must be performed in the principal value (P.V.) sense, and $\bar{\bar{L}}$ is an appropriate depolarizing dyad [12].

III. Microstrip and Optical Circuit Green's Dyads

We now apply boundary conditions to the prototype Hertzian potential solutions above to find specific Hertzian potential Green's dyads for the cases in Fig. 1. For the sake of brevity, some purely algebraic steps are omitted.

A. Microstrip Green's Dyad

First, consider the microstrip integrated circuit background structure of Fig. 3(a). The transformed potentials in the cover medium and film layer decompose into principal and reflected parts as follows:

$$\bar{\pi}_c = \bar{\pi}_c^p + \bar{\pi}_c^s \quad \bar{\pi}_f = \bar{\pi}_f^{s1} + \bar{\pi}_f^{s2} \quad (9)$$

where c and f refer to the cover medium and film layer, respectively. The principal potential $\bar{\pi}_c^p$ is given by (5) with i replaced by c; the scattered potentials are written in terms of the prototype solution (4) as

$$\bar{\pi}_c^s = \bar{A}\exp(-p_c y) \quad \bar{\pi}_f^{s1} = \bar{B}\exp(p_f y) \quad \bar{\pi}_f^{s2} = \bar{C}\exp(-p_f y). \quad (10)$$

We apply boundary conditions to evaluate the coefficient $\bar{A}(\lambda)$; then (9) can be inverse-transformed to yield a general expression for the potential in the cover medium in terms of the impressed current.

Application of tangential Hertzian potential boundary conditions (see the Appendix) at $y = 0$ and $y = -t$ results in an expression for the tangential components of $\bar{A}$ in terms of a tangential reflection coefficient, $R_t(\lambda)$

$$A_\alpha = R_t V_\alpha, \qquad \alpha = x, z \quad R_t = \frac{p_c - p_f \coth p_f t}{p_c + p_f \coth p_f t} \quad (11)$$

where the source term $\bar{V}$ is given by

$$V_\alpha = \int \frac{j_\alpha(\bar{\lambda}; y')}{j\omega\epsilon_c}\frac{e^{-p_c y'}}{2p_c}\,dy', \qquad \alpha = x, y, z. \quad (12)$$

Application of normal boundary conditions at $y = 0$ and $y = -t$ provides an expression for the normal component of $\bar{A}$ in terms of a normal reflection coefficient $R_n(\lambda)$ and a coupling coefficient $C(\lambda)$

$$A_y = R_n V_y + C[j\xi V_x + j\zeta V_z], \qquad R_n = \frac{Kp_c - p_f \tanh p_f t}{Kp_c + p_f \tanh p_f t}$$

$$C = \frac{2(K-1)p_c}{(p_c + p_f \coth p_f t)(Kp_c + p_f \tanh p_f t)}, \quad K = \epsilon_f/\epsilon_c. \quad (13)$$

Having completely specified $\bar{A}$, we are now in a position to solve for the total potential in the cover medium. Inverse-transforming (9) after substitution of (5) and (10)–(13) gives the result in dyadic notation

$$\bar{\Pi}_c(\bar{r}) = \int \bar{\bar{G}}(\bar{r}|\bar{r}')\cdot\frac{\bar{J}(\bar{r}')}{j\omega\epsilon_c}\,dV'. \quad (14)$$

The Hertzian potential Green's dyad in (14) is found to decompose into a principal and a reflected part: $\bar{\bar{G}}(\bar{r}|\bar{r}') = \bar{\bar{I}}G^p(\bar{r}|\bar{r}') + \bar{\bar{G}}^r(\bar{r}|\bar{r}')$, with

$$\bar{\bar{G}}^r(\bar{r}|\bar{r}') = \hat{x}G_t^r\hat{x} + \hat{y}\left(\frac{\partial}{\partial x}G_t^r\hat{x} + G_n^r\hat{y} + \frac{\partial}{\partial z}G_t^r\hat{z}\right) + \hat{z}G_t^r\hat{z} \quad (15)$$

where the scalar components of the reflected Green's dyad are given in terms of 2-D inverse transform integrals

$$\left.\begin{matrix}G_t^r(\bar{r}|\bar{r}')\\ G_n^r(\bar{r}|\bar{r}')\\ G_t^r(\bar{r}|\bar{r}')\end{matrix}\right\} = \iint_{-\infty}^{\infty}\left\{\begin{matrix}R_t(\lambda)\\ R_n(\lambda)\\ C(\lambda)\end{matrix}\right\}\frac{e^{j\bar{\lambda}\cdot(\bar{r}-\bar{r}')}e^{-p_c(y+y')}}{2(2\pi)^2 p_c}\,d^2\lambda. \quad (16)$$

B. Integrated Circuit Green's Dyad

Now consider the optical integrated circuit background structure of Fig. 3(b). The potentials in the cover medium, film layer, and substrate are in this case

$$\bar{\pi}_c = \bar{\pi}_c^p + \bar{\pi}_c^s \quad \bar{\pi}_f = \bar{\pi}_f^{s1} + \bar{\pi}_f^{s2} \quad \bar{\pi}_s = \bar{\pi}_s^s \quad (17)$$

where c, f, and s refer to the cover, film, and substrate, respectively. The principle potential $\bar{\pi}_c^p$ is as in (5) with i replaced by c. The scattered potentials are written in terms of the prototype solutions (4)

$$\bar{\pi}_c^s = \bar{A}\exp(-p_c y) \quad \bar{\pi}_f^{s1} = \bar{B}\exp(p_f y)$$
$$\bar{\pi}_f^{s2} = \bar{C}\exp(-p_f y) \quad \bar{\pi}_s^s = \bar{D}\exp(p_s y). \quad (18)$$

Once $\bar{A}$ is found via application of boundary conditions, (17) can be inverse-transformed to give a general expression for the potential in the cover medium.

Application of tangential boundary conditions at $y = 0$ and $y = -t$ once again gives the tangential components of $\bar{A}$ in terms of a tangential reflection coefficient $R_t(\lambda)$

$$A_\alpha = R_t V_\alpha, \qquad \alpha = x, z \quad R_t = \frac{p_c - p_f R_2}{p_c + p_f R_2} \quad R_2 = \frac{p_s + p_f \tanh p_f t}{p_f + p_s \tanh p_f t} \quad (19)$$

where the source term $\bar{V}$ is given by (12).

Application of normal boundary conditions at $y = 0$ and $-t$ yields an expression for the normal component of $\bar{A}$ in terms of a normal reflection coefficient $R_n(\lambda)$ and a coupling coefficient $C(\lambda)$

$$A_y = R_n V_y + C[j\xi V_x + j\zeta V_z], \qquad R_n = \frac{K_1 p_c - p_f R_4}{K_1 p_c + p_f R_4}$$

$$R_4 = \frac{p_c + K_2 p_f \tanh p_f t}{K_2 p_f + p_c \tanh p_f t} \quad K_1 = \epsilon_f/\epsilon_c \quad K_2 = \epsilon_c/\epsilon_f$$

$$C = \frac{(1+R_t)(1+R_n)}{2K_1 p_c}$$
$$\cdot\left\{\frac{p_f^2(K_2-1)(1+R_2)(1+R_4)e^{-2p_f t}}{K_2 p_f + p_c} + (K_1 - 1)\right\}. \quad (20)$$

We can now solve for the Hertzian potential in the cover by inverse-transforming (17). The result is identical in form to (14).

The Hertzian potential dyad again decomposes into a principle and a reflected part; $\bar{\bar{G}}(\vec{r}|\vec{r}') = \bar{\bar{I}}G^p(\vec{r}|\vec{r}') + \bar{\bar{G}}^r(\vec{r}|\vec{r}')$, with $\bar{\bar{G}}^r$ as in (15) and (16) and R_t, R_n, and C as in (19) and (20).

IV. Applications

In this section, we review some applications of the electric Green's dyads found above in the analysis of waveguiding systems and compare them with specialized versions used by other workers.

A. Microstrip Integral Equation

Consider the microstrip device illustrated in Fig. 1(a). If excitation is provided by an incident electric field $\vec{E}^i$, a surface current $\vec{K}$ is induced on the surface of the microstrip device. This induced current in turn supports a scattered field $\vec{E}^s$ in the system. The total tangential electric field at the strip surface must vanish, or $-\hat{t}\cdot\vec{E}^i = \hat{t}\cdot\vec{E}^s$. The scattered field may be written in terms of the electric dyadic Green's function derived in Section III-A as

$$\vec{E}^s(\vec{r}) = \int \bar{\bar{G}}^e(\vec{r}|\vec{r}')\cdot\frac{\vec{K}(\vec{r}')}{j\omega\epsilon_c}\,dS'. \tag{21}$$

Thus, we obtain an integral equation for the induced surface current on the device

$$\hat{t}\cdot\int \bar{\bar{G}}^e(\vec{r}|\vec{r}')\cdot\frac{\vec{K}(\vec{r}')}{j\omega\epsilon_c}\,dS' = -\hat{t}\cdot\vec{E}^i(\vec{r}). \tag{22}$$

By assuming the microstrip device to be infinitely thin, we recover a specialized version of this equation that has been successfully utilized by several workers in the analysis of thin microstrip structures [5]–[8]. This more general version provides the basis for continuing research on surface wave and radiative loss and coupling in thick microstrip devices.

B. Dielectric Waveguide Integral Equation

Consider the integrated dielectric waveguide of Fig. 1(b). If the system is excited by an impressed field $\vec{E}^i$, then the total field in the system is $\vec{E} = \vec{E}^i + \vec{E}^s$, where $\vec{E}^s$ is the field scattered by the waveguide core. The waveguide core can be replaced by an induced distribution of equivalent polarization $\vec{P}_{eq} = (\epsilon(\vec{r}) - \epsilon_c)\vec{E}(\vec{r})$, and the scattered field can be written in terms of this equivalent polarization as

$$\vec{E}^s(\vec{r}) = \int \bar{\bar{G}}^e(\vec{r}|\vec{r}')\cdot\frac{\vec{P}_{eq}(\vec{r}')}{\epsilon_c}\,dV'. \tag{23}$$

Then, setting $\vec{E} - \vec{E}^s = \vec{E}^i$, we have

$$\vec{E}(\vec{r}) - \int \frac{\epsilon(\vec{r}') - \epsilon_c}{\epsilon_c}\bar{\bar{G}}^e(\vec{r}|\vec{r}')\cdot\vec{E}(\vec{r}')\,dV' = \vec{E}^i(\vec{r}) \tag{24}$$

which is an integral equation for the unknown total field in the waveguiding system. This equation has been utilized successfully in the analysis of propagation and field distribution in integrated optical waveguides [4], and is the basis for continuing research on quantification of surface wave and radiative loss in integrated optics.

Appendix
Hertzian Potential Boundary Conditions

Here, we present an adaptation of Sommerfeld's [9] development of Hertzian potential boundary conditions to assist the reader. Consider the situation in Fig. 4. Electric-type Hertzian

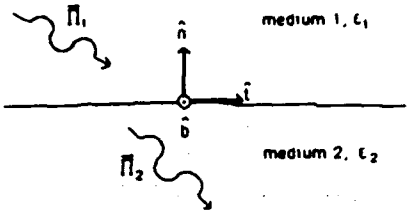

Fig. 4. Hertzian potential at a dielectric interface.

potential exists in regions 1 and 2, separated by a locally planar boundary. The fields in both regions are found in terms of the potential in the region, $\vec{\Pi}_1$ or $\vec{\Pi}_2$, as $\vec{E} = (k^2 + \nabla\nabla\cdot)\vec{\Pi}$, $\vec{H} = j\omega\epsilon\nabla\times\vec{\Pi}$. Let the potential in each region at a point at the interface have components $\vec{\Pi} = \hat{t}\Pi_t + \hat{n}\Pi_n$, with $\hat{t}$ tangent and $\hat{n}$ normal to the interface, and $\hat{b} = \hat{t}\times\hat{n}$. The fields in each region are given by

$$E_t = k^2\Pi_t + \frac{\partial}{\partial t}(\nabla\cdot\vec{\Pi})$$

$$E_b = \frac{\partial}{\partial b}(\nabla\cdot\vec{\Pi}) \quad E_n = k^2\Pi_n + \frac{\partial}{\partial n}(\nabla\cdot\vec{\Pi})$$

$$H_t = -j\omega\epsilon\frac{\partial}{\partial b}\Pi_n \quad H_b = j\omega\epsilon\left(\frac{\partial}{\partial t}\Pi_n - \frac{\partial}{\partial n}\Pi_t\right)$$

$$H_n = j\omega\epsilon\frac{\partial}{\partial b}\Pi_t. \tag{25}$$

Enforcing continuity of tangential E at the interface gives $\nabla\cdot\vec{\Pi}_1 = \nabla\cdot\vec{\Pi}_2$ and

$$\Pi_{t1} = K\Pi_{t2} \tag{26}$$

with $K = \epsilon_2/\epsilon_1$. In a similar fashion, continuity of tangential H yields

$$\Pi_{n1} = K\Pi_{n2} \quad \frac{\partial\Pi_{t1}}{\partial n} = K\frac{\partial\Pi_{t2}}{\partial n}. \tag{27}$$

Finally, $\nabla\cdot\vec{\Pi}_1 = \nabla\cdot\vec{\Pi}_2$ and (26) give

$$\frac{\partial}{\partial n}(\Pi_{n1} - \Pi_{n2}) = (K^{-1} - 1)\frac{\partial\Pi_{t1}}{\partial t}. \tag{28}$$

Equations (26)–(28) are thus the appropriate boundary conditions for electric Hertzian potential at a material interface.

If medium 2 is a perfect conductor, the vanishing of tangential E at the interface yields the following special case:

$$\Pi_{t1} = 0 \quad \frac{\partial\Pi_{n1}}{\partial n} = 0. \tag{29}$$

References

[1] D. Marcuse, *Theory of Dielectric Optical Waveguides*. New York: Academic Press, 1974, ch. 1.

[2] E. A. J. Marcatili, "Dielectric rectangular waveguide and directional coupler for integrated optics," *Bell Syst. Tech. J.*, vol. 48, no. 9, pp. 2071–2102, Sept. 1969.

[3] S-T. Peng and A. A. Oliner, "Guidance and leakage properties of a class of open dielectric waveguides: Part I—mathematical formulations," *IEEE Trans. Microwave Theory Tech.*, vol. MTT-29, pp. 843–855, Sept. 1981.

[4] J. S. Bagby, D. P. Nyquist, and B. C. Drachman, "Integral formulation for analysis of integrated dielectric waveguides," *IEEE Trans. Microwave Theory Tech.*, vol. MTT-33, pp. 906–915, Oct. 1985.

[5] N. K. Uzunoglu, N. G. Alexopoulos, and J. G. Fikioris, "Radiation properties of microstrip dipoles," *IEEE Trans. Antennas Propagat.*, vol. AP-27, pp. 853–858, Nov. 1979.

[6] D. M. Pozar, "Input impedance and mutual coupling of rectangular microstrip antenna," *IEEE Trans. Antennas Propagat.*, vol. AP-30, pp. 1191–1196, Nov. 1982.

[7] S. B. Fonseca and A. J. Giarola, "Microstrip disk antennas, part 1: Efficiency of space wave launching," *IEEE Trans. Antennas Propagat.*, vol. AP-32, pp. 561–567, June 1984.
[8] J. S. Bagby, "Integral equation analysis of propagation in microstrip transmission lines," in *Dig. North American Radio Science Meeting* (Vancouver, Canada), June 1985, p. 178.
[9] A. Sommerfeld, *Partial Differential Equations in Physics*. New York: Academic Press, 1964, pp. 236–265.
[10] R. W. P. King and C. W. Harrison, Jr., *Antennas and Waves: A Modern Approach*. Cambridge: M.I.T. Press, 1969, pp. 15–17.
[11] J. R. Wait, *Electromagnetic Waves in Stratified Media*. New York: MacMillan, 1962, pp. 137–146.
[12] A. D. Yaghjian, "Electric dyadic Green's functions in the source region," *Proc. IEEE*, vol. 68, pp. 248–263, Feb. 1980.

ON THE SOMMERFELD-INTEGRAL REPRESENTATION OF THE ELECTRIC DYADIC GREEN'S FUNCTION FOR LAYERED-MEDIA

Mark S. Viola and Dennis P. Nyquist
Department of Electrical Engineering and Systems Science

Byron C. Drachman
Department of Mathematics

Michigan State University
East Lansing, Michigan 48824

The electric dyadic Green's function for layered media is discussed. It is well known that for the free-space electric dyadic Green's function $\overleftrightarrow{G}_0$, evaluation of the electric field at observation points within the source region requires specification of a depolarizing dyad $\overleftrightarrow{L}$. The dyad $\overleftrightarrow{L}$ is dependent on the geometry of the "principal volume" which excludes the singularity of $\overleftrightarrow{G}_0$. Special considerations are invoked for the layered background media which are appropriate for the electromagnetics of integrated electronics.

The relevant equation which uniquely defines the electric field maintained by arbitrarily located electric currents in a layered environment is established. Beginning with

$$\vec{E}(\vec{r})=(k_c^2 + \nabla\nabla\cdot) \int_V (\overleftrightarrow{G}^p + \overleftrightarrow{G}^r)\cdot\vec{J}(\vec{r}')dV' \qquad (1)$$

and using the Sommerfeld-integral representation for the dyads ("principal" $\overleftrightarrow{G}^p$ has the pertinent singularity, "reflected" $\overleftrightarrow{G}^r$ is well behaved) appearing in the integrand of (1), it is shown that the electric field may be expressed as

$$\vec{E}(\vec{r})=-j\omega\mu_0 \lim_{\delta\to 0}\int_{V-V_\delta} \overleftrightarrow{G}^e(\vec{r};\vec{r}')\cdot\vec{J}(\vec{r}')dV' - \overleftrightarrow{L}\cdot\vec{J}(\vec{r})/j\omega\epsilon_c \qquad (2)$$

where $\overleftrightarrow{G}^e$ and $\overleftrightarrow{L}$ are quantified.

In conclusion, it is shown that for the layered-media electric dyadic Green's function, the Sommerfeld-integral representation is appropriate and leads to an innate option for the principal volume. The correction term in (2) is precisely the depolarizing dyad corresponding to this preferred choice of the excluding region.

T-MTT/36/8:/21764

An Observation on the Sommerfeld-Integral Representation of the Electric Dyadic Green's Function for Layered Media

Mark S. Viola
Dennis P. Nyquist

Reprinted from
IEEE TRANSACTIONS ON MICROWAVE THEORY AND TECHNIQUES
Vol. 36, No. 8, August 1988

An Observation on the Sommerfeld-Integral Representation of the Electric Dyadic Green's Function for Layered Media

MARK S. VIOLA AND DENNIS P. NYQUIST, MEMBER, IEEE

Abstract — The electric dyadic Green's function for layered dielectrics is discussed. It is well known that for the free-space electric dyadic Green's function $\bar{G}_0$, evaluation of the electric field at observation points within the source region requires specification of a "principal volume" along with the corresponding depolarizing dyad $\bar{L}$. Special considerations are invoked for layered background media which are appropriate for the electromagnetics of integrated electronics. It is shown that use of the Sommerfeld-integral representation of the electric dyadic Green's function leads to an innate choice for the depolarizing dyad. A corresponding principal volume is subsequently identified; it is demonstrated that there exists an alternative choice for this excluding region which leads to the same depolarizing dyad.

I. Introduction

There is an increasing interest in the study of optical and electronic circuits immersed in a layered dielectric surround. Conventional differential-operator formulations for the fields within these circuit devices are rendered ineffective due to the inseparability of the applicable boundary conditions for structures having practical shapes. An integral-operator formulation, based on the identification of equivalent volume polarization currents, circumvents this difficulty. Construction of the integral operator requires knowledge of the Green's function for the layered surround.

A general development of the Hertzian potential Green's dyad $\bar{G}$ for layered dielectrics has been discussed by Bagby and Nyquist [1]. Based on the classical method of Sommerfeld [2], the Hertzian potential dyadic Green's function was shown to have scalar components represented by 2-D spectral integrals. As asserted by Yaghjian [3], the singularity of $\bar{G}$ is seen to arise from that part of the dyad which is the Green's function $\bar{G}^p$ ("principal" Green's dyad) for the unbounded-space problem. In Section II, the development in [1] is altered slightly so that identification of a natural depolarizing dyad $\bar{L}$, relevant to the Green's dyad $\bar{G}^e$ for the electric field, may subsequently be made in Section III.

Finally, the electric field is expressed in the standard form as a volume integration of the scalar product of $\bar{G}^e$ with the electric current source J. The volume of integration extends over the support of the current density but excludes the singularity point of $\bar{G}^e$. The excluding region is identified as the "principal volume" which corresponds to the preferred choice of the depolarizing dyad as tabulated in [3]. An alternative excluding region, which is shown to be equivalent, is suggested to be useful in practice due to its simple form.

II. Hertzian Potential Green's Dyad

In this section, the Hertzian potential dyadic Green's function is developed for the trilayered structure depicted in Fig. 1. A film layer of thickness t and refractive index n_f is deposited over a substrate region ($y < -t$) which is characterized by index of refraction n_s. The region ($y > 0$) is the *cover* with refractive index n_c in which electric current density J, maintaining electromagnetic fields in all three regions, is immersed. All media are understood to possess limitingly small dissipation. Although the ensuing analysis may be generalized for a structure having any number of dielectric layers with embedded currents, the situation in Fig. 1 serves for the purpose of illustration, and provides a useful model for the background of practical electronic and optical integrated circuits.

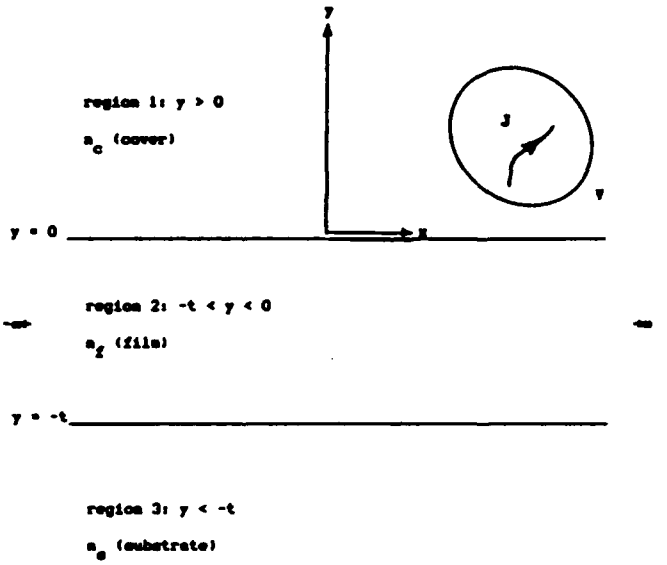

Fig. 1. Trilayered dielectric structure with sources in the cover.

Subsequent analysis assumes: i) time harmonic ($e^{j\omega t}$) dependence of the solutions to Maxwell's equations and ii) all integrals with unspecified limits span the entire space. The Hertzian potential subject to the Lorentz gauge satisfies the Helmholtz equation

$$\left(\nabla^2 + k_i^2\right)\Pi_i = -J/j\omega\epsilon_c \tag{1}$$

in each region ($i = s, f, c$ for substrate, film, cover). Formal operation on (1) with the 2-D Fourier transform

$$F\{\cdot\} = \iint \{\cdot\} e^{-j\lambda\cdot r}\, dx\, dz \tag{2}$$

where $\lambda = \hat{x}\xi + \hat{z}\zeta$, reduces (1) to the ordinary differential equation

$$\left(\partial^2/\partial y^2 - p_i^2\right)\pi(\lambda; y) = -j(\lambda; y)/j\omega\epsilon_c \tag{3}$$

where $\pi = F\{\Pi\}$, $j = F\{J\}$, and $p_i^2 = \xi^2 + \zeta^2 - k_i^2$. Solution of (3) is elementary, and may be written as a sum of primary scattered parts. Thus this decomposition is

$$\pi(\lambda; y) = \delta_{ic}\left\{\int_V g^p(\lambda; y, r')\frac{J(r')}{j\omega\epsilon_c}\, dV'\right\} + W_i^+(\lambda)e^{p_i y} + W_i^-(\lambda)e^{-p_i y} \tag{4}$$

where $g^p(\lambda; y, r') = e^{-j\lambda\cdot r'}e^{-p_c|y-y'|}/2p_c$, and δ_{ic} is a Kronecker delta. The coefficients $W_i^{\pm}$ are determined by satisfying the appropriate boundary conditions [1] across the dielectric interfaces and as $y \to \pm\infty$.

Manuscript received August 10, 1987; revised March 31, 1988. This work was supported in part by the National Science Foundation under Grant ECS-8611958.

The authors are with the Department of Electrical Engineering and Systems Science, Michigan State University, East Lansing, MI 48824.

IEEE Log Number 8821764.

0018-9480/88/0800-1289$01.00 ©1988 IEEE

Inversion of the transform-domain potentials yields the solution to (1) with the potential in the *cover* region given by

$$\Pi_c(r) = \frac{1}{(2\pi)^2}\iint e^{j\lambda\cdot r}\left\{\int_V g^p(\lambda; y, r')\frac{J(r')}{j\omega\epsilon_c}\,dV'\right\}d\xi\,d\zeta + \int_V \bar{\bar{G}}^r(r|r')\cdot\frac{J(r')}{j\omega\epsilon_c}\,dV'. \quad (5)$$

The reflected dyad $\bar{\bar{G}}^r(r|r')$ has scalar components $G_{\alpha\beta}(r|r')$ represented by 2-D Sommerfeld integrals of the generic form

$$G_{\alpha\beta}(r|r') = \frac{1}{(2\pi)^2}\iint C_{\alpha\beta}(\lambda)\,e^{j\lambda\cdot(r-r')}\frac{e^{-p_c(y+y')}}{2p_c}\,d\xi\,d\zeta. \quad (6)$$

Each of the coefficients $C_{\alpha\beta}(\lambda)$ is a well-behaved function of λ in the entire ξ–ζ plane; hence derivatives of $\bar{\bar{G}}^r$ may be obtained by formally differentiating under the spectral integral. Special attention is required in determining derivatives of the principal part of Π.

The spectral integral on the right side of (5) represents the primary part Π^p of the Hertzian potential. It is shown in the Appendix that under the assumption that J and $\nabla\cdot J$ are continuous and of compact support in V, derivatives up to second order of Π^p may be obtained by formally differentiating under the spectral integral. Therefore,

$$\nabla\nabla\cdot\Pi^p(r) = \frac{1}{(2\pi)^2}\iint\nabla\nabla\cdot\left\{e^{j\lambda\cdot r}\left[\int_V g^p(\lambda; y, r')\frac{J(r')}{j\omega\epsilon_c}\,dV'\right]\right\}d^2\lambda \quad (7a)$$

$$= \frac{1}{(2\pi)^2}\left(\iint\nabla\nabla\cdot\left\{e^{j\lambda\cdot r}\left[\int_{y'<y} g^p(\lambda; y, r')\frac{J(r')}{j\omega\epsilon_c}\,dV'\right]\right\}d^2\lambda + \iint\nabla\nabla\cdot\left\{e^{j\lambda\cdot r}\left[\int_{y'>y} g^p(\lambda; y, r')\cdot\frac{J(r')}{j\omega\epsilon_c}\,dV'\right]\right\}d^2\lambda\right) \quad (7b)$$

where the spatial integration has been split into regions in which g^p is continuously differentiable. Tangential derivatives (i.e., derivatives with respect to x and z) of the bracketed term in (7b) operate only on $e^{j\lambda\cdot r}$. However, performing the derivatives with respect to y demands additional considerations. Appropriate use of Leibnitz's rule [4, pp. 321–325] for differentiation under the integral sign reveals that

$$\frac{\partial}{\partial y}\left\{\int_{y'<y} g^p(\lambda; y, r')\frac{J(r')}{j\omega\epsilon_c}\,dV' + \int_{y'>y} g^p(\lambda; y, r')\frac{J(r')}{j\omega\epsilon_c}\,dV'\right\}$$

$$= \int_{y'<y}\frac{\partial}{\partial y}g^p(\lambda; y, r')\frac{J(r')}{j\omega\epsilon_c}\,dV' + \int_{y'>y}\frac{\partial}{\partial y}g^p(\lambda; y, r')\frac{J(r')}{j\omega\epsilon_c}\,dV'$$

$$+ \iint e^{-j\lambda\cdot r'}\left\{\left[\frac{e^{-p_c(y-y')}}{2p_c} - \frac{e^{-p_c(y'-y)}}{2p_c}\right]\frac{J(r')}{j\omega\epsilon_c}\right\}\Bigg|_{y'=y}dx'\,dz'$$

$$= \int_{y'<y}\frac{\partial}{\partial y}g^p(\lambda; y, r')\frac{J(r')}{j\omega\epsilon_c}\,dV' + \int_{y'>y}\frac{\partial}{\partial y}g^p(\lambda; y, r')\frac{J(r')}{j\omega\epsilon_c}\,dV'.$$

A subsequent differentiation with respect to y yields

$$\frac{\partial^2}{\partial y^2}\left\{\int_{y'<y} g^p(\lambda; y, r')\frac{J(r')}{j\omega\epsilon_c}\,dV' + \int_{y'>y} g^p(\lambda; y, r')\frac{J(r')}{j\omega\epsilon_c}\,dV'\right\}$$

$$= \int_{y'<y}\frac{\partial^2}{\partial y^2}g^p(\lambda; y, r')\frac{J(r')}{j\omega\epsilon_c}\,dV' + \int_{y'>y}\frac{\partial^2}{\partial y^2}g^p(\lambda; y, r')\frac{J(r')}{j\omega\epsilon_c}\,dV'$$

$$+ \iint e^{-j\lambda\cdot r'}\left\{\left[\frac{\partial}{\partial y}\frac{e^{-p_c(y-y')}}{2p_c} - \frac{\partial}{\partial y}\frac{e^{-p_c(y'-y)}}{2p_c}\right]\cdot\frac{J(r')}{j\omega\epsilon_c}\right\}\Bigg|_{y'=y}dx'\,dz'$$

$$= \int_{y'<y}\frac{\partial^2}{\partial y^2}g^p(\lambda; y, r')\frac{J(r')}{j\omega\epsilon_c}\,dV' + \int_{y'>y}\frac{\partial^2}{\partial y^2}g^p(\lambda; y, r')\frac{J(r')}{j\omega\epsilon_c}\,dV' - \iint\frac{J(x', y, z')}{j\omega\epsilon_c}e^{-j\lambda\cdot r'}\,dx'\,dz'$$

so that (7b) becomes

$$\nabla\nabla\cdot\Pi^p(r) = \iint\left[\int_V\bar{\bar{g}}(\lambda; r, r')\cdot\frac{J(r')}{j\omega\epsilon_c}\,dV'\right]d^2\lambda - \frac{1}{(2\pi)^2}\iint\left\{\iint\frac{\hat{y}J_y(x', y, z')}{j\omega\epsilon_c}e^{-j\lambda\cdot r'}\,dx'\,dz'\right\}e^{j\lambda\cdot r}\,d^2\lambda$$

$$= \iint\left[\int_V\bar{\bar{g}}(\lambda; r, r')\cdot\frac{J(r')}{j\omega\epsilon_c}\,dV'\right]d^2\lambda - \bar{\bar{L}}\cdot J(r)/j\omega\epsilon_c \quad (8)$$

where $\bar{\bar{L}} = \hat{y}\hat{y}$ and the dyad $\bar{\bar{g}}$ is given by the expression

$$\bar{\bar{g}}(\lambda; r, r') = \begin{cases}\nabla\nabla\left[e^{j\lambda\cdot(r-r')}e^{-p_c(y-y')}/8\pi^2p_c\right], & y'<y\\ \nabla\nabla\left[e^{j\lambda\cdot(r-r')}e^{-p_c(y'-y)}/8\pi^2p_c\right], & y'>y.\end{cases} \quad (9)$$

The term $\bar{\bar{L}}\cdot J$ was extracted from exploitation of the Fourier inversion theorem [5, p. 315], and is found to correspond exactly with that exposed in [3] for a "pillbox" principal volume. The form of $\bar{\bar{g}}$ suggests that the "slice" exclusion in Fig. 2 might be a more natural principal volume pertaining to $\bar{\bar{L}}$. This assertion is verified in part B of Section III.

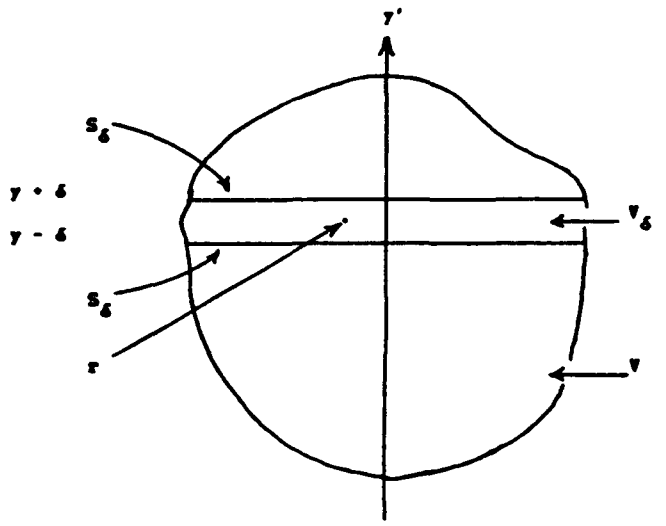

Fig. 2. A "slice" principal volume excluding the singularity point of the electric dyadic Green's function; closed surface S_δ is the boundary of the slice volume.

III. Electric Dyadic Green's Function

A. Development of the Principal Dyad

The electric field E is related to the Hertzian potential by $E = (k_c^2 + \nabla\nabla\cdot)\Pi$. Using (8), the principal part of the field may be written as

$$E^p(r) = -j\omega\mu_0 \iint \left\{ \int_V \bar{\bar{g}}^e(\lambda; r, r') \cdot J(r')\, dV' \right\} d^2\lambda - \bar{\bar{L}} \cdot J(r)/j\omega\epsilon_c \quad (10)$$

where the dyad $\bar{\bar{g}}^e = \bar{\bar{g}}/k_c^2 + (1/4\pi^2)\bar{\bar{I}} g^p e^{j\lambda\cdot r}$.

Equation (10) is a useful expression for the principal part of the electric field due to the simple nature of the integrand appearing in the volume integral. However, (10) is not written in the standard form as a volume integration of the scalar product of a Green's dyad with the electric current density. The depolarizing dyad $\bar{\bar{L}}$ has manifested itself naturally. Recognizing that the corresponding "principal volume" is a pillbox [3] yields the standard form for the electric field:

$$E^p(r) = -j\omega\mu_0 \lim_{v\to 0} \int_{V-v} \bar{\bar{G}}^e(r, r') \cdot J(r')\, dV' - \bar{\bar{L}} \cdot J(r)/j\omega\epsilon_c \quad (11)$$

where v is a pillbox excluding the singularity of $\bar{\bar{G}}^e$ at r and $\bar{\bar{G}}^e$ is given by

$$\bar{\bar{G}}^e(r, r') = \begin{cases} \left(\bar{\bar{I}} + \nabla\nabla/k_c^2\right) \iint e^{j\lambda\cdot(r-r')} \dfrac{e^{-p_c(y-y')}}{2(2\pi)^2 p_c} d^2\lambda, & y' < y \\ \left(\bar{\bar{I}} + \nabla\nabla/k_c^2\right) \iint e^{j\lambda\cdot(r-r')} \dfrac{e^{-p_c(y'-y)}}{2(2\pi)^2 p_c} d^2\lambda, & y' > y. \end{cases} \quad (12)$$

B. Equivalence of Principal Volumes

The principal volume v in (11) was identified to be a pillbox as tabulated in [3]. A more useful, and equivalent, exclusion is the "slice" volume shown in Fig. 2. Starting with the common representation for the free-space Green's function $\psi(r|r') = e^{-jk_c|r-r'|}/4\pi|r-r'|$, it may be shown that for a "slice" principal volume, the correction term $E^c(r)$ for the electric dyadic Green's function for field points in the source region is

$$E^c(r) = -\frac{1}{j\omega\epsilon_c} \lim_{\delta\to 0} \int_{S_\delta} \nabla'\psi(r|r')\, \hat{n}' \cdot J(r')\, dS' \quad (13)$$

where S_δ is shown in Fig. 2. The correction term above is now shown to be equivalent to the correction term corresponding to a pillbox principal volume. The surface integral term in (13) is split into integrations over S_1 and S_2 (planes at $y \pm \delta$, respectively). This yields for (13)

$$E^c(r) = -\frac{1}{j\omega\epsilon_c} \lim_{\delta\to 0} \left\{ -\int_{S_1} \nabla'\psi(r|r')|_{y'=y+\delta} \cdot J_y(x', y+\delta, z')\, dx'dz' + \int_{S_2} \nabla'\psi(r|r')|_{y'=y-\delta} J_y(x', y-\delta, z')\, dx'dz' \right\}. \quad (14)$$

As $\delta \to 0$, S_1 approaches S_2 and $J_y(x', y+\delta, z')$ approaches $J_y(x', y-\delta, z')$ due to the smoothness of the boundary of V and the continuity of J at $y' = y$. Thus, (14) simplifies to

$$E^c(r) = \frac{1}{j\omega\epsilon_c} \lim_{\delta\to 0} \int_S \nabla'\psi(r|r')|_{y'=y-\delta}^{y'=y+\delta} J_y(x', y, z')\, dx'dz' \quad (15)$$

where S extends over the $x'-z'$ plane. Expressing $\nabla'\psi$ in Cartesian form as

$$\nabla'\psi(r|r') = (-jk_c - 1/R)\frac{e^{-jk_cR}}{4\pi R^2} \cdot [\hat{x}(x'-x) + \hat{y}(y'-y) + \hat{z}(z'-z)]$$

where $R = |r - r'|$, it is found that

$$\nabla'\psi(r|r')|_{y'=y-\delta}^{y'=y+\delta} = (-jk_c - 1/R)\frac{e^{-jk_cR_\delta}}{4\pi R_\delta^2} \hat{y}2\delta \quad (16)$$

where $R_\delta = [(x-x')^2 + (z-z')^2 + \delta^2]^{1/2}$. Substitution of (16) into (15) yields

$$E^c(r) = \frac{1}{j\omega\epsilon_c} \lim_{\delta\to 0} \left\{ \hat{y} \int_S 2\delta(-jk_c - 1/R_\delta) \cdot \frac{e^{-jk_cR_\delta}}{4\pi R_\delta^2} J_y(x', y, z')\, dx'dz' \right\}. \quad (17)$$

The integral in (17) may be decomposed into the sum of integrals over $S - C_\nu$ and C_ν. C_ν is a circle centered at (x, z) with radius ν. As $\delta \to 0$, integration over $S - C_\nu$ vanishes. If ν is chosen sufficiently small, then $J_y(x', y, z') \approx J_y(r)$ and $e^{-jk_cR_\delta} \approx 1$ so that (17) becomes

$$E^c(r) = -\frac{1}{j\omega\epsilon_c} \hat{y} J_y(r) \lim_{\delta\to 0} \left\{ \delta \int_{C_\nu} \frac{jk_c + 1/R_\delta}{2\pi R_\delta^2} dx'dz' \right\} \quad (18a)$$

$$= -\frac{1}{j\omega\epsilon_c} \hat{y} J_y(r) \lim_{\delta\to 0} \left\{ \delta \int_0^{2\pi} d\varphi \int_0^{\nu} \frac{jk_c + 1/r_\delta}{2\pi r_\delta^2} \rho\, d\rho \right\} \quad (18b)$$

$$= -\frac{1}{j\omega\epsilon_c} \hat{y} J_y(r) \lim_{\delta\to 0} \left\{ \delta \int_0^{\nu} \frac{jk_c + 1/r_\delta}{r_\delta^2} \rho\, d\rho \right\} \quad (18c)$$

where $r_\delta = (\rho^2 + \delta^2)^{1/2}$. In going from (18a) to (18b), integration over C_ν has been transformed to polar coordinates. Performing the angular integration is trivial and yields (18c). Noting that the integrand in (18c) is a perfect differential, the term in braces becomes

$$\delta \int_0^\nu \frac{jk_c + 1/r_\delta}{r_\delta^2} \rho \, d\rho = \delta \left\{ jk_c \ln\left(\rho^2 + \delta^2\right)^{1/2} - \left(\rho^2 + \delta^2\right)^{-1/2} \right\} \Big|_0^\nu$$

$$= \delta \left\{ jk_c \left[\ln\left(\nu^2 + \delta^2\right)^{1/2} - \ln \delta \right] + \left[1/\delta - \left(\nu^2 + \delta^2\right)^{-1/2} \right] \right\}$$

$$= 1 \quad (\text{as } \delta \to 0). \tag{19}$$

Finally, substitution of (19) into (18c) yields

$$E^c(r) = -\frac{1}{j\omega\epsilon_c} \hat{y} J_y(r)$$

which is precisely the same correction term appearing in (11). Therefore integration excluding a "slice" principal volume is equivalent to a pillbox exclusion, and evaluation of (11) may use either of these volumes.

IV. Conclusions

In the study of layered-media electromagnetics, Sommerfeld integrals are used to represent scalar components of the electric dyadic Green's function. The principal part of the electric field may be written as a sum of a spectral integral along with a correction term that appears naturally. The spectral integration may be replaced with the more standard volume integral as in (11). Recognition of the depolarizing dyad, which has manifested itself innately, identifies the appropriate principal volume (a pillbox). An equivalent excluding region to the pillbox is suggested to be useful in practice due to its simple form.

Appendix

It is now shown that the differentiation under the spectral integral as in (7) is a legitimate operation. Without loss of generality, justifying this interchange of operations for the following is sufficient:

$$\iint_{\lambda > k_r} \nabla\nabla \cdot \left[e^{j\lambda \cdot r} \int_V g^p(\lambda; y, r') J(r') \, dV' \right] d^2\lambda. \tag{A1}$$

In (A1), k_r is the real part of k_c. Evaluation of p_c is made on the Riemann sheet with $\mathrm{Re}\{p_c\} > 0$.

Assuming that J and $\nabla \cdot J$ are continuous and have compact support in V, use of the vector identity $\nabla \cdot \{\varphi A\} = \varphi \nabla \cdot A + \nabla\varphi \cdot A$ along with the divergence theorem on (A1) yields

$$\iint_{\lambda > k_r} \nabla\nabla \cdot \left[e^{j\lambda \cdot r} \int_V g^p(\lambda; y, r') J(r') \, dV' \right] d^2\lambda$$

$$= \iint_{\lambda > k_r} \nabla \left[e^{j\lambda \cdot r} \int_V \nabla' \cdot J(r') \, g^p(\lambda; y, r') \, dV' \right] d^2\lambda$$

$$= \iint_{\lambda > k_r} \nabla \left[e^{j\lambda \cdot r} \int F\{\nabla' \cdot J(r')\} \frac{e^{-p_c|y-y'|}}{2p_c} \, dy' \right] d^2\lambda \tag{A2}$$

where $F\{\nabla \cdot J\}$ is the Fourier transform of $\nabla \cdot J$ as defined by (2).

Next, use $p_c = p_r + jp_i$, where p_r and p_i are the real and imaginary parts of p_c, respectively. The exponential $e^{-p_r|y-y'|}$ is of constant sign for all y. By the generalized first mean value theorem for integrals [4, p. 117], the right side of (21) may be written as

$$\iint_{\lambda > k_r} \nabla \left[e^{j\lambda \cdot r} \mathrm{Re}\left\{ F\{\nabla' \cdot J(x', \eta, z')\} e^{-jp_c|y-\eta|} \right\} \cdot \int_{y_{\min}}^{y_{\max}} \frac{e^{-p_r|y-y'|}}{2p_c} \, dy' \right] d^2\lambda$$

$$+ j \iint_{\lambda > k_r} \nabla \left[e^{j\lambda \cdot r} \mathrm{Im}\left\{ F\{\nabla' \cdot J(x', \theta, z')\} e^{-jp_c|y-\theta|} \right\} \cdot \int_{y_{\min}}^{y_{\max}} \frac{e^{-p_r|y-y'|}}{2p_c} \, dy' \right] d^2\lambda \tag{A3}$$

where $y_{\min} < (\eta, \theta) < y_{\max}$ ($J = 0$ for all $y' < y_{\min}$, $y > y_{\max}$). The spatial integration in (22) is trivial and leads to

$$\iint_{\lambda > k_r} \nabla \left[e^{j\lambda \cdot r} \mathrm{Re}\left\{ F\{\nabla \cdot J(x', \eta, z')\} \cdot e^{-jp_c|y-\eta|} \right\} \frac{\varphi(p_r; y)}{2p_r p_c} \right] d^2\lambda$$

$$+ j \iint_{\lambda > k_r} \nabla \left[e^{j\lambda \cdot r} \mathrm{Im}\left\{ F\{\nabla' \cdot J(x', \theta, z')\} \cdot e^{-jp_c|y-\theta|} \right\} \frac{\varphi(p_r; y)}{2p_r p_c} \right] d^2\lambda \tag{A4}$$

where $\varphi(p_r; y) = \{2 - e^{-p_r(y - y_{\min})} - e^{-p_r(y_{\max} - y)}\}$. Since $\nabla \cdot J$ is continuous and of compact support in V, $\nabla \cdot J \in L^2$ (i.e., the space of square integrable functions). In particular, for each y, $\nabla \cdot J$ is an L^2 function in the $\xi - z$ plane. Using a standard theorem from Fourier transform theory [5, pp. 310–313], the 2-D Fourier transform of $\nabla \cdot J$ is an L^2 function in the $\xi - \zeta$ plane. Thus, $F\{\nabla \cdot J\} = 0(\lambda^{-1-\epsilon})$ as $(\lambda \to \infty, \epsilon > 0)$. The integrand in (A4) is dominated in magnitude by a function which is independent of r and $0(\lambda^{-2-\epsilon})$. The Weierstrauss M test [4, p. 470] guarantees that the integral in (A4) converges uniformly, whereby a standard theorem from advanced calculus [4, p. 474] justifies the interchange of differentiation and spectral integration.

References

[1] J. S. Bagby and D. P. Nyquist, "Dyadic Green's functions for integrated electronic and optical circuits," *IEEE Trans. Microwave Theory Tech.*, vol. MTT-35, pp. 206–210, Feb. 1987.

[2] A. Sommerfeld, *Partial Differential Equations in Physics*. New York: Academic Press, 1964, pp. 236–265.

[3] A. D. Yaghjian, "Electric dyadic Green's function in the source region," *Proc. IEEE*, vol. 68, pp. 248–263, Feb. 1980.

[4] J. M. H. Olmsted, *Advanced Calculus*. Englewood Cliffs, NJ: Prentice-Hall, 1961.

[5] H. F. Weinberger, *A First Course in Partial Differential Equations*. New York: Wiley, 1965.

ELECTRIC DYADIC GREEN'S FUNCTION FOR LAYERED MEDIA WITH DIELECTRIC/MAGNETIC CONTRAST

Yi Yuan* and Dennis P. Nyquist
Department of Electrical Engineering
Michigan State University
East Lansing, Michigan 48824

In the study of layered environments in electronic and optical integrated circuits, integral-operator formulations are increasingly exploited. Construction of such integral operators requires an appropriate Green's function. In this paper, we present the development of a general electric dyadic Green's function for layered structures with magnetic as well as dielectric contrast. The general properties of that Green's dyad are studied.

In the tri-layered environment, a film of thickness t with constitutive parameters (ε_f, μ_f) is deposited over a substrate $(y<-t)$ described by (ε_s, μ_s). The region $(y>0)$ is the cover with parameters (ε_c, μ_c). The arbitrarily directed electric current $\vec{J}$ is immersed in the cover or film region. By Sommerfeld's classical method, a Hertzian-potential dyadic Green's function is found whih satisfies general boundary conditions. The electric Green's dyad is expressed in terms of its Hertzian counterpart as

$$\bar{\bar{G}}^e(\vec{r}|\vec{r}') = (k_c^2 + \nabla\nabla\cdot)\bar{\bar{G}}(\vec{r}|\vec{r}') + \bar{\bar{L}}\delta(\vec{r}-\vec{r}')$$

$$\bar{\bar{G}}(\vec{r}|\vec{r}') = \bar{\bar{I}}G^p(\vec{r}|\vec{r}') + \bar{\bar{G}}^r(\vec{r},\vec{r}')$$

where $\bar{\bar{G}}$ is the Hertzian-potential Green's dyad, $\bar{\bar{L}}$ is a depolarizing dyad, G^p is the principal Green's function, and $\bar{\bar{G}}^r$ is a reflected Green's dyad. The scalar components of the reflected dyad are obtained in 2-D spectral integral representations. The dyadic Green's functions are reducible in certain special cases, such as that of a conducting substrate layer.

The source-point singularity of the electric Green's dyad is studied, and depolarizing dyad $\bar{\bar{L}}$ is identified. It is demonstrated that the electric Green's dyad for layered media of general contrast is reciprocal. Pole singularities of implicated reflection coefficients lead to general discrete surface-wave-mode eigenvalue equations.

The electric dyadic Green's function obtained is applied to the microstrip transmission-line structure with magnetic (ferrite) film and conductor substrate. The EFIE's based upon that Green's function are solved by the MoM and by a perturbation approximation. Numerical results are obtained and compared with those of a structure having a purely dielectric surround.

Research Paper No. [15]

DYADIC GREEN'S FUNCTIONS FOR EM FIELDS IN THE LAYERED PC/IC ENVIRONMENT -- REPRESENTATION, PROPERTIES AND APPLICATIONS

Dennis P. Nyquist
Department of Electrical Engineering
Michigan State University
East Lansing, Michigan 48824

The study of EM interactions among electronic/optical devices in the layered PC/IC environment has become a contemporary topic in electromagnetics research. Interest is in microstrip or dielectric-waveguide based circuits operating at microwave, millimeter, or optical wavelengths. Such circuits are typically located adjacent to a planar, tri-layered substrate/film/cover surround. In microwave and most mm-wave circuits, the dielectric substrate layer is replaced by a good conductor. This paper exposes dyadic Green's functions useful or the integral-operator description of such circuits, as well as certain of their general properties and applications.

Dyadic Green's functions for the Hertz potential and electric field maintained by electric currents immersed in a tri-layered substrate/film/cover surround are obtained in Sommerfeld integral representation; they are cast into a form useful for the description of the EM field in the PC/IC environment. Arbitrary contrast of dielectric/magnetic properties among the several linear, isotropic, homogeneous media in the tri-layered surround is accomodated. A substrate with negative-infinite imaginary permittivity provides the special case of a conducting layer. Alternative representations, arising from real-line Fourier inversion and its subsequent conversion to a singularity expansion involving pole and branch-point singularities, are exposed.

Several general properties of the Green's dyads are identified. Pole singularities of integrands in the dyad representations correspond to TE/TM surface waves supported by the asymmetric substrate/film/cover surround with appropriate dielectric/magnetic contrast among layers. The electric Green's dyad is demonstrated to be reciprocal, and its source-point singularity is exposed. The latter singularity leads to an innate contribution to the electric field at a source point which is absent in conventional eigenfunction expansions of that field. A mixed-potential formulation identifies a scalar potential maintained by charge immersed in the tri-layered environment.

The Green's dyads are applied to obtain an integral-operator description for electronic/optical components in PC/IC configurations. Application to open waveguides leads to quantification of the complete propagation-mode (including radiation) spectrum as well as an excitation theory for discrete modes. A coupled-mode perturbation theory for systems of adjacent open waveguides is exposed. The integral-operator formulation also provides a description for coupling of patch antennas and other devices among themselves and associated transmission systems. Typical numerical results will be presented.

Research Paper No. [17]

A NOTE ON THE MIXED POTENTIAL REPRESENTATION OF ELECTRIC FIELDS IN LAYERED MEDIA

M.J. Cloud and D.P. Nyquist

ABSTRACT

A mixed potential formulation is given for electric fields in layered environments. Contributions to the field from charges are identified explicitly through a scalar Green's function for layered media. The outcome is a computationally expedient Sommerfeld integral representation.

I. Introduction

The study of electric fields due to surface currents in millimeter-wave integrated circuits [1,2] brings to light some facts about the alternative representation of Hertz potentials. Despite their apparent simplicity, these observations have not appeared previously in this form. The points discussed in this paper bear directly upon the divergent spectral integrations which are offered on several occasions [3,4] in the recent literature; it is hoped that ultimately they will find application in avoiding comparatively awkward formulations.

II. Hertz Potential Green's Dyad Formulation

Consider the configuration of layered dielectric media over a conducting half-space as shown in Figure 1. The electric field $\vec{E}(\vec{r})$ in the cover, maintained by surface currents embedded in that same layer, decomposes linearly into two parts as $\vec{E}(\vec{r}) = \vec{E}^{p}(\vec{r}) + \vec{E}^{r}(\vec{r})$. The fields of the right member may be termed the primary and reflected components. A Hertz potential representation of $\vec{E}$ based upon this decomposition is given by Bagby and Nyquist [1,2] as follows:

$$\vec{E}(\vec{r}) = (k_c^2 + \nabla\nabla\cdot) \int_S \overleftrightarrow{G}(\vec{r},\vec{r}')\cdot[\vec{K}(\vec{r}')/j\omega\epsilon]dS' \qquad (1)$$

where $\vec{K}(\vec{r})$ describes source currents on surface S, and $\overleftrightarrow{G} = \overleftrightarrow{I}G^{p} + \overleftrightarrow{G}^{r}$ is the decomposition of the Hertz potential Green's dyad into primary and reflected components. The dyad scalar components are given as double spectral (Sommerfeld-type) integrals:

$$G^{p}(\vec{r},\vec{r}') = \iint_{-\infty}^{\infty} \frac{\exp[j\vec{\lambda}\cdot(\vec{r} - \vec{r}')]\exp[-p_c|y - y'|]}{2(2\pi)^2 p_c} \, d^2\lambda \qquad (2)$$

$$\begin{bmatrix} G_t^r(\vec{r},\vec{r}') \\ G_n^r(\vec{r},\vec{r}') \\ G_c^r(\vec{r},\vec{r}') \end{bmatrix} - \iint_{-\infty}^{\infty} \begin{bmatrix} R_t(\lambda) \\ R_n(\lambda) \\ C^n(\lambda) \end{bmatrix} \frac{\exp[j\vec{\lambda}\cdot(\vec{r} - \vec{r}')]\exp[-p_c|y - y'|]}{2(2\pi)^2 p_c} \, d^2\lambda \quad (3)$$

where $\overleftrightarrow{G}^r = \hat{x}G_t^r\hat{x} + \hat{y}[(\partial G_c^r/\partial x)\hat{x} + G_n^r\hat{y} + (\partial G_c^r/\partial z)\hat{z}] + \hat{z}\,G_t^r\hat{z}$. The R_t, R_n, and C are reflection and coupling coefficients detailed in [1,2]. Note that $p_c = [\lambda^2 - k_c^2]^{1/2}$ is a wavenumber parameter, $\vec{\lambda} = \hat{x}\lambda_x + \hat{z}\lambda_z$ is a vector spatial frequency, and $d^2\lambda = d\lambda_x d\lambda_z$.

The first term (with k_c^2 factor) in $\vec{E}(\vec{r})$ is proportional to the vector Hertz potential contribution to $\vec{E}$ (produced directly by currents $\vec{K}$), while the second term is subsequently treated as the negative gradient of scalar potential. In the present formulation, and in many similar ones [3,4], it is found that boldly exchanging the order of differentiation (i.e., the $\nabla\nabla\cdot$ operation) with integration too many times leads to convergence problems with the resulting inner-nested spectral integrals. Care will be taken in the present development to allow only one such interchange; moreover, the impact of the derivative on the Green's function is subsequently minimized by a technique of integration-by-parts.

Figure 2 illustrates the geometry of surface S, supporting currents of integrated electronics. Assume that $\vec{K}(\vec{r})$ is a continuous function everywhere on S, except possibly at the boundary C_p of subregion S_p. The exception is made because, although one physically expects continuous currents, discontinuities could be introduced mathematically by subsectional basis functions in numerical solutions. C_p^+ and C_p^- are auxiliary boundary contours just outside and inside of C_p. Take C_0 to be the outer contour of S. Let $S' = S\text{-}S_p$, with $\hat{n}'$ the outward normal unit vector to S'. It is important to note here that principal Green's function G^p may in fact be represented either in Sommerfeld integral form, or simply as $\exp(-jkR)/4\pi R$; the latter form points out explicitly the nature of its source-point

($R = |\vec{r} - \vec{r}'| = 0$) singularity. This singularity, unless handled properly, invalidates a subsequent application of the divergence theorem. To maintain complete rigor a small area should be excluded from S, at the location $\vec{r}$, to preclude the coincidence of $\vec{r}$ and $\vec{r}'$ during the spatial integration in (1). However, at points where $\vec{K}$ is continuous there is no contribution from either the excluded area or its boundary contour. Therefore, the exclusion process is not detailed here. Points of surface current discontinuity are handled in the following section.

III. Primary Component of Electric Field

Consider first the primary component of $\vec{E}$. The electric scalar potential contribution to $\vec{E}^P$ is $-\nabla\Phi^P$, where

$$\Phi^P = -(1/j\omega\epsilon)\nabla\cdot\int_S G^P\vec{K}dS'$$

$$= -(1/j\omega\epsilon)\left[\int_{S'}\nabla\cdot(G^P\vec{K})dS' + \int_{S_p}\nabla\cdot(G^P\vec{K})dS'\right]. \qquad (4)$$

This expression is subsequently cast into a form which explicitly exposes its electric charge sources. Although the method is conventional, it is included here to guide the identification of similar contributions to the reflected potential. The procedure is less obvious in the latter case.

Exchanging the divergence and spatial integration prompts vector manipulation of the integrand as follows:

$$\nabla\cdot(G^P\vec{K}) = G^P\nabla\cdot\vec{K} + \nabla G^P\cdot\vec{K} = -\nabla'\cdot(G^P\vec{K}) + G^P\nabla'\cdot\vec{K}. \qquad (5)$$

Into the last term a substitution from the surface continuity equation, $\nabla\cdot\vec{K} = -j\omega\sigma$, is made. The scalar potential becomes

$$\Phi^p = (1/j\omega\epsilon)[\int_{S'}\nabla'\cdot(G^p\vec{K})dS' + \int_{S_p}\nabla'\cdot(G^p\vec{K})dS']$$

$$+ (1/\epsilon)\int_S(G^p\sigma)dS' \qquad (6)$$

to which the 2-D divergence theorem is applied to give

$$\Phi^p = (1/\epsilon)[(1/j\omega)\oint_{C_0}G^p(\hat{n}'\cdot\vec{K})dl'$$

$$+ (1/j\omega)\oint_{C_p}G^p[\hat{n}'\cdot(\vec{K}^+ - \vec{K}^-)dl'$$

$$+ \int_S G^p\sigma dS']$$

$$= (1/\epsilon)[\oint_{C_0}G^p\rho_{10}dl' + \oint_{C_p}G^p\rho_{1p}dl' + \int_S G^p\sigma dS'] \qquad (7)$$

where $\vec{K}^+$ and $\vec{K}^-$ are values of surface current on C_p^+ and C_p^-, respectively. Thus Φ^p is written in terms of line and surface charges, while the original derivatives have been effectively removed from G^p.

IV. Reflected Component

For the reflected potential,

$$\Phi^r = (-1/j\omega\epsilon)\nabla\cdot\int_S\overleftrightarrow{G}^r\cdot\vec{K}\,dS' \qquad (8)$$

one may follow the same general sequence of steps as above, but this time exploiting the specific form of $\overleftrightarrow{G}^r$. Following the procedure beginning with equation (5), and defining a scalar Green's function $G^r = G_t^r + \partial G_c^r/\partial y$,

$$\nabla\cdot(\overleftrightarrow{G}^r\cdot\vec{K}) = \nabla\cdot\{\hat{x}G_t^rK_x - \hat{y}[(\partial G_c^r/\partial x)K_x + (\partial G_c^r/\partial z)K_z] + \hat{z}G_t^rK_z\}$$

$$=)\partial G_t^r/\partial x)K_x + (\partial G_t^r/\partial z)K_z$$

$$+ (\partial/\partial y)[(\partial G_c^r/\partial x)K_x + (\partial G_c^r/\partial z)K_z]$$

$$= (\nabla_{xz}G_t^r)\cdot\vec{K} + [\nabla_{xz}(\partial G_c^r/\partial y)]\cdot\vec{K}$$

$$= (\nabla G^r)\cdot\vec{K} = (-\nabla' G^r)\cdot\vec{K} \qquad (9)$$

Carrying the analogous steps to completion, one finally arrives at

$$\Phi^r = (1/\epsilon)[\oint_{C_0} G^r\rho_{10}dl' + \oint_{C_p} G^r\rho_{1p}dl' + \int_S G^r\sigma dS'] \qquad (10)$$

Therefore the reflected scalar potential is expressible in terms of effective charges weighted by an appropriate Green's function. It is noted that convenient form of the scalar reflected Green's function arose from the specific form of the Hertz potential Green's dyad cited earlier. Since the conversion process has effectively removed derivatives from this function, the new formulation is expected to be computationally efficient. Finally, the $\vec{E}$ field in the cover region is expressed as

$$\vec{E} = -j\omega\mu\int_S \overleftrightarrow{G}\cdot\vec{K}dS - \nabla(1/\epsilon)[\oint_{C_0} G\rho_{10}dl' + \oint_{C_p} G\rho_{1p}dl' + \int_S G\sigma dS'] \qquad (11)$$

where $G = G^p + G^r$ is a Sommerfeld integral representation of the scalar potential Green's function for layered media. The gradient operator may (at interior points) be exchanged with the spectral integrals without rendering those Sommerfeld integrals non-convergent.

V. Summary and Conclusions

The preceding sections illustrate a procedure for avoiding the needless imposition of derivatives onto the Green's function, thus avoiding convergence problems. In the process of converting to a less singular formulation, unknown surface and line charges are introduced explicitly into the problem. Presumably, for many applied problems, these charge functions could be expanded in suitable moment method basis sets along with the original surface currents.

References

[1] J.S. Bagby, D.P. Nyquist, and B.C. Drachman, "Integral formulation for analysis of integrated dielectric waveguides," IEEE Trans. Microwave Theory Tech., vol. MTT-33, no. 10, pp. 906-915, October 1985.

[2] J.S. Bagby and D.P. Nyquist, "Dyadic Green's functions for integrated electronic and optical circuits," IEEE Trans. Microwave Theory Tech., vol. MTT-35, pp. 206-210, February 1987.

[3] D.M. Pozar, "Input impedance and mutual coupling of rectangular microstrip arrays," IEEE Trans. Antennas Propagat., vol. AP-30, no. 6, pp. 1191-1196, November 1982.

[4] N.K. Uzunoglu, N.G. Alexopoulis, and J.G. Fikloris, "Radiation properties of microstrip dipoles," IEEE Trans. Antennas Propagat., vol. AP-27, no. 6, pp. 853-858, November 1979.

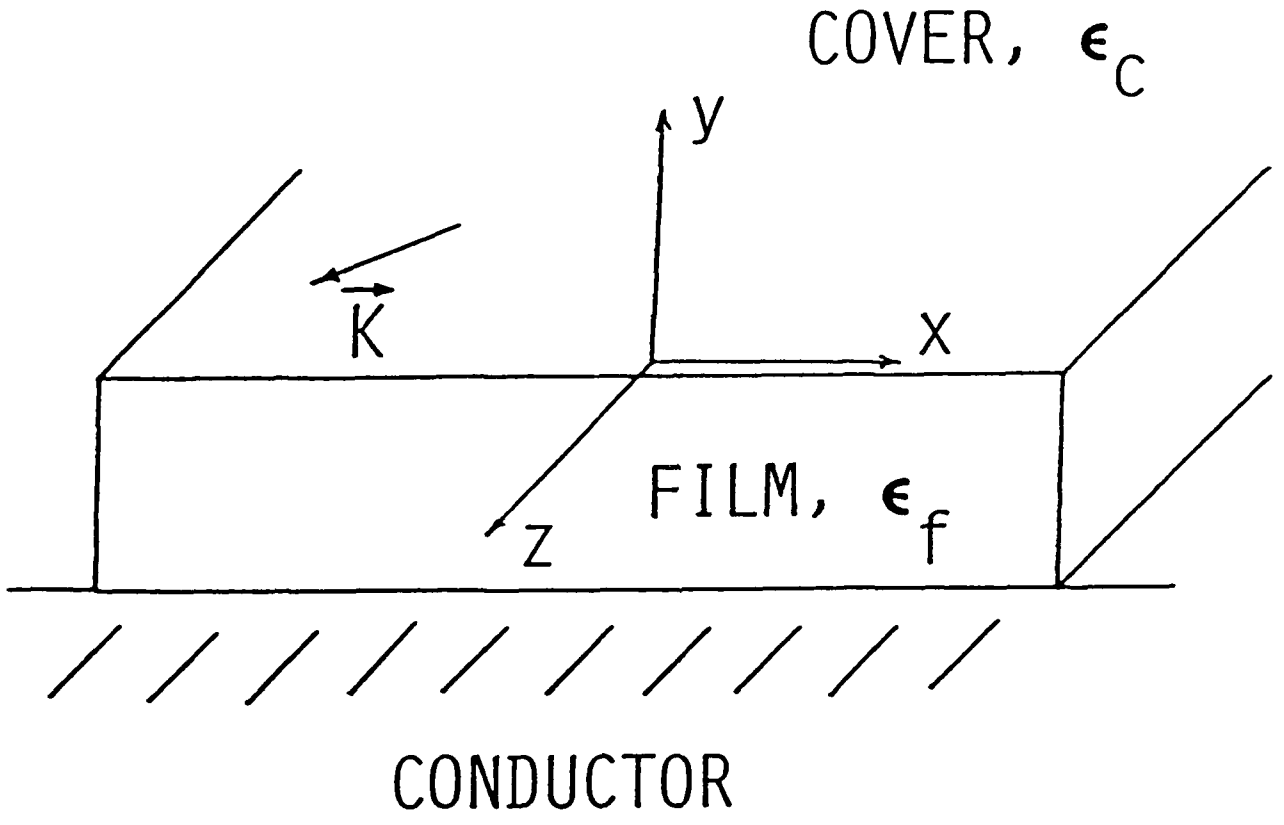

Figure 1. Configuration of Layered Media

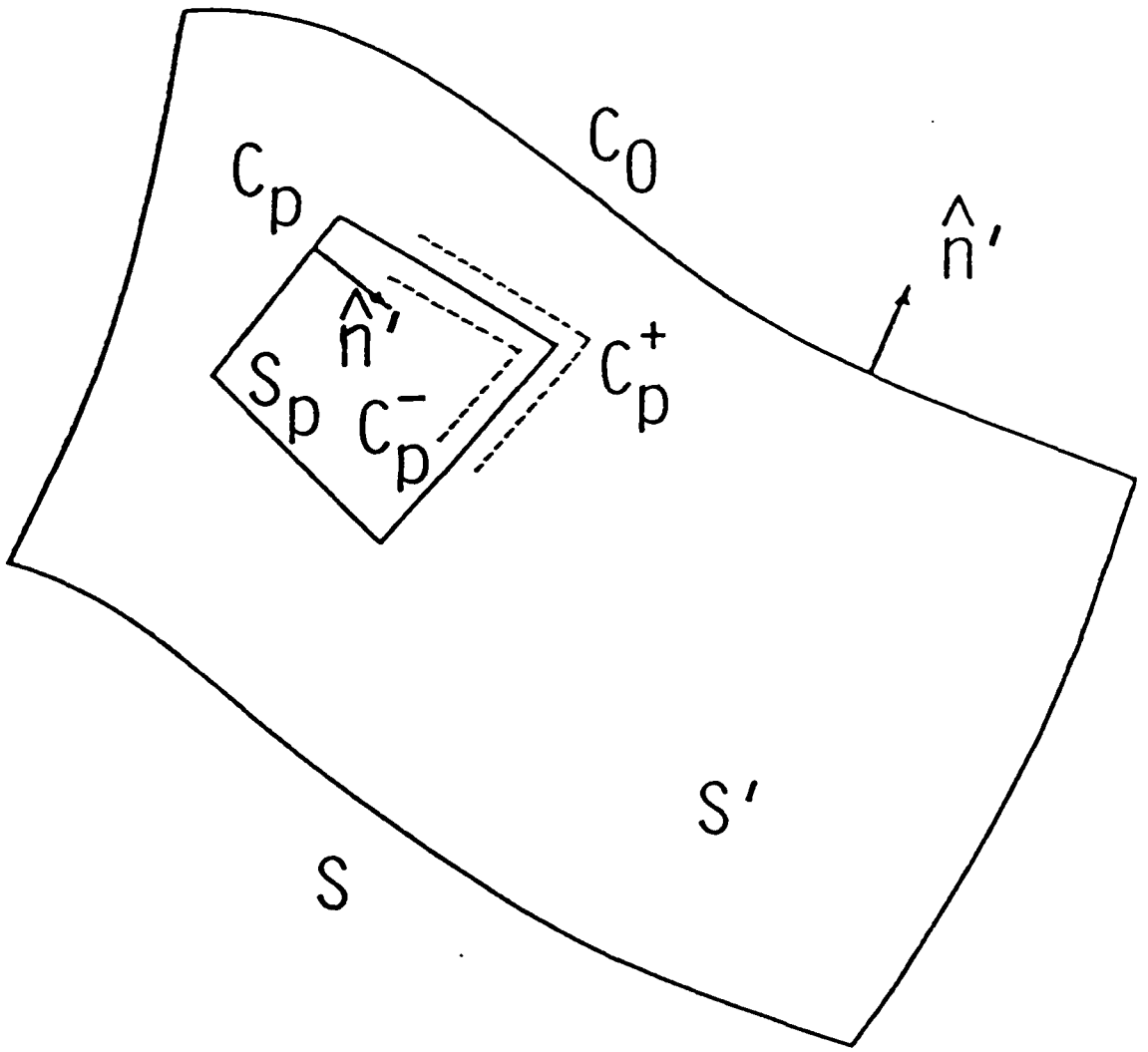

Figure 2. Geometry of Surface over which Currents Exist

4.2 Mathematical methods--analytical and numerical

Efforts on this topic were devoted to the formulation and computation of Sommerfeld-integral type representations for relevant Green's function kernels. Analytical/numerical methods to accomodate the slowly-convergent (and sometimes apparently divergent) behavior of those representations, arising when the source-point singularity is implicated, were developed. These initial preparatory investigations were necessary to acquire confidence in the construction, computation, and use of the dyadic kernels described in Section 4.1. Studies on the computation of Green's function kernels are reported in [1,8,12], while properties of the source-point singularity are addressed in [8].

Research Paper No. [1]

ACCURATE EVALUATION OF SOMMERFELD INTEGRALS USING THE FAST FOURIER TRANSFORM

B.C. Drachman
Department of Mathematics
D.P. Nyquist and M.J. Cloud
Department of Electrical Engineering and Systems Science
Michigan State University
East Lansing, MI 48824

Application of the conventional Hertzian-potential-based formulation of layered media electromagnetics necessitates evaluation of Sommerfeld-type integrals. An efficient and accurate method of computing these integrals is presented.

The Fast Fourier Transform (FFT) may be used in a straight-forward fashion to obtain accurate integrations of periodic functions. It is explained how, in these cases, the numerical integration method corresponds to the Corrected Trapezoidal rule (with error proportional to the fourth power of the step size). Attempts to use the FFT in such a fashion on aperiodic functions result in significant errors because, in these cases, the integration method corresponds to the Rectangular rule (error proportional to the first power of the step size). Thus it is often believed that the FFT is a quick but inaccurate way to compute an integral. When used in conjunction with Simpson's rule, however, the FFT gives extremely accurate results for aperiodic functions. An error analysis suggests a technique for integral truncation and choice of partition density. Examples are given in which this method is applied to the numerical evaluation of Sommerfeld integrals.

The method exploits the efficiency of the FFT algorithm, while deriving additional benefit from the fact that a single call of the FFT algorithm returns sample values of the Sommerfeld integral at many spatial locations. Moreover, this technique should be well adapted for use with the point-matching Galerkin's method of moments which requires values of the Sommerfeld integrals at a set of locations on a structure.

ON SOMMERFELD-INTEGRAL ELECTRIC FIELD KERNELS FOR MICROSTRIP-BASED CIRCUITS

D.P. Nyquist, M.S. Viola, M.J. Cloud and M. Havrilla
Department of Electrical Engineering
Michigan State University
East Lansing, MI 48824

Microstrip circuits are fabricated over the film/cover interface of a planar, layered conductor/film/cover surround environment. In an electric-field integral equation description of such circuits, the electric field tangential to metallic microstrip conductors, maintained by surface currents on those conductors, is required. A spectral approach through Hertz potentials leads to sommerfeld-type integral representations for required Green's function kernels.

Let the microstrip conductors reside at $y=0^+$, adjacent to the x-z film/cover interface plane. The field $e(x,\zeta)$ at the conductor surface, maintained by surface current $k(x,\zeta)$ on that conductor (both in the axial Fourier-transform domain; transform variable ζ), is then

$$e(x,\zeta) = \lim_{y\to 0^+} (k_c^2 + \tilde{\nabla}\tilde{\nabla}\cdot) \int_{cond} \bar{\bar{g}}_\zeta(x,y|x',0)\cdot k(x',\zeta)dx'$$

where $k_c = n_c k_0$ (n_c = cover index), $\tilde{\nabla} = \nabla_{xy} + \hat{z}j\zeta$ and $\bar{\bar{g}}_\zeta$ is a Hertz potential Green's dyad in Sommerfeld-integral representation. It is convenient to pass the spatial integral and the differential operator, in turn, through the spectral integral over ξ, since the former operations can all be performed in closed form. This procedure is valid provided the details (source-point singularity) are handled carefully and the $y\to 0^+$ limit is performed lastly. In much of the recent literature, the latter limit is exchanged with the spectral integral; this invalidates the differential-operator exchange and leads to a divergent spectral integration. Consequently, uncertainty has arisen in the choice of appropriate expansion and testing functions for use in MoM solutions to associated EFIE's.

In fact, pulse basis functions and point matching lead to convergent spectral integrals if the $y\to 0^+$ limit is performed appropriately. MoM matrix elements are represented by

$$I_{\alpha\beta} = \lim_{y\to 0^+} \int_0^\infty W_{\alpha\beta}(\xi) e^{-p_c y} \frac{\sin(\xi\delta)}{\xi} \begin{pmatrix}\sin\xi x_m \\ \cos\xi x_m\end{pmatrix}\begin{pmatrix}\sin\xi x_n \\ \cos\xi x_n\end{pmatrix} d\xi$$

where $W_{\alpha\beta}$ is a complicated function of ξ (carrying surface-wave poles of the surround) and $p_c = (\xi^2+\zeta^2-k_c^2)^{1/2}$. The most slowly convergent case is $\alpha=\beta=x$, where $W_{xx}(\xi) \propto \xi$ for large arguments, leading to an undamped oscillatory integrand when $y=0$. It is demonstrated, however, that the $y\to 0^+$ limit does indeed exist, and the convergence rates of the various $I_{\alpha\beta}$ are compared.

Research Paper No. [12]

Accurate Evaluation of Sommerfeld Integrals Using the Fast Fourier Transform

B. DRACHMAN*,**, M. CLOUD*, AND D. NYQUIST*

Abstract - Accurate numerical integration of Sommerfeld-type integrals by the Fast Fourier Transform algorithm is considered. Several examples illustrate in the process.

I. INTRODUCTION

The purpose of this note is to observe that the FFT combines naturally with Simpson's rule for Sommerfeld-type integral computation. Standard references, such as [1,2,3], discuss the FFT for periodic functions only; however, even relatively simple Sommerfeld integrals have aperiodic integrands.

A principal advantage of using the FFT is that a single subroutine call yields a set of sample values of an integral (i.e., the integral for various values of an integrand parameter). Such samples could be useful in

---

*This work partially supported by Office of Naval Research under Contract N0014-86-K-0609.

**Partially supported by DARPA.

B. Drachman is with the Department of Mathematics, M. Cloud and D. Nyquist are with the Department of Electrical Engineering, Michigan State University, East Lansing, Michigan 48824.

themselves; for example, the parameter might be a spatial coordinate variable in a moment method solution. In other applications Sommerfeld integrals represent Green's functions nested within other spatial integrals. Samples from the FFT might be useful in approximating the outer-nested integral.

II. SUMMARY OF NEWTON-COTES NUMERICAL INTEGRATION METHODS

To estimate an integral such as

$$I = \int_a^b f(t)dt \tag{1}$$

suppose [a,b] is partitioned into N subintervals $[t_i,t_{i+1}]$ with $t_i = a + hi$, $i = 0,1,2,\ldots,N-1$. The step size h is (b-a)/N. Table 1 summarizes several well-known integration rules, provided f(t) is sufficiently smooth. Note that η is some point in (a,b), and N is even for Simpson's rule. These rules are summarized here for reference in later sections.

III. NUMERICAL INTEGRATION WITH THE FFT

The FFT algorithm computes the discrete Fourier transform

$$S_{k+1} = \sum_{n=0}^{N-1} A_{n+1} \exp(j2\pi kn/N); \quad k = 0,1,2,\ldots,N-1 \tag{2}$$

of the sequence $A_1,\ldots,A_N$. This may be viewed as numerical integration to approximate

$$I(x) = \int_0^\infty g(t)\exp(jxt)dt \tag{3}$$

as follows. First, choose T sufficiently large so that the improper integral in (3) is adequately approximated by

$$I(x) = \int_0^T g(t)\exp(jxt)dt \qquad (4)$$

for x in the range of interest. Make a change of variables, transforming the interval of integration to $[0,2\pi]$:

$$I(x) = (T/2\pi) \int_0^{2\pi} g(tT/2\pi)\exp(jxtT/2\pi)dt \qquad (5)$$

Partition this new interval into N equal segments, each of width $2\pi/N$. The rectangular rule (see Table 1) then yields the approximation

$$I(x_k) = h \sum_{n=0}^{N-1} g(nh)\exp(j2\pi nk/N) \ , \qquad (6)$$

where $h = T/N$ and $x_k = 2\pi k/T$. Comparison of equations (1) and (6) shows $I(x_k) = hS_{k+1}$, where $A_{n+1} = g(nh)$. Therefore, the FFT is directly invoked for efficient computation of $I(x)$ by the rectangular rule.

The great accuracy found by those using the FFT for periodic functions is easily explained. Observe (see Table 1) that if $g(t)$ is periodic and sufficiently smooth on $[0,T]$, the rectangular and corrected trapezoidal rules are identical. Thus fourth-order accuracy is obtained. For aperiodic $g(t)$ the method does not correspond with corrected trapezoidal rule, but to rectangular rule, and is therefore accurate only to first-order.

For $g(t)$ aperiodic, better accuracy is obtained by weighting the integrand sample values $g(nh)$ prior to the FFT call. Reference to Table 1 shows that the simple procedure of letting $A_1 = g(0) + g(hN)$, $A_2 = 4g(h)$, $A_3 = 2g(2h)$, $A_4 = 4g(3h)$, ..., implements Simpson's rule within a factor

of h/3.

To demonstrate the consequences of this improvement, consider the following example: In order to compute the transform

$$g(x) = \frac{1}{\sqrt{2\pi}} \int_{-\infty}^{\infty} e^{-t^2/2}\, e^{jxt} dt$$

$$= \frac{2}{\sqrt{2\pi}} \text{Real} \int_{0}^{\infty} e^{-t^2/2}\, e^{jxt}\, dt$$

which we approximate by

$$\frac{2}{\sqrt{2\pi}} \int_{0}^{T} e^{-t^2/2}\, e^{jxt}\, dt$$

(Take the real part.) We choose $T = 4\pi$ and $N = 2^{10}$. The FFT computes $g(x_k)$ at 1024 sample points. To check accuracy, let $x_k = 1$. Then

$$\frac{2\pi k}{T} = 1, \qquad \frac{2\pi k}{4\pi} = 1 \quad \text{so} \quad k = 2.$$

Since by (2), $S_{k+1} = \sum_{i=0}^{N-1} A_{i+1}\, e^{2\pi jik/N}$,

S_3 corresponds to $g(x_2)$, that is $g(x_2) = \frac{\sqrt{2\pi}}{\pi} \frac{T}{N} S_3$.

Except for a constant factor, $e^{-t^2/2}$ is its own transform. Hence $g(1)$ should be $e^{-.5}$. Direct FFT with unweighted integrand sample values (i.e., rectangular rule) produces an answer correct to only one significant figure. The Simpson's rule scheme gives 13 digit accuracy using a CDC-750 computer and the FFT routine from the IMSL library.

For another example, suppose sample values of $K_0(x)$ are needed, where K_0 is the modified Bessel function of order 0, a Green's function for the Helmholtz wave equation. For example, the sample values might be needed to carry out a numerical integration involving $K_0(x)$ in another problem.

Although there are better methods for estimating $K_o(x)$, we use

$$K_o(x) = \frac{1}{2}\int_{-\infty}^{\infty} \frac{e^{jxt}}{(t^2+1)^{1/2}}\,dt \tag{7}$$

In order to make the integrand decay more quickly, use integration by parts four times and obtain

$$\frac{2}{3}x^4K_o = \int_{-\infty}^{\infty} \frac{8t^4-24t^2+3}{(t^2+1)^{9/2}}\,e^{jxt}\,dt \tag{8}$$

so

$$K_o(x) = \frac{3}{x^4}\int_{0}^{\infty} \frac{8t^4-24t^2+3}{(t^2+1)^{9/2}}\,e^{jxt}\,dt \tag{9}$$

with ∞ replaced by $T = 4\pi$ and $N = 1024$, a single FFT call with Simpson's rule returned values $K_o(1),\ldots,K_o(10)$ to 6 place accuracy.

IV. ERROR ANALYSIS

Two types of error are introduced in the previous computations: truncation and resolution errors. First, consider the truncation error. The error introduced by truncating an improper integral is bounded by proper choice of the stopping point T. Assuming g(t) decays monotonically for large t, the truncation error is an alternating series due to the oscillation of g(t)exp(jxt). Approximation of an alternating series $\sum_{i=1}^{\infty}(-1)^i a_i$, a_i positive, monotonically converging to 0, by the nth partial sum $\sum_{i=1}^{n}(-1)^i a_i$ causes an error bounded by a_{n+1}. Choose T sufficiently large so that the area enclosed by one of the half-oscillations is negligible compared to the estimated integral.

We now discuss why incorporating Simpson's rule into the FFT gives dramatic improvement in our examples. This effect is not obvious, as can be seen in the following case: if, in equation (1), $f(t)$ is a highly oscillatory function such as $\sin(At)$ with $A \gg 1$, the derivatives increase in magnitude, and the error bounds in Table 1 may actually increase with higher-order integration methods. For example, if $h = 1$ and $A > 12$ the error bound in trapezoidal rule is larger than in rectangular rule.

However, in our examples the integrals are of the form of equation (4), where $g(t)$ is slowly varying in the sense that its derivatives all have same order magnitude (all bounded by M, say) on the interval $[0,T]$.

Suppose $I(x_k)$ is desired for equally-spaced points $x_0 = 0, x_1, x_2, \ldots, x_S = \beta$. First choose T sufficiently large so that $I(x_k)$ is a good approximation to the original improper integral for all x_k in $[0,\beta]$, and each x_k is included in the set $\{2\pi k/T;\ k = 0,1,2,\ldots,N-1\}$. For example, suppose $T = 4\pi$ and $I(0), I(1), \ldots, I(10)$ are desired. Our first choice of N is to make N a power of 2 such that $(N/2) > 2\pi k_{max}$, where $x_{max} = 2\pi k_{max}/T = \beta = 10$ (see the Nyquist Criterion [4]). In this case $k_{max} = 20$, and $N = 256$ becomes the first choice.

Letting E_1 denote the error bound given by Table 1 for rectangular rule applied to equation (4), we have

$$E_1 < |(T^2/2)[j(x/N)g(c) + (1/N)g'(c)]| \qquad (10)$$

where $0 < c < T$. For Simpson's rule, the error bound is

$$E_4 < |(T/N)^4(T/180)(g^{iv}(c) + 4jxg'''(c) + 6(jx)^2g''(c) + 4(jx)^3g'(c) + (jx)^4g(c))| \ . \qquad (11)$$

Assuming that g and the various derivatives of g are all bounded by M,

$$E_1 < (T/N)(T/2)M[x + 1] \tag{12}$$

$$E_4 < (T/N)^4(T/180)M[1 + 4x + 6x^2 + 4x^3 + x^4] \tag{13}$$

Consider first the case for which $0 < x \leq 1$. Then

$$E_1 \leq ThM \tag{14}$$

$$E_4 < Th^4M(16/180) < E_1 \quad \text{for} \quad h = (T/N) < 1 \tag{15}$$

Otherwise, when $x > 1$

$$E_1 < MT(xT/N) < MT(1/2) \tag{16}$$

$$\begin{aligned} E_4 &< (T/180)(T/N)^4M[1 + 4x + 6x^2 + 4x^3 + x^4] \\ &< (MT/180)[(6)(5)x^4(T/N)^4] < MT(1/2)^4/60 < E_1 \end{aligned} \tag{17}$$

since $(xT/N) < (1/2)$.

For this first choice of N we therefore expect more accuracy from Simpson's rule. In actual practice, however, the choice of N is determined as is commonly done, by doubling the number of partitions N (each step reusing previously computed quantities) until convergence is obtained in a Rhomberg scheme. In this process, each time N is doubled the ratio (xT/N) is halved, hence the inequality $E_4 < E_1$ in (17) is strengthened.

A single call to FFT provides values for the next iteration in Rhomberg's method [4] simultaneously for all sample points $\{x_k\}$. In this way, a

"parallel-processing" numerical integration algorithm is achieved on a serial computer via the FFT.

V. APPLICATION

As an example relevant to electromagnetics, suppose that the Sommerfeld-type integral

$$I(x,y,g) = \int_{-\infty}^{\infty} \frac{\exp(jxt)\exp(-p|y|)dt}{2p} \qquad (18)$$

where $p^2 = t^2 + g^2$, is required at $2M$ evenly-spaced values $x_k \in [0,2W]$. Let $T = (2\pi M)L$, where L is an integer large enough for adequate approximation. Taking the real part of the integral allows replacement of the lower limit by zero. By its definition,

$$x_k = 2\pi k/T = k/LM; \quad k = 0,1,2,\ldots,N-1 \; . \qquad (19)$$

Choose N for desired resolution, and recover every L'th evaluation by the FFT.

Results from this technique are identical to those obtained by other methods; moreover, the FFT/Simpson's rule combination is much faster since a single call to FFT returns the required sequence of integrals for the set $\{x_k\}$. This example is closely related to the last example.

VI. CONCLUSION

Numerical integration for aperiodic functions with the FFT is greatly improved by the concurrent use of Simpson's rule. Some algorithms that

already make use of the FFT could benefit from this slight modification. It also appears to be a promising technique for the evaluation of Sommerfeld-type integrals.

REFERENCES

[1] E.O. Brigham, The Fast Fourier Transform, Englewood Cliffs: Prentice-Hall, 1974.

[2] A. Papoulis, Signal Analysis, New York: McGraw-Hill, 1977.

[3] J.W. Cooley and J.W. Tukey, "An algorithm for Machine Calculation of Complex Fourier Series," Math. Computation, Vol. 19, pp. 297-301, Apr. 1965.

[4] S.D. Conte and C. de Boor, Elementary Numerical Analysis, 3rd Ed., New York: McGraw-Hill, 1980.

Integration Rule	Error
1. $h \sum_{i=0}^{N-1} f(t_i)$	$h(b-a)f'(\eta)/2$
2. $h \left[\frac{f(a) + f(b)}{2} + \sum_{i=1}^{N-1} f(t_i) \right]$	$-h^2(b-a)f''(\eta)/12$
3. $h \left[\frac{f(a) + f(b)}{2} + \sum_{i=1}^{N-1} f(t_i) \right] + \frac{h^2}{12} [f'(a) - f'(b)]$	$h^4(b-a)f^{(iv)}(\eta)/720$
4. $\frac{h}{3} [f(a) + 4f(t_1) + 2f(t_2) + \ldots + f(b)]$	$-h^4(b-a)f^{(iv)}(\eta)/180$

TABLE 1

Numerical integration methods. The rule names are: (1) rectangular, (2) trapezoidal, (3) corrected trapezoidal, and (4) Simpson's.

4.3 EM interactions among integrated microstrip devices

This research topic includes the scattering of microstrip waves by integrated devices and the large-scale interactions among such devices. Interactions in the MMIC environment have been conceptualized through an EFIE description of the microstrip/device system, based upon the electric dyadic kernels exposed in Section 4.1. The general electromagnetic formulation for such interactions is presented in [16].

Coupling among microstrip devices can be studied through a perturbation solution which exploits currents supported by isolated system components. Significant scattering of microstrip waves is anticipated only when they interact with near-resonant devices. The quasi-closed-form Chebychev series representations for microstrip line and device currents detailed in Sections 4.5-4.6 permits the quantification of scattering coefficients based upon such a perturbation formulation.

The description of microstrip-based circuits by integral-operator equations which exploit the electric Green's dyad kernels leads to a number of general properties and phenomena associated with such circuits. An excitation theory for discrete microstrip line and cavity modes is obtained, which yields the excitation amplitudes as overlap integrals of impressed currents with the modal fields of those devices. A coupled-mode perturbation theory for propagation constant or resonant frequency shifts due to coupling among systems of multiple microstrip lines or cavities is developed, again based upon the integral-operator description of the sysyem. Research paper [16] exposes all these results.

Large-scale interactions among systems of microstrip devices can be quantified by the methods and approximations described in [16]. The research topics of Sections 4.4-4.6 are, in fact, specializations of such interactions, consequently [16] again provides the electromagnetic foundation for the study of those topics.

DEDUCTION OF EM PHENOMENA IN MICROSTRIP CIRCUITS FROM AN INTEGRAL-OPERATOR DESCRIPTION OF THE SYSTEM

Dennis Paul Nyquist

Department of Electrical Engineering, Michigan State University, East Lansing, Michigan, USA 48824

Abstract

An electric-field integral equation (EFIE) description of microstrip-based circuits permits the relatively general deduction of EM phenomena which influence the behavior of those circuits. Prior efforts by many researchers have used the EFIE formulation to study specific microstrip devices. The present research exploits an EFIE description to study more broadly the EM phenomena and interactions in microstrip circuits. Included are the following topics: 1) identification of the complete propagation-mode spectrum for microstrip from a singularity expansion of its current, including an excitation theory for discrete modes; 2) excitation of patch-device resonances, which arise from temporal pole singularities; and 3) formulation of a coupled-mode perturbation theory leading to propagation constant and resonant frequency shifts due to coupling among microstrip lines and patch resonators.

1. Introduction

An integral-operator formulation is presented for electromagnetic interactions in microstrip-based electronic circuits. It is a full-wave formulation based upon the electric dyadic Green's function for currents immersed in the layered integrated electronics environment. Full-wave integral equation methods have been used extensively for the study of specific microstrip devices. A survey of such methods applied to the study of discrete microstrip propagation modes is included in [1], while a similar treatment for microstrip patch antennas is exposed in [2]. The present research attempts to deduce more broadly those EM phenpmena which influence the behavior of microstrip circuits from an electric-field integral equation description of the circuit system.

2. EFIE Description of Microstrip Circuits

The microstrip circuit configuration consists of conducting circuit devices embedded in the cover layer adjacent to the film/cover interface of a tri-layered conductor/film/cover environment. A dielectric film layer of thickness t and refractive index n_f occupies $-t<y<0$ between a perfect conductor in $y<-t$ and a dielectric cover of index n_c in $y>0$. Circuit components, of generally non-vanishing thickness, are consequently located in $y\geq 0$, where the y axis is normal and the x,z axes tangential to the film/cover interface. Total circuit surface S is composed of N components, where the component contributed by the n'th circuit element is S_n. Fig. 1 depicts the circuit configuration in cross section, and indicates a general pair of device elements.

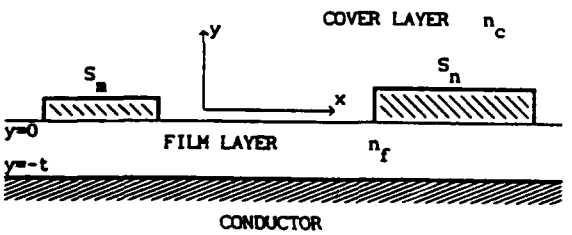

Figure 1. Configuration of microstrip-based electronic circuit.

Impressed current $\vec{J}^i$ maintains impressed electric field $\vec{E}^i$, which excites surface current $\vec{K}$ on the conducting circuit system. Induced current $\vec{K}$ maintains a scattered field $\vec{E}^s$. The boundary condition for tangential $\vec{E}$ at the circuit surface requires $\hat{t}\cdot(\vec{E}^i+\vec{E}^s)=0$, where $\hat{t}$ is a unit tangent vector at any point on that surface. Expressing $\vec{E}^s$ in terms of electric dyadic Green's function $\overline{G}^e$ for the layered environment leads to the electric-field integral equation (EFIE) for $\vec{K}$ induced on the circuit

$$\hat{t}\cdot\int_S \overline{G}^e(\vec{r}|\vec{r}')\cdot\vec{K}(\vec{r}')dS' = -\frac{jk_c}{\eta_c}\vec{E}^i(\vec{r}) \qquad (1)$$

for all $\vec{r}\in S$, where $k_c=n_c k_0$ and $\eta_c=\eta_0/n_c$ with k_0,η_0 the free-space wavenumber and impedance.

The electric Green's dyad [3,4] can be expressed as $\overline{G}^e(\vec{r}|\vec{r}') = PV(k_c^2+\nabla\nabla\cdot)\overline{G}(\vec{r}|\vec{r}') + \overline{L}\delta(\vec{r}-\vec{r}')$ where $\overline{G}$ is a Hertzian potential Green's dyad. Notation PV indicates that $\overline{G}^e$ should be integrated in a principal value sense [5] by excluding an innate "slice" principal volume [6] to accomodate the source-point singularity at y=y', and $\overline{L}=-\hat{y}\hat{y}$ is an associated depolarizing dyad. The Hertz potential Green's dyad is expressed as $\overline{G}=\overline{I}G^p+\overline{G}^r$, where G^p yields the principal wave excited by $\vec{K}$ in an unbounded cover and

$$\overline{G}^r(\vec{r}|\vec{r}') = \hat{x}G_t^r\hat{x} + \hat{y}\left(\frac{\partial G_c^r}{\partial x}\hat{x} + G_n^r\hat{y} + \frac{\partial G_c^r}{\partial z}\hat{z}\right) + \hat{z}G_t^r\hat{z}$$

yields the reflected wave scattered by the layered environment. G_t^r yields potential components tangential to the film/cover interface, while G_n^r yields normal potential due to normal current and G_c^r couples tangential current to normal potential. Reciprocity of the electric Green's dyad leads to $G^e_{\alpha\beta}(\vec{r}|\vec{r}') = G^e_{\beta\alpha}(\vec{r}'|\vec{r})$.

The several dyad components have Sommerfeld integral representations

$$G^p(\vec{r}|\vec{r}') = \iint_{-\infty}^{\infty}\frac{e^{j\vec{\lambda}\cdot(\vec{r}-\vec{r}')}e^{-p_c|y-y'|}}{2(2\pi)^2 p_c}d^2\lambda$$

$$\begin{Bmatrix} G_t^r(\vec{r}|\vec{r}') \\ G_n^r(\vec{r}|\vec{r}') \\ G_c^r(\vec{r}|\vec{r}') \end{Bmatrix} = \iint_{-\infty}^{\infty}\begin{Bmatrix} R_t(\lambda) \\ R_n(\lambda) \\ C(\lambda) \end{Bmatrix}\frac{e^{j\vec{\lambda}\cdot(\vec{r}-\vec{r}')}e^{-p_c(y+y')}}{2(2\pi)^2 p_c}d^2\lambda$$

where $\vec{\lambda} = \hat{x}\xi+\hat{z}\zeta$, $\lambda^2 = \xi^2+\zeta^2$, and $d^2\lambda = d\xi d\zeta$. Wavenumber parameters are $p_\ell = (\lambda^2-n_\ell^2k_0^2)^{1/2}$; $\Re e(p_\ell)>0$ for $\ell = f,c$. Reflection and coupling coefficients are

$$R_t = \frac{A_t(\lambda)}{Z^h(\lambda)}, \qquad R_n = \frac{A_n(\lambda)}{Z^e(\lambda)}, \qquad C = \frac{2(N_{fc}^2-1)p_c}{Z^h(\lambda)Z^e(\lambda)}$$

with

$$\left.\begin{aligned} A_t &= p_c - p_f\coth(p_f t) \\ Z^h &= p_c + p_f\coth(p_f t) \end{aligned}\right\} \qquad \left.\begin{aligned} A_n &= N_{fc}^2p_c - p_f\tanh(p_f t) \\ Z^e &= N_{fc}^2p_c + p_f\tanh(p_f t) \end{aligned}\right\}$$

where contrast factor $N_{fc} = n_f/n_c$, and $Z^{h,e} = 0$ is associated with TE and TM surface-wave poles, respectively, of the layered surround environment.

3. Propagation-Mode Spectrum of Microstrip

The microstrip line configuration is that specialization of Fig. 1 where the conducting elements have infinite extent along the waveguiding z-axis. Infinite axial symmetry renders the integral operator in EFIE (1) convolutional in the axial variable, and Fourier transformation on that variable is consequently prompted. Transform-domain quantities are denoted by lower-case letters such that $\mathcal{F}_z\{\vec{f}(\vec{\rho},z)\} = \vec{f}(\vec{\rho},\zeta)$ for all such quantities, where $\vec{\rho} = \hat{x}x+\hat{z}z$ is the 2-D transverse position vector and ζ is the transform variable corresponding to z. Subsequent to application of the convolution theorem, EFIE (1) becomes

$$\hat{t}\cdot\int_C \bar{\bar{g}}^e(\vec{\rho}|\vec{\rho}';\zeta)\cdot\vec{k}(\vec{\rho}',\zeta)d\ell' = -\frac{jk_c}{\eta_c}\vec{e}^i(\vec{\rho},\zeta) \qquad (2)$$

for all $\vec{\rho}\in C$, where C is the boundary contour about the microstrip conductor in the transverse plane. Green's dyad $\bar{\bar{g}}^e(\vec{\rho}|\vec{\rho}';\zeta) = PV(k_c^2+\bar{\bar{\nabla}}\bar{\bar{\nabla}}\cdot)\bar{\bar{g}}(\rho|\rho';\zeta) + \bar{\bar{I}}\delta(\rho-\rho')$ where $\bar{\bar{\nabla}} = \nabla_t+\hat{z}j\zeta$ with ∇_t the transverse operator and $\bar{\bar{g}}(\vec{\rho}|\vec{\rho}';\zeta) = \mathcal{F}_z\{\bar{\bar{G}}(\vec{\rho}|\vec{\rho}';z)\}$. The transform-domain electric Green's dyad has the useful reciprocal property $g^e_{\alpha\beta}(\vec{\rho}|\vec{\rho}';\zeta) = g^e_{\beta\alpha}(\vec{\rho}'|\vec{\rho};-\zeta)$.

Discrete propagation modes correspond to pole singularities of $\vec{k}(\vec{\rho},\zeta)$ at $\zeta=\mp\zeta_p$, near which

$$\vec{k}(\vec{\rho},\zeta) \approx a_p^\pm\vec{k}_p^\pm(\vec{\rho})/(\zeta\pm\zeta_p)^\ell \qquad (3)$$

where $\vec{k}_p^\pm$ is the eigenmode current of a wave propagating in the $\pm z$ direction. It is demonstrated in Sec. 4 that $\ell=1$, so the poles are simple. If representation (3) for $\zeta\approx\mp\zeta_p$ is exploited in EFIE (2) then, since $\vec{e}^i(\vec{\rho},\zeta)$ is regular at $\mp\zeta_p$, $\vec{k}_p^\pm$ must satisfy the homogeneous EFIE

$$\hat{t}\cdot\int_C \bar{\bar{g}}^e(\vec{\rho}|\vec{\rho}';\zeta)\cdot\vec{k}_p^\pm(\vec{\rho}') = 0 \ \ldots \text{ for all } \vec{\rho}\in C \qquad (4)$$

with non-trivial solutions only for $\zeta=\mp\zeta_p$. The discrete propagation modes are consequently described by EFIE (4).

The discrete propagation modes corresponding to simple-pole singularities of $\vec{k}(\vec{\rho},\zeta)$ constitute one contribution to the singularity expansion of that current. Square root branch-point singularities in the integral representation of $\bar{\bar{g}}^e$ lead to similar singularities in $\bar{\bar{g}}^e$ and $\vec{k}$, with associated branch cuts in the complex ζ-plane. If the real-line inversion integral is deformed into the upper|lower half ζ-plane for $z>z'|z<z'$, then the space-domain current becomes

$$\vec{k}(\vec{\rho},z) = \pm j\sum_p a_p^\pm\vec{k}_p^\pm(\vec{\rho})e^{\mp j\zeta_p z} - \frac{1}{2\pi}\int_{C_b^\pm}\vec{k}(\vec{\rho},\zeta)e^{j\zeta z}d\zeta \qquad (5)$$

where the sum of discrete modes is contributed by pole singularities and the continuous-spectrum contribution arises from deforming the integration path about the branch cuts along $C_b^\pm$. The continuous spectrum current $\vec{k}(\vec{\rho},\zeta)$ is consequently identified as the forced solution to EFIE (2) for points ζ along $C_b^\pm$. A discrete-mode excitation theory for amplitudes $a_p^\pm$ is exposed in the next section.

4. Excitation and Coupling of Microstrip Lines

The amplitude coefficients $a_p^\pm$ and pole order ℓ in representation (3) are established here. If the reciprocal property of $\bar{\bar{g}}^e$ is exploited subsequent to applying the testing operator (which implements the $\hat{t}\cdot$ operation)

$$\lim_{\zeta\to\mp\zeta_p}\int_C d\ell\ \vec{k}_p^\mp(\vec{\rho})\cdot(\text{——})$$

to EFIE (2), then expansion of $\bar{\bar{g}}^e$ in a Taylor's series about $\mp\zeta_p$ is prompted. Invoking defining EFIE (4) for $\vec{k}_p^\pm$ leads to vanishing of the contribution from the first term of that expansion. The leading non-vanishing term is consequently the first-order contribution proportional to $(\zeta\pm\zeta_p)$. When representation (3) for $\vec{k}$ is used in the resulting operator equation, it is clear that the leading term can annul at most a first-order pole; it is thus established that $\ell=1$.

If reciprocity of $\bar{\bar{g}}^e$ is invoked again, and only leading terms are retained, propagation-mode amplitudes excited by $\vec{e}^i$ are obtained as

$$a_p^\pm = \mp\frac{jk_c}{\eta_c}\int_C\vec{k}_p^\pm(\vec{\rho})\cdot\vec{e}^i(\vec{\rho},\mp\zeta_p)d\ell \qquad (6)$$

where $\vec{k}_p$ satisfies the normalization constraint

$$C_p^\pm = \int_C d\ell\int_C d\ell'\vec{k}_p^\mp(\vec{\rho})\cdot\frac{\partial\bar{\bar{g}}^e(\vec{\rho}|\vec{\rho}';\zeta)}{\partial\zeta}\bigg|_{\mp\zeta_p}\cdot\vec{k}_p^\pm(\vec{\rho}') = \pm 1 \qquad (7)$$

Coupling coefficient (6) is an overlap integral of the impressed field with the discrete eigenmode current. If $\vec{e}^i$ maintained by $\vec{j}^i$ is expressed in terms of $\bar{\bar{g}}^e$, and the reciprocity of $\bar{\bar{g}}^e$ is subsequently exploited, then an alternative coupling coefficient involving the overlap integral of $\vec{j}^i$ and $\vec{e}_p^\pm$ is obtained. Using the latter excitation amplitudes in expression (5) leads to the discrete-mode current

$$\vec{k}_d(\vec{r}) = -\frac{k_c}{\eta_c}\sum_p\vec{k}_p^\pm(\vec{\rho})\int_{V'}\vec{j}^i(\vec{r}')\cdot\vec{e}_p^\pm(\vec{\rho}')e^{-j\zeta_p|z-z'|}dv'$$
$$\ldots \text{ for } (z-z')\approx\pm. \qquad (8)$$

The discrete system eigenmode currents supported by N coupled microstrip lines again correspond to simple-pole ζ-plane singularities, and satisfy the coupled system of homogeneous EFIE's

$$\hat{t}_m\cdot\sum_{n=1}^N\int_{C_n}\bar{\bar{g}}^e(\vec{\rho}|\vec{\rho}';\zeta)\cdot\vec{k}_{np}^\pm(\vec{\rho}')d\ell' = 0 \ \ldots \text{ all } \vec{\rho}\in C_m,$$
$$\cdot \text{ for } m=1,2,\ldots,N \qquad (9)$$

with non-trivial solutions for $\zeta=\mp\zeta_p$. For nearly-

degenerate coupling, the system-mode ζ_p is near to all the $\zeta_{np}^{(0)}$ associated with eigenmode currents $k_{np}^{\pm(0)}$ of the individual isolated microstrip. If reciprocity of $\overline{\overline{G}}^e$ is exploited subsequent to application of the operator

$$\int_{C_m} d\ell\, \vec{k}_{mp}^{\mp(0)}(\vec{\rho})\cdot(\text{——}) \ \ldots \text{ for } m=1,2,\ldots,N$$

to EFIE's (9), then expansion of $\overline{\overline{G}}^e$ in a Taylor's series about $\zeta=\mp\zeta_{np}^{(0)}$ is prompted. The leading-term contribution vanishes for m=n by virtue of the defining EFIE for $\vec{k}_{np}^{\pm(0)}$, while the first-order term annuls the simple poles of $\vec{k}(\vec{\rho},\zeta)$. Retaining only the leading non-vanishing terms, subsequent to the perturbation approximation $\vec{k}_{np}^{\pm} \cong a_n^{\pm}\vec{k}_{np}^{\pm(0)}$, leads to the homogeneous system of algebraic equations

$$a_m^{\pm}\bar{C}_{mm}^{\pm}[\zeta\pm\zeta_{mp}^{(0)}] + \sum_{n\neq m} C_{mn}^{\pm}a_n^{\pm} \cong 0 \ \ldots \ m=1,2,\ldots,N \quad (10)$$

with non-trivial solution only when $\det[\zeta] \cong 0$. Coupling coefficients are given by overlap integrals of the m'th strip current with the n'th strip field as

$$C_{mn}^{\pm} = \frac{jk_c}{\eta_c}\int_{C_m} \vec{k}_{mp}^{\mp(0)}(\vec{\rho})\cdot\vec{e}_{np}^{\pm(0)}(\vec{\rho})\,d\ell \quad (11)$$

while normalization coefficients $\bar{C}_{mm}^{\pm}$ are given by expression (7) applied to isolated eigenmode currents $\vec{k}_{mp}^{\mp(0)}$ on the m'th strip.

For nearly degenerate coupling of two microstrip, the perturbation approximation to system-mode propagation eigenvalues leads to $\zeta = \bar{\zeta}\pm\delta$. $\bar{\zeta} = (\zeta_1+\zeta_2)/2$ is the average of isolated phase constants and $\delta = (\Delta^2+K^2)^{1/2}$ where $\Delta = (\zeta_1-\zeta_2)/2$ and $K^2 = C_{12}C_{21}$ with normalization $\bar{C}_{mm}^{+}=1$.

5. Excitation and Coupling of Patch Resonators

Currents excited on a resonant patch device by impressed radiation satisfy EFIE (1), where S is descriptive of a single patch or a coupled system of such resonant devices. Resonant currents are associated with pole singularities at $\omega=\omega_p$ in the temporal frequency domain, such that

$$\vec{k}(\vec{r},\omega) \cong a_p(\omega)\vec{k}_p(\vec{r})/(\omega-\omega_p)^{\ell} \ \ldots \ \omega \text{ near } \omega_p \quad (12)$$

where $\vec{k}_p(\vec{r})$ is the normalized resonant eigencurrent. Subsequent to using representation (12) in EFIE (1), and recognizing that $\vec{E}^{i}$ is regular at ω_p, it is evident that $\vec{k}_p$ must satisfy the homogeneous EFIE

$$\hat{t}\cdot\int_S \overline{\overline{G}}^e(\vec{r}|\vec{r}';\omega)\cdot\vec{k}_p(\vec{r}')\,dS' = 0 \ \ldots \text{ all } \vec{r}\in S \quad (13)$$

with non-trivial solution only for $\omega=\omega_p$. Equation (13) defines the resonant patch eigenmode.

If reciprocity of $\overline{\overline{G}}^e$ is exploited subsequent to application of the operator $\int_S dS\,\vec{k}_p(\vec{r}')\cdot(\text{——})$ to EFIE (1), then expansion of $\overline{\overline{G}}^e$ in a Taylor's series about $\omega=\omega_p$ is prompted. The first term of the resulting expression vanishes by virtue of definition (13) for $\vec{k}_p$, so the leading non-vanishing term is linear in $(\omega-\omega_p)$; it can annul at most a simple pole, which establishes $\ell=1$. If representation (12) is used in the resulting expression, and reciprocity is again invoked, then the excitation amplitude is obtained as the overlap integral

$$a_p(\omega) = -\frac{jk_c}{\eta_c C_p}\int_S \vec{k}_p(\vec{r})\cdot\vec{E}^{i}(\vec{r},\omega)\,dS \quad (14)$$

where normalization constant C_p is

$$C_p = \int_S dS\,\vec{k}_p(\vec{r})\cdot\int_S \frac{\partial\overline{\overline{G}}^e(\vec{r}|\vec{r}';\omega)}{\partial\omega}\bigg|_{\omega_p}\cdot\vec{k}_p(\vec{r}')\,dS'. \quad (15)$$

An EFIE-based coupled-mode perturbation theory for a nearly-degenerate coupled system of N resonant devices is based upon the coupled system (13) of IE's. A procedure analogous to that which lead to (10) above yields the algebraic equations

$$[\omega-\omega_p^{(0)}]a_m + \sum_{n\neq m} C_{mn}a_n \cong 0 \ \ldots \text{ for } m=1,2,\ldots,N \quad (16)$$

which yields the system-mode resonance frequency as the solution to $\det[\omega] \cong 0$, where $\omega_p^{(0)}$ are the isolated resonant frequencies. Coupling coefficients are given by the overlap integral of isolated currents and fields

$$C_{mn} = \frac{jk_c}{\eta_c}\int_{S_m} \vec{k}_{mp}^{(0)}(\vec{r})\cdot\vec{E}_{np}^{(0)}(\vec{r})\,dS \quad (17)$$

where currents are normalized by equating coefficients similar to (15) to unity.

6. Concluding Remarks

Several general properties of EM phenomena in microstrip-based circuits have been deduced from an integral-operator description of the circuit system. The complete propagation-mode spectrum of a microstrip line was identified from a singularity expansion of its current. It is believed that this is the first such treatment of the continuous spectrum. An excitation theory for discrete modes along isolated microstrip and a coupled-mode perturbation theory for nearly-degenerate coupling among any number of microstrip were exposed. Patch device resonances were identified with temporal pole singularities, while excitation and perturbation coupling theories for such resonant elements were advanced. Typical numerical results will be included in the oral exposition of the paper.

7. References

[1] N. Fache and D. DeZutter, "Rigorous full-wave space-domain solution for dispersive microstrip lines," IEEE MTT-S Trans. 36(4) 731-737, April 1988.

[2] W. C. Chew and Q. Liu, "Resonance frequency of a rectangular microstrip patch," IEEE AP-S Trans. 36(8) 1045-1056, Aug. 1988.

[3] J. S. Bagby, D. P. Nyquist, and B. C. Drachman, "Integral formulation for analysis of integrated dielectric waveguides," IEEE MTT-S Trans. 33(10) 906-915, Oct. 1985.

[4] J. S. Bagby and D. P. Nyquist, "Dyadic Green's functions for integrated electronic and optical circuits," IEEE MTT-S Trans. 35(2) 206-210, Feb. 1987.

[5] A. D. Yaghjian, "Electric dyadic Green's function in the source region," Proc. IEEE 68(2) 248-263, Feb. 1980.

[6] M. S. Viola and D. P. Nyquist, "An observation on the Sommerfeld integral representation of the electric dyadic Green's function for layered media," IEEE MTT-S Trans. 36(8) 1289-1292, August 1988.

4.4 Propagation-mode spectrum of microstrip guiding structures

Research on the complete propagation-mode spectrum of microstrip guiding structures exploits a transform-domain integral-operator description of the structure and is based upon a singularity expansion of the microstrip current [16]. It includes an excitation theory for discrete and continuous spectral components. Discrete propagation modes correspond to pole singularities in the complex transform plane, while the continuous spectrum arises from integration about branch cuts associated with branch-point singularities of the Green's dyad kernels [2,5,7,16].

The discrete-mode quantification has been generalized [13,15] to include the possibility of a ferrimagnetic thin-film layer. This study is based upon a transform-domain EFIE description for current induced on the microstrip; the dyadic Green's function kernel described above is exploited. The discrete (principal, and several higher-order) modes are now quite well understood. A new Chebychev-Galerkin's MoM numerical solution has been implemented using Chebychev polynomials, modulated by appropriate square-root edge-condition factors, for expansion and testing of the transverse dependence of unknown eigenmode currents (both longitudinal and transverse).

Results indicate that the transverse current component is negligible for the principal discrete eigenmode, but becomes important in the higher-order modes. This method provides a rapidly convergent quasi-closed-form solution for the eigenmode currents, since analytical expressions for the current components are available subsequent to numerical quantification of expansion coefficients in the Chebychev series. Convergence is so rapid that two terms suffice for the principal mode, and at most four need be retained for even the second higher-order mode. It was found that coupling to surface-wave modes of the layered surround, and consequent leakage phenomena, is unlikely to occur for practical configurations with dielectric thin-film layers. Presence of a ferrimagnetic film layer may alter this conclusion, however, and numerical studies remain to be completed. The quasi-closed-form solutions for discrete eigenmode currents are particularly suitable for application in perturbation-type studies of their coupling with adjacent devices and other nearby microstrip lines. Extensive numerical results are presented in connection with the formulation for coupled microstrip lines exposed in Section 4.5.

Radiation fields of the continuous spectrum have been conceptually iden-

tified as forced solutions to the EFIE's at points along transform-plane branch cuts. Their numerical quantification has been ititiated through a MoM formulation [7] for the forced microstrip currents. Additional research on potentially efficient approximate iterative solutions remains to be completed. The radiation field is required for any serious investigation of scattering by discontinuities along open microstrip in MMIC's. Since no suitable representation of the radiation field in microstrip-based circuits is presently available, this topic constitutes one of the major unsolved problems in the theory of such circuits. It is conjectured that a suitable formulation can be obtained based upon the integral-operator description of microstrip, since that full-wave theory at least provides for a conceptual definition of the radiation field and its spectrum [7,16].

Research papers [2,5,7] follow on the subsequent pages, while papers [13,15] were included in Section 4.1 and paper [16] was appended to Section 4.3.

RADIATIVE AND SURFACE WAVE LOSSES IN MICROSTRIP TRANSMISSION LINES: J. S. Bagby, Department of Electrical Engineering, University of Texas at Arlington, Arlington, Texas 76019, and D. P. Nyquist, Department of Electrical Engineering and Systems Science, Michigan State University, East Lansing, Michigan 48824.

An exact dyadic integral equation is utilized in the analysis of propagation in uniform integrated microstrip transmission lines. The object of the analysis is to predict and quantify the radiative and surface wave losses in such systems.

The axially-transformed surface current $\vec{k}(\vec{\rho};\zeta)$ of a natural mode on an integrated microstrip line satisfies the homogeneous integral equation:

$$\hat{t}\cdot(k_c^2 + \nabla\nabla\cdot) \oint_{\ell} \overleftrightarrow{g}(\vec{\rho}|\vec{\rho}';\zeta)\cdot\vec{k}(\vec{\rho}';\zeta)\, d\ell' = 0, \quad \vec{\rho} \in \ell$$

where k_c is the wavenumber in the cover region, $\overleftrightarrow{g}(\vec{\rho}|\vec{\rho}';\zeta)$ is the Hertzian potential Green's dyad of the background structure, ζ is the complex propagation constant of the mode, t is a unit tangent to the transmission line, and ℓ is the cross-sectional contour of the line.

The integral representation of the Green's dyad exhibits singularity when the real part of ζ is less than the propagation constant of a surface wave mode in the integrated circuit background structure. It is shown that for the dominant mode of the line the singularity is not implicated, and all losses are due to radiation into the cover medium. For higher order modes, however, the singularity is implicated, requiring inclusion of a residue term representing excitation of surface waves in the film layer. For higher order modes, higher losses are observed due to excitation of surface waves in the film layer.

This equation is solved numerically by the method of moments for narrow and wide microstrip transmission lines. The above-described effects are demonstrated in both cases.

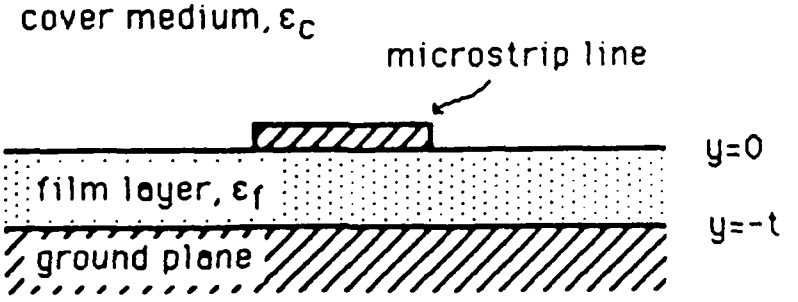

Research Paper No. [5]

COMPLETE PROPAGATION-MODE SPECTRUM OF MICROSTRIP GUIDING STRUCTURES

M.J. Cloud and D.P. Nyquist
Department of Electrical Engineering
and Systems Science
B.C. Drachman, Department of Mathematics
Michigan State University
East Lansing, Michigan 48824

Results of investigating the propagation-mode spectrum for longitudinally-invariant microstrip systems are presented. The influence of a layered conductor/film/cover background environment is rigorously accounted for.

Surface current eigenmodes $\vec{K}(\vec{r})$ are solutions of a homogeneous electric field integral equation (EFIE). The EFIE, which is enforced at all points $\vec{r}$ on the conducting microstrip surface S, may be stated as

$$\hat{t} \cdot (k^2 + \nabla \nabla \cdot) \int_S \overleftrightarrow{G}(\vec{r},\vec{r}') \cdot \vec{K}(\vec{r}') \, dS' = 0$$

where k is the wavenumber in the cover medium, $\hat{t}$ is a unit tangent vector to S, and $\overleftrightarrow{G}(\vec{r},\vec{r}')$ is a Hertz potential Green's dyad. This dyad depends explicitly upon the thickness and permittivity of the film layer. Often neglected transversely-flowing surface currents are retained in the model through a coupled integral equation approach, and are quantified along with the longitudinal components.

Emphasis is placed on leaky microstrip modes associated with transversely propagating surface waves of the background environment. Numerical solution is performed by Galerkin's method using entire-domain basis functions.

Research Paper No. [7]

Ph.D. DISSERTATION ABSTRACT

by

Michael John Cloud

Department of Electrical Engineering
Michigan State University
East Lansing, Michigan 48824

December 1987

Electromagnetic waves in millimeter-wave integrated circuits are studied. Dielectric film and cover regions overlay a conducting half-space in the configuration modeled, forming a non-uniform background for integrated devices. Emphasis is placed on the microstrip transmission line in this environment.

This research exploits an integral-operator description of the system. Constructed through Hertz potentials, an electric field integral equation (IE) quantifies microstrip surface currents. Complex plane analysis in the axial Fourier transform domain leads to the rigorous identification of discrete and continuous eigenvalue spectra. Discrete modes are associated with simple pole singularities, while the continuous spectrum arises from branch-cut integrals. These modal spectra are subsequently linked to natural and forced solutions of the IE.

Discrete wave modes are associated with the homogeneous IE, which is solved by the moment method for electrically-thin microstrip. The current density function is expanded in both subsectional and entire-domain basis functions. Results clearly validate: (1) the dominant axial current approximation for narrow strips, and (2) the edge singularity for axial currents. Dispersion characteristics are given for several modes; those for the fundamental mode compare favorably with results already in the literature.

Solution of the forced IE, at points along the complex-plane branch cut, yields spectral components of the strip radiation modes. The forcing function is taken to be the electric field impressed by a vertical monopole current that resides in the film layer. Preliminary moment-method results are given.

The transform-domain IE is also a basis for the study of coupling phenomena in axially-uniform multi-strip systems. System propagation modes are characterized by coupled currents sharing simple-pole singularities. Perturbation approximations apply for loose coupling, leading to an overlap-integral description of the coupling phenomenon.

Finally, a novel approach to the numerical evaluation of Sommerfeld integrals, using the Fast Fourier Transform, is advanced.

4.5 Coupling between adjacent microstrip lines

Discrete system modes of a coupled multi-microstrip configuration can be studied based upon a transform-domain integral-operator description of the system. Those system modes arise fron pole singularities in the complex transform plane. A Chebychev-Galerkin's solution to the homogeneous coupled EFIE's for discrete eigenmode currents of an adjacent microstrip system has been developed [10]. A manuscript [18] describing this accurate and rapidly-convergent full-wave formulation is presently in the review cycle. The isolated-strip eigenmode propagation constant is found to split when two adjacent microstrip become coupled, leading to two new system modes having symmetric and antisymmetric parity among the associated currents on the two lines. This formulation again leads to concise quasi-closed-form solutions for the eigenmode currents supported by coupled microstrip. Included in [18] are extensive numerical results for both isolated and coupled microstrip configurations.

An EFIE-based coupled-mode perturbation theory for coupling among any number of adjacent microstrip lines has been formulated [11,14,16]. It leads to a simple formulation for propagation eigenvale shifts and relative amplitudes of the various line currents for discrete system modes. Since the general Green's dyad kernels are exploited, both dielectric and ferrimagnetic thin-film layers can be accomodated. The simple quasi-closed-form Chebyshev series expressions for the isolated eigenmode currents are well suited for application in this coupled-mode theory. Numerical implementation leads to results which agree almost exactly with those of the numerical MoM solution except when the lines are very closely spaced. A research paper manuscript describing this integral-operator-based perturbation formulation is presently in preparation.

Papers [10,11,14,18] are appended here, while paper [16] was included in Section 4.3.

ENTIRE-BASIS MOM ANALYSIS OF COUPLED MICROSTRIP TRANSMISSION LINES

C.-H. Lee, J.S. Bagby
Department of Electrical Engineering
University of Texas at Arlington
Arlington, Texas 76019

Y. Yuan, D.P. Nyquist
Department of Electrical Engineering and System Science
Michigan State University
East Lansing, Michigan 48824

A system of exact dyadic integral equations is utilized in the analysis of propagation in uniform coupled integrated microstrip transmission lines. Axially-transformed natural mode surface currents on N coupled microstrip transmission lines satisfy the homogeneous coupled dyadic integral equations:

$$\hat{t}_j \cdot \sum_{i=1}^{N} \int_{\ell_i} \overleftrightarrow{g}^{e}(\rho \mid \rho'; \zeta) \cdot \vec{k}_i(\rho')\, d\ell' = 0, \quad j = 1, \ldots, N$$

where $\vec{k}_i$ is the transformed surface current on the i^{th} strip, $\overleftrightarrow{g}^{e}$ is the electric Green's dyad of the background structure, ζ is the unknown propagation constant of the coupled mode, $\hat{t}_j$ is a unit tangent to the j^{th} strip, and ℓ_i is the cross-sectional contour of the i^{th} strip.

The above integral equation is solved by the method of moments. Longitudinal and transverse currents are expanded in entire basis functions consisting of Tchebyshev polynomials of the first and second kind with multiplicative factors incorporating the proper edge behavior. This formulation is shown to converge to accurate results in as few as three terms.

Numerical results in the form of dispersion curves and surface current distributions are presented for the dominant and first three higher order modes, both even and odd, for the case of two identical coupled lines.

Research Paper No. [11]

EFIE-BASED PERTURBATION APPROXIMATION FOR COUPLED MICROSTRIP LINES

Yi Yuan and Dennis P. Nyquist
Department of Electrical Engineering
Michigan State University
East Lansing, MI 48824

To solve the eigenvalue problem of coupled microstrip lines, a full-wave analysis based on an electric dyadic Green's function is developed. The electric field integral equations (EFIE's) are solved, by a Galerkin's MoM technique with Chebychev polynomial basis functions, for both isolated and coupled microstrip. The direct numerical solution becomes very time consuming for a coupled microstrip system, consequently an approximate coupled-mode perturbation formulation is pursued.

In this paper, we present an EFIE-based perturbation approximation to solve for the system eigenmodes of N coupled microstrip lines. In solving the coupled EFIE's, the eigenmode current of the isolated line (which is obtained by a Galerkin's MoM solution to the isolated EFIE in a convenient Chebychev polynomial series) is used as a first-order perturbation approximation for nearly-degenerate eigenmode currents of the loosely-coupled system. The EFIE's yield a matrix equation

$$\bar{C}_{mm} a_m [\zeta - \zeta_{mp}^{(0)}] + \sum_{n \neq m} C_{mn} a_n = 0 \quad \text{... for } m=1,2,\ldots,N$$

where ζ is the unknown propagation eigenvalue, $\zeta_{mp}^{(0)}$ is that eigenvalue for the p'th mode on the n'th isolated microstrip, a_n is the current amplitude, and the C_{mn} are coupling coefficients involving field/current overlap integrals. ζ is that value which leads to a non-trivial solution for the a_n. Since the C_{mn} are ζ-independent, the numerical procedure is relatively efficient. For the special case of two-line coupling, it is found that the propagation eigenvalues split and shift symmetrically away from their isolated limit as the two microstrip become closely spaced.

A numerical implementation of the perturbation method is developed. The numerical results of the perturbation approximation are compared with those of the MoM numerical solution. Computation times are also compared, and the validity range of the perturbation approximation is investigated.

Research Paper No. [14]

COUPLED MICROSTRIP TRANSMISSION LINES: FULL-WAVE PERTURBATION THEORY AND EXPERIMENTAL VALIDATION

Yi Yuan*, John Vezmar, Gregory King and Dennis Nyquist
Department of Electrical Engineering
Michigan State University
East Lansing, Michigan 48824

The coupling between adjacent, parallel microstrip transmission lines in the micro/mm-wave PC/IC environment is studied both analytically and experimentally. A numerically efficient coupled-mode theory is obtained through a full-wave, EFIE-based perturbation approximation. The perturbation theory leads to propagation eigenvalue shifts associated with symmetric and antisymmetric coupling of both the principal and higher-order propagation modes. Experimental measurements are made on PC-board implementations of coupled microstrip pairs at micro/mm wavelengths to confirm the predicted coupling lengths.

A full-wave EFIE formulation for the currents on N coupled microstrip lines, located in the cover layer at the film/cover interface of a tri-layered conductor/film/cover environment, is based upon the Sommerfeld-integral representation of an appropriate electric Green's dyadic. The perturbation solution to those coupled EFIE's exploits a rapidly-convergent, modulated Chebychev series numerical solution for the isolated strip currents as the zero'th-order approximate induced current in the coupled system. Propagation eigenvalues ζ for coupled system modes satisfy

$$\bar{C}_{mm} a_m [\zeta - \zeta_{mp}^{(0)}] + \sum_{n \neq m} C_{mn} a_n = 0 \quad \text{... for } m = 1,2,\ldots,N$$

where $\zeta_{mp}^{(0)}$ is the phase constant for the p'th mode on the m'th isolated microstrip, a_n is the current amplitude on the n'th strip, $\bar{C}_{mm}$ is a normalization constant, and the C_{mn} are coupling coefficients involving field/current overlap integrals. For the case of two coupled lines, the propagation eigenvalues split and shift symmetrically away from their isolated limit as the microstrip become closely spaced. A simple coupled-mode theory leads to the coupling length in terms of the eigenvalue shifts.

The coupling length is measured experimentally, at micro/mm wavelengths on PC-board implementations of two coupled microstrip, to validate the perturbation-theory predictions for similar system parameters. A monopole microcoax probe is used to measure the axial electric field amplitude distribution along the coupled system. The probe is inserted through the conducting ground screen into the film and/or cover layers to measure the normal electric field there. A pattern of small holes is drilled through the PC board to implement probe insertion. A harmonic heterodyne detector assures measurement linearity. A new theoretical study of higher-order mode coupling is included.

Research Paper No. [18]

ENTIRE-DOMAIN BASIS MOM ANALYSIS OF COUPLED MICROSTRIP TRANSMISSION LINES

C.-H. Lee, J. S. Bagby
Department of Electrical Engineering
University of Texas at Arlington
Arlington, TX 76019

Y. Yuan, D. P. Nyquist
Department of Electrical Engineering
Michigan State University
East Lansing, MI 48824

Abstract

A full-wave spectral-domain integral equation formulation is used to analyze coupled microstrip transmission lines. A method of moments solution is implemented utilizing entire-domain basis functions which incorporate appropriate edge conditions for transverse and longitudinal current components, allowing for closed-form evaluation of spatial integrals. In contrast with earlier subdomain basis solutions, improved accuracy is obtained using far fewer terms. Numerical results in the form of propagation contants and current distributions are presented for the dominant and first two higher-order modes, and are compared to results of other techniques.

1. Introduction

The problem of analysis of coupled microstrip transmission lines is one of both considerable practical interest, and of long history. Traditionally, various quasi-static methods [1-5] have been used to compute the propagation characteristics of the coupled system. However, such methods are inherently inaccurate at higher frequencies, and are also found to be inadequate at low frequencies for many useful combinations of substrate thickness and dielectric constant [6]. In such cases a more accurate full-wave analysis must be utilized.

Recently, an exact spectral-domain coupled integral equation formulation has been introduced [8]. A subdomain basis method of moments solution of the coupled equations has been implemented and yields accurate results in the form of current distributions and propagation constants for the dominant and several higher-order modes [7]. However, this method requires a large number of basis functions to achieve desired accuracy, yielding long computation time.

In this paper an entire-domain basis method of moments solution is utilized. The basis functions are chosen carefully to incorporate the proper behavior at the edges of the strips. Besides allowing closed-form evaluation of spatial integrals, it is found that good accuracy is obtained (in the case of an isolated microstrip) for as few as three basis functions for each current component of low-order modes, yielding a compact approximate closed-form solution for currents and a substantial savings in computation time.

In section 2 the mathematical formulation and numerical solution technique are introduced. Numerical results in the form of propagation constants and strip current distributions are presented in Section 3. Conclusions and areas for further investigation are given in Section 4.

2. Formulation

Consider the coupled microstrip geometry depicted in Figure 1. The integral equation satisfied by the unknown surface current with an assumed propagation dependence of $\exp[j(\omega t-\zeta z)]$ on an isolated microstrip transmission line is given in [8]. This equation can easily be extended to an N coupled microstrip transmission line structure [7], and takes the following form:

$$\hat{t}_j\cdot(\tilde{\nabla}\tilde{\nabla}\cdot+k_c^2)\sum_{i=1}^{N}\int_{\ell_i}\overleftrightarrow{g}(\vec{\rho}\,|\,\vec{\rho}\,';\zeta)\cdot\vec{k}_i(\vec{\rho}\,')\,d\ell'=0,\quad \vec{\rho}\in\ell_j,\ j=1,\ldots,N. \tag{1}$$

where $\vec{k}_i$ is the axially-transformed surface current on the i^{th} strip, $\overleftrightarrow{g}$ is the transformed electric Hertzian potential Green's dyad of the microstrip background structure, ζ is the unknown propagation constant of the coupled mode, $\hat{t}_j$ is a unit tangent to the j^{th} strip, ℓ_i is the cross-sectional contour of the i^{th} strip, and $\tilde{\nabla}=\nabla_t+j\zeta\hat{z}=\hat{x}\frac{\partial}{\partial x}+\hat{y}\frac{\partial}{\partial y}+j\zeta\hat{z}$ is the transformed del operator.

The Hertzian potential Green's dyad decomposes into a principal and a reflected part, $\overleftrightarrow{g}=\overleftrightarrow{I}g^p+\overleftrightarrow{g}^r$, where g^p is the 2-dimensional unbounded-space Green's function in integral representation, and

$$\overleftrightarrow{g}^r(\vec{\rho}\,|\,\vec{\rho}\,')=\hat{x}g_t^r\hat{x}+\hat{y}\left(\frac{\partial}{\partial x}g_c^r\hat{x}+g_n^r\hat{y}+j\zeta g_c^r\hat{z}\right)+\hat{z}g_t^r\hat{z} \tag{2}$$

The scalar components of the reflected Green's dyad are given in terms of inverse transform integrals:

$$\left.\begin{matrix} g_t^r(\vec{\rho}|\vec{\rho}') \\ g_n^r(\vec{\rho}|\vec{\rho}') \\ g_c^r(\vec{\rho}|\vec{\rho}') \end{matrix}\right\} = \int_{-\infty}^{\infty} \left\{\begin{matrix} R_t(\lambda) \\ R_n(\lambda) \\ C(\lambda) \end{matrix}\right\} \frac{e^{j\xi(x-x')} e^{-p_c(y+y')}}{4\pi p_c} d\xi \qquad (3)$$

Here $\lambda^2 = \xi^2 + \zeta^2$, $p_c^2 = \lambda^2 - k_c^2$, $p_f^2 = \lambda^2 - k_f^2$, and the reflection and coupling coefficients are given by

$$R_t = \frac{p_c - p_f \coth(p_f t)}{p_c + p_f \coth(p_f t)} \qquad R_n = \frac{K p_c - p_f \tanh(p_f t)}{K p_c + p_f \tanh(p_f t)}$$

$$C = \frac{2(K-1)p_c}{[p_c + p_f \coth(p_f t)][K p_c + p_f \tanh(p_f t)]} \quad , \quad K = \frac{\varepsilon_f}{\varepsilon_c} \qquad (4)$$

2.1 Two identical microstrip lines

Now consider a coupled system of two identical microstrip lines. Assume that the lines are infinitely thin and are extended axially to infinity, as shown in Figure 2, where **b** is half of the spacing between the centers of the two strips and **w** is half of the strip width.

In this case, the integral equation becomes

$$\hat{t}_j \cdot \lim_{y\to 0} \sum_{i=1}^{2} \int_{\ell_i} (k_c^2 + \tilde{\nabla}\tilde{\nabla}\cdot)\, \vec{\vec{g}}(\vec{\rho}\,|x', y'=0;\zeta) \cdot \vec{k}_i(x', y'=0;\zeta)\, dx' = 0, \quad j = 1, 2 \qquad (5)$$

where interchange of differentiation and integration is valid since $y \neq 0$. As $y \to 0$, the contour involved in the integration is only the path along the x-axis and is denoted as ℓ_{x_i}. For the specialized structure, the tangential unit vector $\hat{t}$ and the surface current $\vec{k}$ can be expressed as

$$\hat{t} = \hat{x} t_x + \hat{z} t_z, \quad \vec{k} = \hat{x} k_x + \hat{z} k_z$$

To evaluate equation (5), we rewrite the integral representations of the scalar components g^p and $g^r_{t,n,c}$ as

$$g^{p,r}_{t,n,c}(\vec{\rho}\,|x';\zeta) = \int_{-\infty}^{\infty} i^{p,r}_{t,n,c}(\vec{\rho}\,|x';\zeta,\xi)\, d\xi \qquad (6)$$

with

$$i^p = \frac{e^{j\xi(x-x')} e^{-p_c|y|}}{4\pi p_c}$$

$$\left.\begin{matrix} i^r_t \\ i^r_n \\ i^r_c \end{matrix}\right\} = \left\{\begin{matrix} R_t \\ R_n \\ C \end{matrix}\right\} \frac{e^{j\xi(x-x')} e^{-p_c y}}{4\pi p_c}$$

where the fact y'=0 has been applied. Substitute (6) into (5) to obtain

$$\hat{t}_j \cdot \lim_{y\to 0} \sum_{i=1}^{2} \int_{\ell_{x_i}} \int_{-\infty}^{\infty} (k_c^2 + \tilde{\tilde{\nabla}}\tilde{\tilde{\nabla}}\cdot)\, \vec{i}(\rho \mid x';\zeta,\xi)\cdot \vec{k}\,(x';\zeta)\, d\xi\, dx' = 0 \qquad (7)$$

Notice that the operator $\tilde{\nabla}$ is now $\tilde{\tilde{\nabla}} = j\xi\hat{x} + \frac{\partial}{\partial y}\hat{y} + j\zeta\hat{z}$ since $\frac{\partial}{\partial x} \to j\xi$ when we interchange $\frac{\partial}{\partial x}$ and $\int d\xi$.

After some algebraic manipulation, we obtain

$$\hat{t}\cdot \vec{i}\cdot \vec{k} = (i^p + i_t^r)(t_x k_x + t_x k_z) \qquad (8)$$

$$\hat{t}\cdot \tilde{\tilde{\nabla}}\tilde{\tilde{\nabla}}\cdot \vec{i}\cdot \vec{k} = (j\xi t_x + j\zeta t_z)[(i^p + i_t^r)(j\xi k_x + j\zeta k_z) - p_c i_c^r (j\xi k_x + j\zeta k_z)] \qquad (9)$$

Substituting (8) and (9) into (7) and taking the limit $y \to 0$ in the results, we obtain two coupled equations by letting $\hat{t} = \hat{x}$ and $\hat{t} = \hat{z}$. They are

$$\hat{x}: \sum_{i=1}^{2} \int_{\ell_{x_i}} \int_{-\infty}^{\infty} \frac{e^{j\xi(x-x')}}{4\pi p_c} [k_c^2(1+R_t)k_x - \xi(1+R_t-p_cC)(\xi k_x+\zeta k_z)]\, d\xi\, dx' = 0$$

$$\hat{z}: \sum_{i=1}^{2} \int_{\ell_{x_i}} \int_{-\infty}^{\infty} \frac{e^{j\xi(x-x')}}{4\pi p_c} [k_c^2(1+R_t)k_z - \zeta(1+R_t-p_cC)(\xi k_x+\zeta k_z)]\, d\xi\, dx' = 0$$

The final form of the integral equations for the two indentical microstrip line structure can be obtained by resolving ℓ_{x_i} as $\ell_{x_1} = [-b-w, -b+w]$ and $\ell_{x_2} = [b-w, b+w]$.

$$\hat{x}: \int_{-b-w}^{-b+w} \int_{-\infty}^{\infty} \frac{e^{j\xi(x-x')}}{4\pi p_c} [k_c^2 R k_{x1} - \xi(R-C')(\xi k_{x1}+\zeta k_{z1})]\, d\xi\, dx' + \int_{b-w}^{b+w} \int_{-\infty}^{\infty} \frac{e^{j\xi(x-x')}}{4\pi p_c} [k_c^2 R k_{x2} - \xi(R-C')(\xi k_{x2}+\zeta k_{z2})]\, d\xi\, dx' = 0 \qquad (10)$$

$$\hat{z}: \int_{-b-w}^{-b+w} \int_{-\infty}^{\infty} \frac{e^{j\xi(x-x')}}{4\pi p_c} [k_c^2 R k_{z1} - \zeta (R - C')(\xi k_{x1} + \zeta k_{z1})] \, d\xi \, dx'$$

$$+ \int_{b-w}^{b+w} \int_{-\infty}^{\infty} \frac{e^{j\xi(x-x')}}{4\pi p_c} [k_c^2 R k_{z2} - \zeta (R - C')(\xi k_{x2} + \zeta k_{z2})] \, d\xi \, dx' = 0 \qquad (11)$$

Here k_{x1}, k_{z1} and k_{x2}, k_{z2} are transverse and axial currents for strip 1 and strip 2, respectively, and

$$R = 1 + R_t = \frac{2 p_c}{p_c + p_f \coth(p_f t)}$$

$$C' = p_c C = \frac{2(K-1)p_c^2}{[p_c + p_f \coth(p_f t)][K p_c + p_f \tanh(p_f t)]}$$

Equations (10) and (11) are the coupled integral equations for the microstrip structure depicted in figure 2. They have a non-trivial solution for k_{xi}'s and k_{zi}'s only when $\zeta = \zeta_m$ is an eigenvalue; here m=0,1,2,..., is the

mode number. In practical analysis, we can take advantage of the symmetry in x inherent in the coupled structure to further simplify the I.E.'s. For symmetric eigenmodes the currents exhibit even symmetry and we let $k_{x1}(x') = k_{x2}(-x')$ and $k_{z1}(x') = k_{z2}(-x')$; similarly, for antisymmetric mode we let $k_{x1}(x') = -k_{x2}(-x')$ and $k_{z1}(x') = -k_{z2}(-x')$ since the currents now have an odd symmetry. Then the coupled I.E. can eventually be written in terms of just $k_{x2}(x')$ and $k_{z2}(x')$. We will solve the coupled I.E.s by the method of moments using entire-domain basis functions.

2-2 Entire-domain basis MoM solution

The MoM solution to equations (10) and (11) depends on a reasonable choice of basis functions. These basis functions should incorporate the edge conditions that $\vec{k}_z$ is singular and $\vec{k}_x$ is zero at the edges of the microstrips. In this paper, instead of using subdomain basis MoM for which the solutions satisfy the electromagnetic boundary conditions only at discrete points, we use entire-domain bases for expansion of the unknown surface currents and testing. The main advantage of entire-domain bases lies in problems where the unknown function is assumed a priori to follow a known pattern [9]. In such cases, entire-domain functions may render an acceptable representation of the unknown while using far fewer terms than would be necessary for subdomain bases.

Based on the results presented in [7], it is found that Chebyshev polynomials multiplied by an appropriate edge-factor are one of the best sets that fit the solution currents of this coupled microstrip structure well. In our

work we choose Chebyshev polynomials of the second kind $U_n(x')$ to expand the unknown transverse transmission line currents since the latter can accurately be represented with a linear combination of just few functions of this kind. By similar reason, the same polynomials of the first kind $T_n(x')$ have been used for axial currents expansion. Use of these functions has the added advantage of allowing spatial integrals to be evaluated in closed form.

From above discussion, we expand $k_{x2}(x')$ and $k_{z2}(x')$ as follows:

$$k_{x2}(x') \cong \sqrt{1-\left(\frac{x'-b}{w}\right)^2} \sum_{n=0}^{N-1} a_n U_n\left(\frac{x'-b}{w}\right)$$

$$k_{z2}(x') \cong \frac{1}{\sqrt{1-\left(\frac{x'-b}{w}\right)^2}} \sum_{n=0}^{N-1} b_n T_n\left(\frac{x'-b}{w}\right)$$

where a_n and b_n are expansion coefficients representing the contribution of each order of the Chebyshev polynomials $U_n(x')$ and $T_n(x')$ to the unknown surface currents and the factors in front of the summation terms give $U_n(x')$ and $T_n(x')$ the correct edge behavior.

To test the coupled I.E.s after doing the expansion of unknown currents, we follow Galerkin's method and utilize the same functions for testing. We need the tabulated integral formulas listed in [10] and in the appendix for the calculation involved in current expansion and testing. For the sake of brevity, we omit some purely algebraic steps and finally obtain the I.E.'s for the coupled structure as

symmetric modes:

$$\hat{x}: \sum_{n=0}^{N-1} a_n\,(n+1) \int_{-\infty}^{\infty} \frac{e^{j\xi b}}{\xi^2 p_c} \left[\cos(\xi b)\,\mathrm{Re}\left\{j^n\right\} - \sin(\xi b)\,\mathrm{Im}\left\{j^n\right\}\right]\left[k_c^2 R - \xi^2 (R - C')\right] J_{m+1}(\xi w)\, J_{n+1}(\xi w)\, d\xi$$

$$- \sum_{n=0}^{N-1} b_n w\, \zeta \int_{-\infty}^{\infty} \frac{e^{j\xi b}}{p_c} \left[\cos(\xi b)\,\mathrm{Re}\left\{j^n\right\} - \sin(\xi b)\,\mathrm{Im}\left\{j^n\right\}\right] (R - C')\, J_{m+1}(\xi w)\, J_n(\xi w)\, d\xi = 0$$

$$\hat{z}: \sum_{n=0}^{N-1} a_n\,(n+1)\,\zeta \int_{-\infty}^{\infty} \frac{e^{j\xi b}}{p_c} \left[\cos(\xi b)\,\mathrm{Re}\left\{j^n\right\} - \sin(\xi b)\,\mathrm{Im}\left\{j^n\right\}\right] (R - C')\, J_m(\xi w)\, J_{n+1}(\xi w)\, d\xi$$

$$- \sum_{n=0}^{N-1} b_n w \int_{-\infty}^{\infty} \frac{e^{j\xi b}}{p_c} \left[\cos(\xi b)\,\mathrm{Re}\left\{j^n\right\} - \sin(\xi b)\,\mathrm{Im}\left\{j^n\right\}\right]\left[k_c^2 R - \zeta^2 (R - C')\right] J_m(\xi w)\, J_n(\xi w)\, d\xi = 0$$

antisymmetric modes:

$$\hat{x}: \sum_{n=0}^{N-1} a_n (n+1) \int_{-\infty}^{\infty} \frac{j e^{j\xi b}}{\xi^2 p_c} \left[\cos(\xi b)\,\mathrm{Im}\left\{j^n\right\} + \sin(\xi b)\,\mathrm{Re}\left\{j^n\right\}\right]\left[k_c^2 R - \xi^2 (R - C')\right] J_{m+1}(\xi w)\, J_{n+1}(\xi w)\, d\xi$$

$$- \sum_{n=0}^{N-1} b_n\, w\, \zeta \int_{-\infty}^{\infty} \frac{j e^{j\xi b}}{p_c} \left[\cos(\xi b)\,\mathrm{Im}\left\{j^n\right\} + \sin(\xi b)\,\mathrm{Re}\left\{j^n\right\}\right] (R - C')\, J_{m+1}(\xi w)\, J_n(\xi w)\, d\xi = 0$$

$$\hat{z}: \sum_{n=0}^{N-1} a_n (n+1)\,\zeta \int_{-\infty}^{\infty} \frac{j e^{j\xi b}}{p_c} \left[\cos(\xi b)\ \mathrm{Im}\left\{j^n\right\} + \sin(\xi b)\ \mathrm{Re}\left\{j^n\right\}\right] (R - C')\, J_m(\xi w)\, J_{n+1}(\xi w)\, d\xi$$

$$- \sum_{n=0}^{N-1} b_n\, w \int_{-\infty}^{\infty} \frac{j e^{j\xi b}}{p_c} \left[\cos(\xi b)\ \mathrm{Im}\left\{j^n\right\} + \sin(\xi b)\ \mathrm{Re}\left\{j^n\right\}\right] \left[k_c^2 R - \zeta^2 (R - C')\right] J_m(\xi w)\, J_n(\xi w)\, d\xi = 0$$

The integration limits $(-\infty, \infty)$ in the variable ξ can be reduced to $[0, \infty)$ by considering m and n to be even or odd respectively. Those terms which are odd with respect to ξ will integrate to zero , and those even terms will survive and the final I.E.s can be written as two times the same integral with the integration limits $[0, \infty)$. In matrix form the I.E.s can be written as

$$\begin{bmatrix} Z_{xx} & Z_{xz} \\ Z_{zx} & Z_{zz} \end{bmatrix} \begin{bmatrix} a_0 \\ \vdots \\ a_{N-1} \\ b_0 \\ \vdots \\ b_{N-1} \end{bmatrix} = \begin{bmatrix} 0 \\ \vdots \\ 0 \\ 0 \\ \vdots \\ 0 \end{bmatrix}$$

$2N \times 2N \qquad 2N \times 1 \qquad 2N \times 1$

where each element in the Z matrix is in terms of a spectral integral on ξ, and $a_0,\ldots,a_{N-1}$, $b_0,\ldots,b_{N-1}$ are coefficients for expansion polynomials. We have 2N equations for 2N unknowns. To obtain a non-trivial solution, the determinant of the coefficient matrix must vanish. Since Matrix elements depend on the propagation constant ζ, we can iterate to find ζ_m for the eigenmodes. Some typical calculated results will be shown in next section.

3. Numerical results

A computer program in Fortran 77 using the method described above was prepared to calculate the propagation constants (or eigenvalues) and currents for the fundamental and higher order modes of the coupled microstrip structure. For convenience in comparison with the results in [14] and [15], the case with a dielectric constant of $n_f=k_f/k_o=3.13$, $n_c=1.0$, $t = 0.635$ mm, $w = 1.5$ mm and a varying distance **b** has been calculated and will be presented here.

3-1 Eigenvalues

Table 1 shows the eigenvalues for the fundamental and first two higher order modes at operating frequencies near cutoff. For each mode at the specific frequency, it can be seen that they agree with the well known fact that $\zeta_a<\zeta_{iso}<\zeta_s$, where ζ_a, ζ_{iso} and ζ_s are eigenvalues corresponding to antisymmetric, isolated, and symmetric modes, respectively. The smaller the spacing **b/w**, the larger (smaller) the eigenvalues for symmetric (antisymmetric) system modes. When the separation of the two coupled microstrips is large enough (in our work, about $b/w \geq 2$), the eigenvalues converge to the corresponding isolated one. Indeed, the symmetric and antisymmetric modes can be viewed as emerging from the corresponding isolated mode. Figure 3 shows the case of EH_0 Mode. While **(b-w)/w** is getting smaller, eigenvalues of the EH_0 symmetric and antisymmetric system modes are separated further, and ultimately, when two microstrips contact on inside edges, the EH_0 symmetric mode goes to the EH_0 mode of an isolated strip with double width, and the EH_0 antisymmetric mode goes to the EH_1

mode of the same width-doubled strip.

The behavior of eigenvalues for this coupled structure agrees very well with the results obtained by using the analysis in [1].

3-2. Currents

The axial and transverse currents for each mode mentioned above are shown in figures 4, 5 and 6 (since currents have either even or odd symmetry, only k_{x2} and k_{z2} for each mode are shown here.). In numerically quantifying the currents, we found that three Chebyshev polynomials are enough to accurately represent the unknown surface currents on an isolated microstrip. However, for currents on each microstrip of the coupled system, we need the first five to obtain an accurate result. It can be seen in Figure 4-a, b, 5-b and 6-b that due to the repulsion of the surface charge, currents for symmetric modes have smaller value near the inside edge than at the outside edge. On the other hand, due to the attraction of charge, the antisymmetric modes have larger current near the inside edge. This behavior of currents is not so obvious in figure 5-a and figure 6-a, since at such low frequencies, the effective width of the strip is so narrow that it can not fit the complete pattern of the currents. At higher frequency (40 GHz for EH_1 mode or 90 GHz for EH_2 mode, for example) we did find that transverse currents for EH_1 and EH_2 have the same behavior as mentioned above. In all cases, we can see the currents for isolated line lie between the two groups of currents of symmetric and antisymmetric system modes as expected.

Conclusions

A full-wave spectral-domain integral equation formulation has been presented for analysis of coupled microstrip transmission lines. A method of moments solution utilizing entire-domain basis functions which incorporate appropriate edge conditions for transverse and longitudinal current components allows for closed-form evaluation of spatial integrals. In contrast with earlier subdomain basis solutions, improved accuracy is obtained using far fewer terms. Numerical results in the form of propagation constants and current distributions for the dominant and first two higher-order modes compare favorably to results of other techniques.

A more difficult problem is the solution in the case of lossy modes. This condition occurs when the propagation constant falls below the eigenvalue of a surface-wave mode supported by the integrated circuit background slabguide structure. In this case singularties in the spectral integrands move close to the real axis, and complex-plane evaluation techniques become necessary . Work along these lines is proceeding, and is expected to yield results in the near future.

References

[1] K. C. Gupta, Ramesh Garg, and I. J. Bahl, Microstrip Lines and Slotlines, Norwood MA: Artech House, Inc., 1979, p. 303.

[2] Günter Kowalski and Reinhold Pregla, "Dispersion characteristics of single and coupled microstrips," AEÜ, Vol. 26, 1972, pp. 276-280.

[3] Ramesh Garg and I. J. Bahl, "Characteristics of coupled microstriplines, "IEEE Trans. Microwave Theory Tech., Vol. MTT-27,No.7,July 1979, pp. 700-705.

[4] Thomas G. Bryant and Jerald A. Weiss, "Parameters of microstrip transmission lines and of coupled pairs of microstrip lines," IEEE Trans. on Microwave Theory Tech., Vol. MTT-16, No. 12, Dec. 1968, PP. 1021-1027.

[5] E. G. Farr, C. H. Chan and R. Mittra,"A frequency-dependent coupled-mode analysis of multiconductor microstrip lines with application to VLSI interconnection problems," IEEE Trans. on Microwave Theory Tech. Vol. MTT-34, No. 2, Feb. 1986, pp. 307-310.

[6] Juan R. Mosing and Tapan K. Sarkar, "Comparison of quasi-static and exact electromagnetic fields from a horizontal electric dipole above a lossy dielectric backed by an imperfect ground plane," IEEE Trans. Microwave Theory Tech., Vol. MTT-34, No. 4, April 1986, pp.379-387.

[7] C.-H. Lee and J. S. Bagby, "Analysis of coupled microstrip transmission lines with EFIE method," 1988 International Radio Science (URSI) Meeting, Syracuse, NY, June 1988, digest p. 318.

[8] J. S. Bagby and D. P. Nyquist, "Dyadic Green's function for integrated electronic and optical circuits,"IEEE Trans. Microwave Theory Tech., Vol. MTT-35, No. 2, Feb. 1987, pp. 206-210.

[9] Constantine A. Balanis, Antenna Theory, Harper & Row, Publishers, New York, 1982, pp. 301-313.

[10] I. S. Gradshteyn and I. M. Ryzhik, Table of Integrals, Series, and Products, New York Academic Press, 1980, p. 836.

[11] Jerry M. Grimm, The Usage of Alternative Green's Functions Formulations in the Analysis of Microstrip Transmission Lines, M.S. Thesis, The University of Texas at Arlington, 1988, Chap. 3,4.

[12] I. E. Rana and N. G. Alexopoulos, "Current distribution and input impedance of printed dipoles," IEEE Trans. Antennas Propagat., Vol. AP-29, No. 1, Jan. 1985, pp. 99-105.

[13] Milton Abramowitz and Irene A. Stegun, Handbook of Mathematical Functions, Dover Pub. Inc., NY, 1972, pp. 390-397.

[14] Helmut Ermert, "Guiding and Radiation Characteristics of Planar Waveguides," IEE Microwave, Optics and Acoustics, Vol. 3, March 1979, pp. 59-62.

[15] Arthur A. Oliner, "Leakage from higher modes on microstrip line with application to antennas," Radio Sci., Vol. 22, No. 6, Nov. 1987, pp. 907-912.

Appendix

Other than the tabulated integral formulas listed in [10], we need to develop formulas for evaluating following integrals:

$$\int_{-1}^{1} \sqrt{1-x^2}\cos ax\, U_n(x)\,dx \quad \ldots (1) \qquad \int_{-1}^{1} \sqrt{1-x^2}\sin ax\, U_n(x)\,dx \quad \ldots (2)$$

$$\int_{-1}^{1} \cos ax\, T_n(x)\,\frac{dx}{\sqrt{1-x^2}} \quad \ldots (3) \qquad \int_{-1}^{1} \sin ax\, T_n(x)\,\frac{dx}{\sqrt{1-x^2}} \quad \ldots (4)$$

To evaluate (1) and (2), refer to Gradshteyn's book, eq. (7-321), p. 830, which is

$$\int_{-1}^{1} (1-x^2)^{v-\frac{1}{2}} e^{iax} C_n^{v}(x)\,dx = \frac{\pi\, 2^{1-v}\, i^n\, \Gamma(2v+n)}{n!\,\Gamma(v)}\, a^{-v} J_{v+n}(a)$$

Since $U_n(x) = C_n^{(1)}(x)$, where $C_n(x)$ is the Gegenbauer polynomial, The above formula can be specialized to

$$\int_{-1}^{1} \sqrt{1-x^2}\, e^{iax} U_n(x)\,dx = \frac{\pi\, i^n\, \Gamma(n+2)}{n!\,\Gamma(1)}\, a^{-1} J_{n+1}(a) = \frac{i^n\, \pi\,(n+1)}{a} J_{n+1}(a)$$

Thus we obtain following formulas for (1) and (2):

$$\int_{-1}^{1} \sqrt{1-x^2}\, \cos ax\, U_n(x)\, dx = \frac{\pi\,(n+1)}{a}\, J_{n+1}(a)\, \mathrm{Re}\{i^n\}$$

$$\int_{-1}^{1} \sqrt{1-x^2}\, \sin ax\, U_n(x)\, dx = \frac{\pi\,(n+1)}{a}\, J_{n+1}(a)\, \mathrm{Im}\{i^n\}$$

Similar procedure can be taken for evaluating (3) and (4). We now refer to eq. (7-355), p. 836, the same book:

$$\int_{0}^{1} T_{2n+1}(x)\, \sin ax\, \frac{dx}{\sqrt{1-x^2}} = (-1)^n\, \frac{\pi}{2}\, J_{2n+1}(a)$$

$$\int_{0}^{1} T_{2n}(x) \cos ax\, \frac{dx}{\sqrt{1-x^2}} = (-1)^n\, \frac{\pi}{2}\, J_{2n}(a)$$

From this we can write

$$\int_{-1}^{1} \cos ax\, T_n(x)\, \frac{dx}{\sqrt{1-x^2}} = \begin{cases} 0\,, & \text{for odd } n. \\ (-1)^{n/2}\, \pi\, J_n(a)\,, & \text{for even } n. \end{cases}$$

$$\int_{-1}^{1} \sin ax\, T_n(x) \frac{dx}{\sqrt{1-x^2}} = \begin{cases} (-1)^{\frac{n-1}{2}} \pi J_n(a), & \text{for odd } n. \\ 0, & \text{for even } n. \end{cases}$$

Also notice that

$$\int_{-1}^{1} e^{iax} T_n(x) \frac{dx}{\sqrt{1-x^2}} = \int_{-1}^{1} \cos ax\, T_n(x) \frac{dx}{\sqrt{1-x^2}} + i \int_{-1}^{1} \sin ax\, T_n(x) \frac{dx}{\sqrt{1-x^2}}$$

$$= \begin{cases} i\,(-1)^{\frac{n-1}{2}} \pi J_n(a), & \text{for odd } n. \\ (-1)^{n/2} \pi J_n(a), & \text{for even } n. \end{cases}$$

$$= i^n \pi J_n(a), \qquad \text{for any } n.$$

Thus we obtain folowing integral formulas for use.

$$\int_{-1}^{1} \cos ax\, T_n(x) \frac{dx}{\sqrt{1-x^2}} = \mathrm{Re}\left\{ i^n \pi J_n(a) \right\} = \pi J_n(a)\, \mathrm{Re}\left\{ i^n \right\}$$

$$\int_{-1}^{1} \sin ax \; T_n(x) \frac{dx}{\sqrt{1-x^2}} = \mathrm{Im}\left\{ i^n \pi J_n(a) \right\} = \pi J_n(a) \; \mathrm{Im}\left\{ i^n \right\}$$

Table 1: Eigenvalues

Mode / b/w	10 GHz EH_0	20 GHz EH_1	40 GHz EH_2	
1.10	3.00638	2.17164	2.23297	Symmetric modes
1.25	2.98567	2.12381	2.21197	
1.50	2.95200	2.09482	2.19654	
Isolated	2.89586	2.06867	2.17533	
1.50	2.83309	2.05419	2.15925	Antisymmetric modes
1.25	2.78686	2.01026	2.11995	
1.10	2.75250	1.94495	2.05663	

Figure captions :

1. Figure 1: General system of N coupled microstrip lines.

2. Figure 2: Two identical thin coupled microstrip lines.

3. Figure 3: Dependence of propagation phase constant ζ for EH_0 system modes of two coupled microstrip lines upon line spacing; symmetric and antisymmetric system modes emerge from the isolated EH_0 mode.

4. Figure 4: (a) Transverse currents; (b) axial currents for EH_0 coupled mode.

5. Figure 5: (a) Transverse currents; (b) axial currents for EH_1 coupled mode.

6. Figure 6: (a) Transverse currents; (b) axial currents for EH_2 coupled mode.

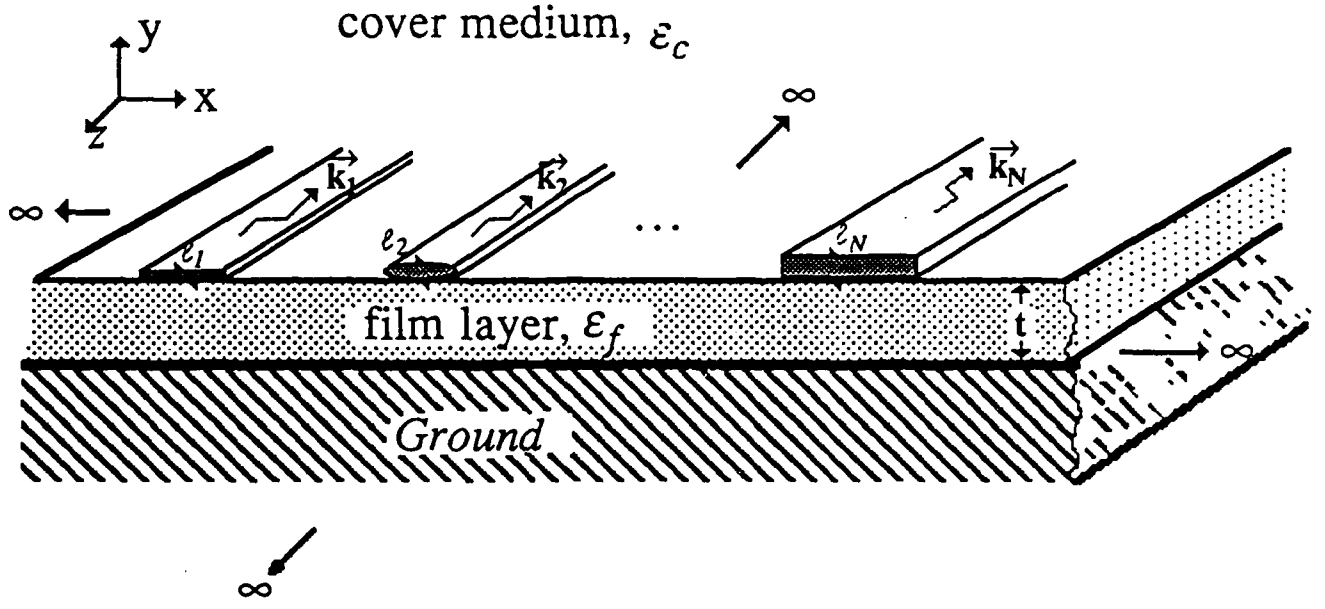
cover medium, ε_c
y
x
z
$\vec{k}_1$
$\vec{k}_2$
$\vec{k}_N$
ℓ_1
ℓ_2
ℓ_N
film layer, ε_f
t
Ground

Fig. 1

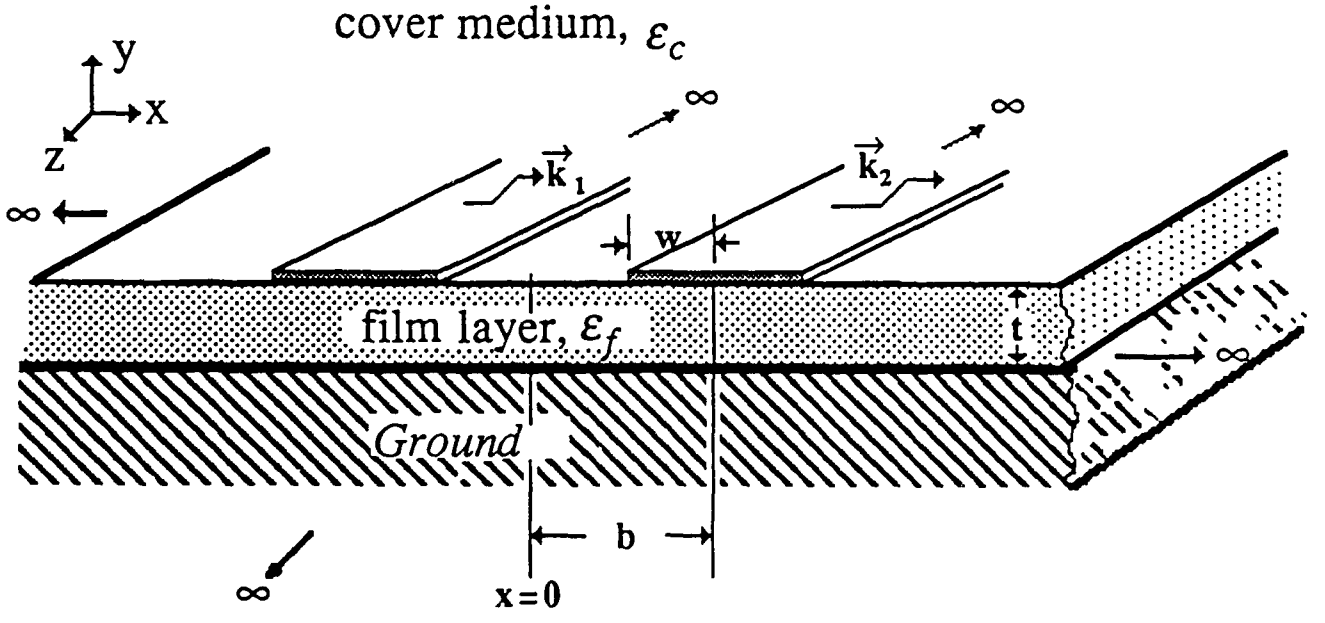
cover medium, ε_c
y
x
z
$\vec{k}_1$
$\vec{k}_2$
w
film layer, ε_f
t
Ground
b
x=0

Fig. 2

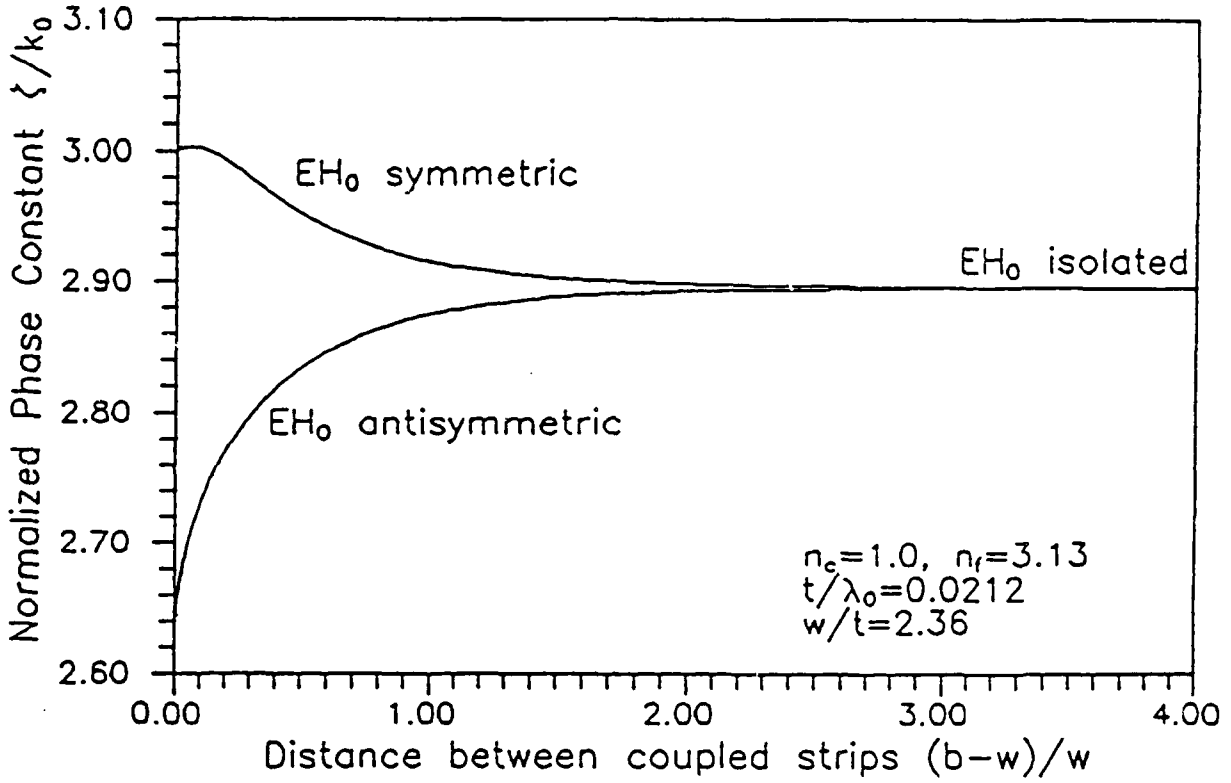

Figure 3. Dependence of propagation phase constant ζ for EH_0 system modes of two coupled microstrip lines upon line spacing; symmetric and antisymmetric system modes emerge from the isolated EH_0 mode.

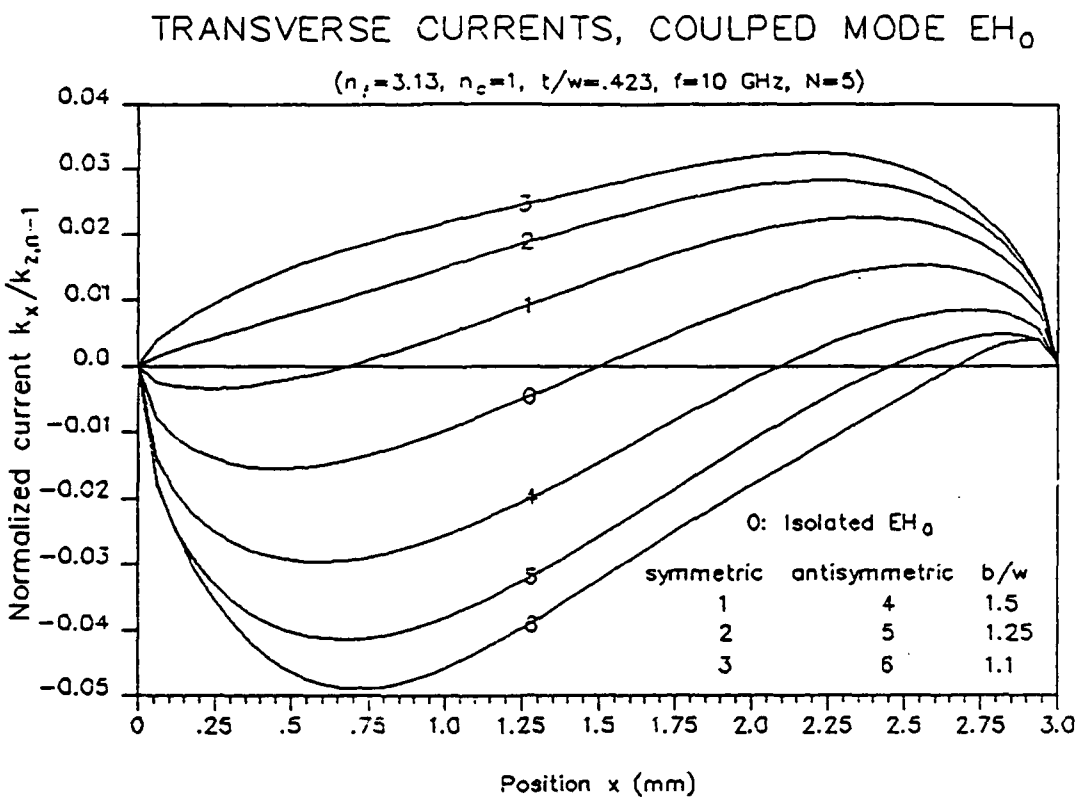
TRANSVERSE CURRENTS, COULPED MODE EH0
(nf=3.13, nc=1, t/w=.423, f=10 GHz, N=5)
Normalized current kx/kz,n-1
0.04
0.03
0.02
0.01
0.0
-0.01
-0.02
-0.03
-0.04
-0.05
0
.25
.5
.75
1.0
1.25
1.5
1.75
2.0
2.25
2.5
2.75
3.0
Position x (mm)
0: Isolated EH0
symmetric antisymmetric b/w
1 4 1.5
2 5 1.25
3 6 1.1

(a)

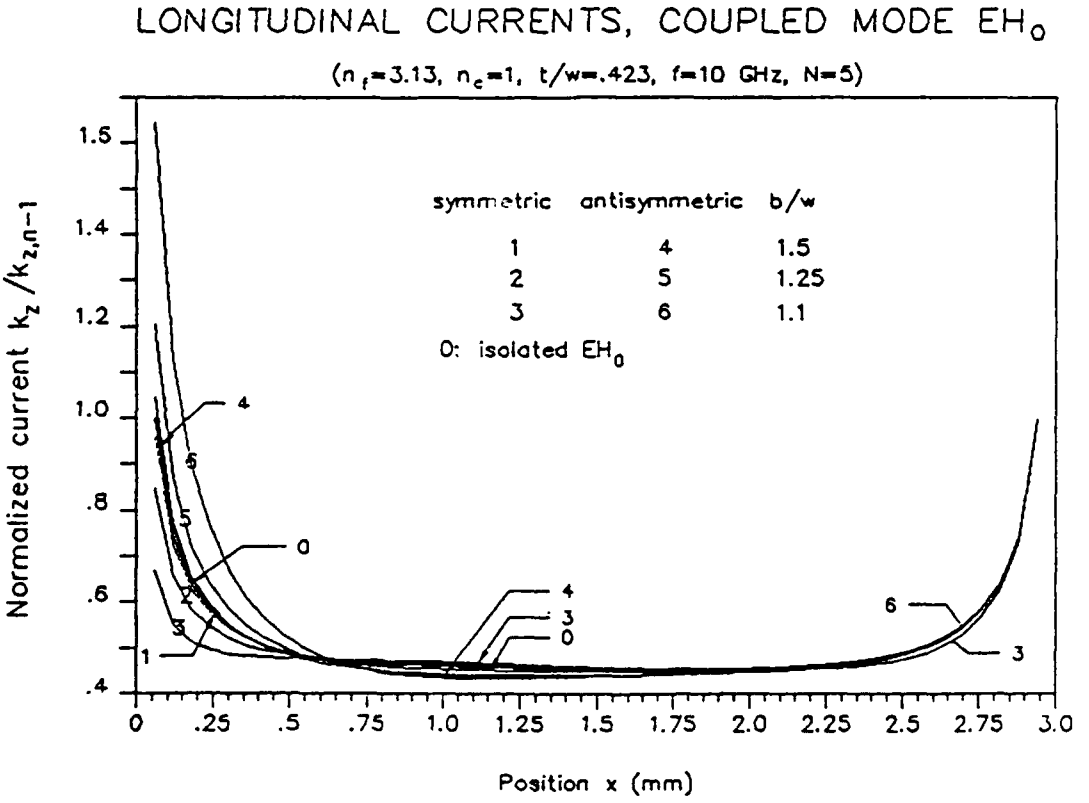
LONGITUDINAL CURRENTS, COUPLED MODE EH0
(nf=3.13, nc=1, t/w=.423, f=10 GHz, N=5)
Normalized current kz/kz,n-1
1.5
1.4
1.2
1.0
.8
.6
.4
0
.25
.5
.75
1.0
1.25
1.5
1.75
2.0
2.25
2.5
2.75
3.0
Position x (mm)
symmetric antisymmetric b/w
1 4 1.5
2 5 1.25
3 6 1.1
0: isolated EH0

Figure 4.

(b)

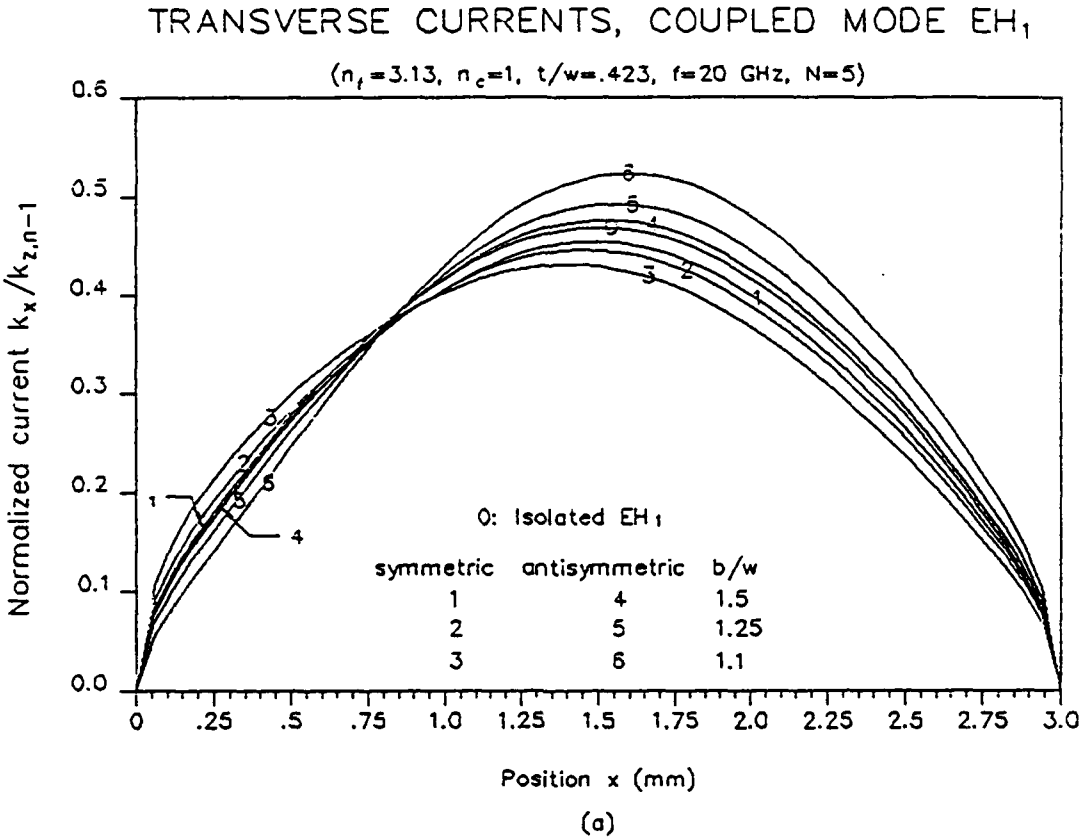
TRANSVERSE CURRENTS, COUPLED MODE EH1
(nf=3.13, nc=1, t/w=.423, f=20 GHz, N=5)
Normalized current kx/kz,n-1
0: Isolated EH1
symmetric antisymmetric b/w
1 4 1.5
2 5 1.25
3 6 1.1
Position x (mm)

(a)

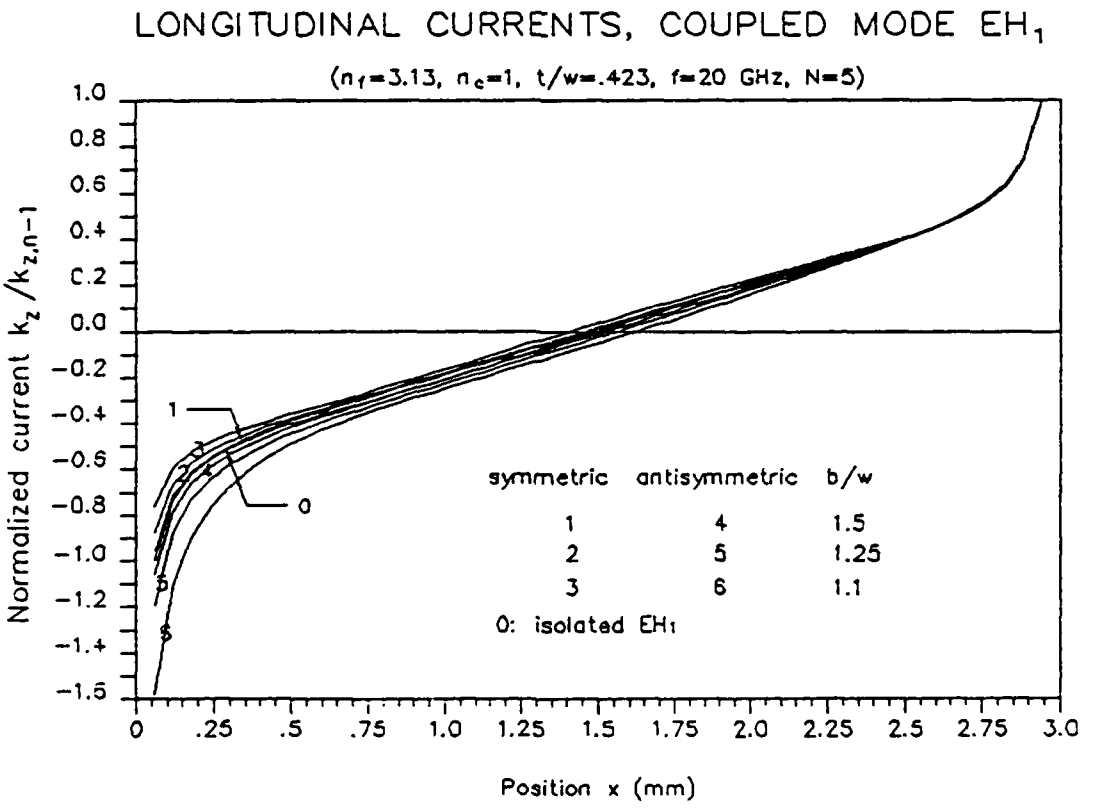
LONGITUDINAL CURRENTS, COUPLED MODE EH1
(nf=3.13, nc=1, t/w=.423, f=20 GHz, N=5)
Normalized current kz/kz,n-1
symmetric antisymmetric b/w
1 4 1.5
2 5 1.25
3 6 1.1
0: isolated EH1
Position x (mm)

(b)

Figure 5.

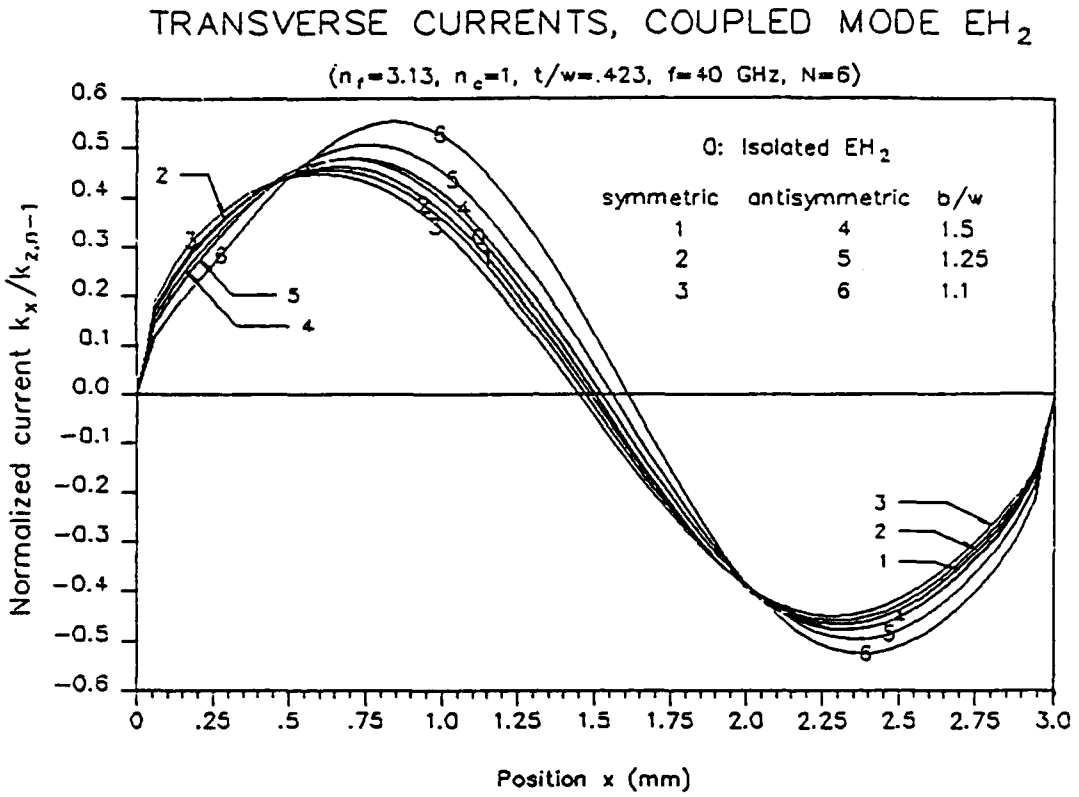
TRANSVERSE CURRENTS, COUPLED MODE EH2
(nf=3.13, nc=1, t/w=.423, f=40 GHz, N=6)
0: Isolated EH2
symmetric antisymmetric b/w
1 4 1.5
2 5 1.25
3 6 1.1
Normalized current kx/kz,n-1
Position x (mm)

(a)

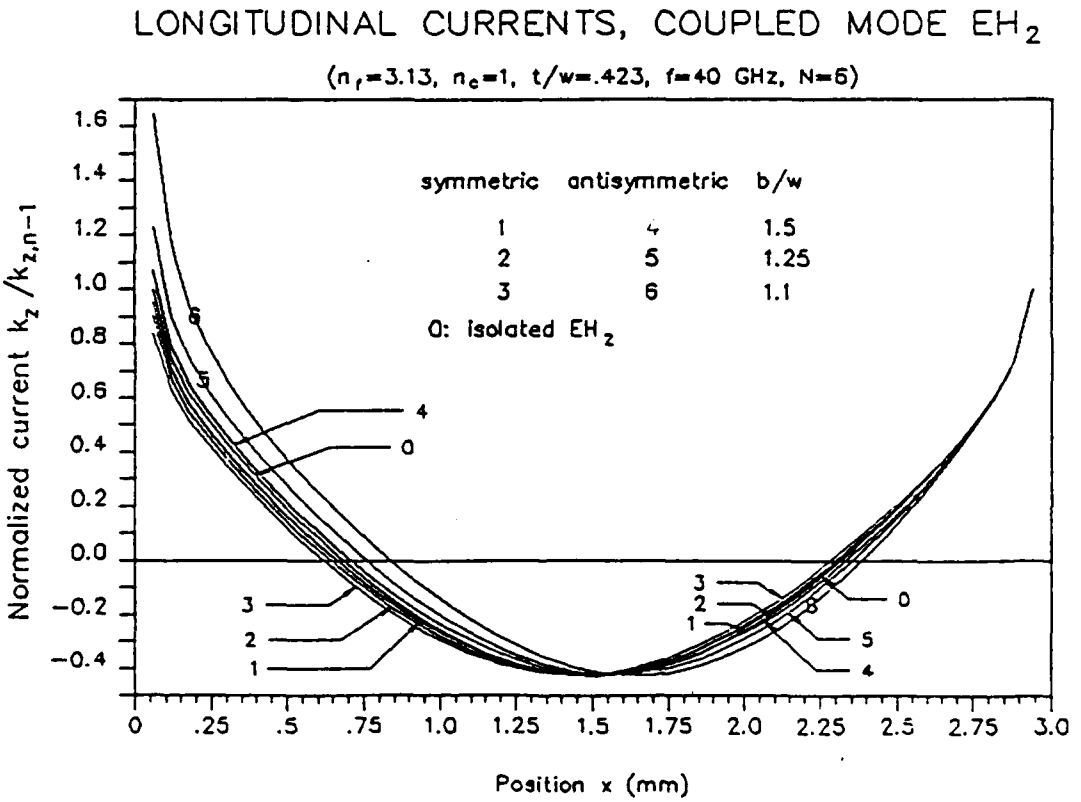
LONGITUDINAL CURRENTS, COUPLED MODE EH2
(nf=3.13, nc=1, t/w=.423, f=40 GHz, N=6)
symmetric antisymmetric b/w
1 4 1.5
2 5 1.25
3 6 1.1
0: Isolated EH2
Normalized current kz /kz,n-1
Position x (mm)

(b)

Figure 6.

4.6 EM response of microstrip patch devices and antennas

A rigorous description for natural resonance modes of microstrip patch devices in the MMIC environment, and the excitation of those modes, has been completed [16] based upon an EFIE description of such devices immersed in a layered dielectric/ferrimagnetic surround. Natural resonances arise from simple-pole singularities in the temporal complex transform plane, and are quantified as the non-trivial solutions to resulting homogeneous integral-operator equations. Numerical quantification of those modes for a circular-patch device is implemented [6] using Chebyshev series representations, appropriately modulated by square-root edge singularity factors, for the induced current components. Complex natural frequencies of several resonance modes and the associated natural-mode currents are obtained. A M.S. degree thesis on this topic is presently in preparation.

An EFIE-based coupled-mode perturbation theory for the system-mode resonant frequencies and relative current amplitudes describing an ensemble of coupled microstrip antennas in the MMIC environment [16] has been generalized to permit the presence of ferrimagnetic film layers. This perturbation approximation exploits natural-mode currents of isolated devices to obtain coupling coefficients for system-mode currents as overlap integrals of the current on one device with the resonant field of another.

Scientific paper [16] was included with Section 4.3, while paper [6] is appended here.

Research Paper No. [6]

INTEGRAL EQUATION FORMULATION FOR NATURAL MODES OF A CIRCULAR PATCH ANTENNA IN A LAYERED ENVIRONMENT

Eric W. Blumbergs, Dennis P. Nyquist, and Paul F. Havala

Department of Electrical Engineering and Systems Science
Michigan State University, East Lansing, Michigan 48824

This paper investigates the natural resonant modes of a circular path device immersed in an integrated conductor, film, and cover environment. A full two-dimensional EFIE description which totally accounts for the layered environment is developed. This development uses a polar coordinate Sommerfeld-integral representation of the dyadic Green's Function. The possibility of surface waves of the layered background is also included.

The natural mode formulation is based on a pair of coupled EFIE's. These equations are of the following form:

$$\sum_{n=-\infty}^{\infty} e^{jn\theta} \sum_{\nu=\rho,\theta} \int_0^a a_{\nu n}(\rho') K_{\alpha\nu}(\rho|\rho') d\rho' = -j \frac{k_0}{\zeta} E_\alpha^i(\rho,\theta)$$

for $\alpha=\rho,\theta$ where $a_{\nu n}(\rho')$ are radially dependent Fourier expansion coefficients of surface currents on the patch, $K_{\alpha\nu}(\rho|\rho')$ are kernels arising from the Hertzian potential Green's dyad, and $E_\alpha^i(\rho,\theta)$ are components of the impressed field tangent to the patch surface. Natural modes satisfy the homogeneous specialization of $E_\alpha^i(\rho,\theta)=0$.

Orthogonality of the $\exp(jn\theta)$ leads to independent systems of homogeneous equations for each n. Numerical solutions for natural frequencies and eigenfields are pursued by Galerkin's method. The special case n=0 leads to independent IE's for a_ρ and a_θ; corresponding field components are coupled for higher-order modes. Representative results are presented.

4.7 Experimental measurement of EM interactions in MMIC's

A complete V-band mm-wave instrumentation setup has been acquired and installed. Funds provided in the 10/1/87 to 12/31/88 reneral period allowed the purchase of a required local oscillator for the harmonic-mixer detector and MS-DOS PCB design software for use on the personal computer in MSU's new millimeter-wave laboratory. Low-loss PCB microstrip circuits are being fabricated to simulate the MMIC environment. Interactions between microstrip waves and adjacent patch devices are being studied experimentally to quantify the associated coupling and radiative scattering. The measured results provide for validation of the analytically predicted scattering characteristics. Validation of the coupled-mode perturbation theory for adjacent microstrip lines will be accomplished through experimental measurements on PCB implementations of such a coupled-line configuration.